The Gut Microbiota and Inflammation-Related Diseases, from Molecular Basis to Therapy 2021

Lead Guest Editor: Hongmei Jiang
Guest Editors: Xiaolu Jin, Li Zhang, and Guan Yang

The Gut Microbiota and Inflammation-Related Diseases, from Molecular Basis to Therapy

2021

The Gut Microbiota and Inflammation-Related Diseases, from Molecular Basis to Therapy 2021

Lead Guest Editor: Hongmei Jiang
Guest Editors: Xiaolu Jin, Li Zhang, and Guan Yang

Contents

Research Article

T Cell Subsets and the Expression of Related MicroRNAs in Patients with Recurrent Early Pregnancy Loss

Ya-ni Yan [iD],[1] **Jian Zhang,**[2] **Na Yang,**[1] **Chaochao Chen,**[1] **and Weiwei Li**[1]

[1]*Department of Reproductive Medicine, Qinhuangdao Maternal and Child Health Care Hospital, Qinhuangdao, Hebei 066000, China*
[2]*Jiulongshan Hospital of Qinhuangdao, Qinhuangdao, Hebei 066000, China*

Correspondence should be addressed to Ya-ni Yan; 18732780@qq.com

This study explored the role of T cell subsets and the expression of related microRNAs in patients with recurrent early pregnancy loss (EPL). Fifty patients with EPL loss between May 2018 and May 2021 were randomly selected as the EPL group, and 50 pregnant women with normal pregnancies or normal delivery outcomes were randomly selected as the control group. The expression levels of T cell subset-related markers and T cell subset-related miRNAs, in addition to the frequencies of T cell subsets, in peripheral blood of the two groups were analyzed. In terms of T cell-related markers, the results showed that the expression levels of the transcriptional regulator TBX-21 (T-bet) and interferon regulatory factor 4 (IRF4) were significantly upregulated in peripheral blood of the patients in the EPL group ($P < 0.05$), whereas the expression levels of GATA binding protein 3 (GATA3) and glucocorticoid-induced tumor necrosis factor receptor (GITR) were significantly downregulated ($P < 0.05$). In the EPL group, the expression of mir-106b, mir-93, and mir-25 was upregulated (1.51 ± 0.129, 1.43 ± 0.132, and 1.73 ± 0.156, respectively) in regulatory T (Treg) cell-related T cell subsets, whereas the expression of miR-146a and miR-155 was downregulated ($P < 0.05$). The frequencies of Treg and exhausted T cells in the EPL group were significantly lower than those in the control group ($P < 0.05$). The cell frequencies of T helper 17 (Th17) cells and exhausted Treg cells in the EPL group were significantly higher than those in the control group ($P < 0.05$). In conclusion, immune cells and associated miRNA profiles can be used as prognostic biomarkers for the treatment of human reproductive disorders, such as EPL.

1. Introduction

Early pregnancy loss (EPL) is defined as pregnancy loss within 12 weeks of gestation and includes miscarriages and biochemical pregnancy loss [1]. EPL, which includes spontaneous miscarriages, the most common type of EPL, embryonic abortion, and intrauterine fetal death, accounts for approximately 80% of pregnancy losses [2]. Recurrent EPL is a major concern in human reproduction and the focus of much research due to its complex etiology, poor prognosis, and adverse effects on the physical and mental health of pregnant women [3]. Immune abnormalities, mainly T cell subsets and related miRNA abnormalities, are known to play a vital role in the occurrence of EPL [4, 5].

Studies have shown that regulatory T (Treg) cells play an important role in the process of immune regulation and the survival of the fetus in the uterus [6, 7]. T helper 17 (Th17) cells, a newly recognized subpopulation of effector helper T cells, have the ability to promote host defense against extracellular pathogens and modulate inflammatory, chronic, and autoimmune diseases [6, 7]. A recent study showed that Th17 and Treg cells are strongly associated not only with successful pregnancies but also with pregnancy disorders, such as preeclampsia (PE) and recurrent spontaneous abortion (RSA), in which the frequency of Treg cells is decreased and the frequency of Th17 cells is increased [8]. Hadfield et al. and McCracken et al. showed that in the third trimester of pregnancy, the inability to mount a sufficient Th1 response resulted in diminished expression of the Th1 transcriptional regulator TBX-21 (T-bet) [9, 10]. They also showed that reconstitution of T-bet expression restored cytokine synthesis in T cells.

Some studies in recent years have shown that compared with normal pregnancies, miRNAs in exosomes and plasma of patients with RSA show significant changes [11, 12], in which miR-559, miR-146b-5p, miR-320b, and miR-221-3p were significantly upregulated, while miR-101-3p was significantly downregulated. This finding indicates that miRNAs can regulate RSA through a variety of potential mechanisms involving different target genes and binding sites. However, the specific mechanism is unclear and needs to be further explored. Liu et al. found that the expression of miR-93 and target B cell lymphoma-2-like 2 (BCL2L2) was increased in chorionic villi of RSA patients compared to that in women with normal pregnancies and that BCL2L2 expression adversely affected the balance of apoptosis, cell proliferation, migration, and invasion, promoting the development of RSA [13]. Other research demonstrated that miR-155-5p regulated RSA by activating the nuclear factor kappa-light-chain-enhancer of activated B cells signaling pathway [14]. And the overexpression of miR-155-5p was followed by a decrease in the release of inflammatory cytokines, including interleukin- (IL-) 6, interferon-γ (IFN-γ), tumor necrosis factor-α, and IL-10 from decidual stromal cells, thereby inhibiting the apoptosis of decidual stromal cells [14].

In this study, we explored the role of T cell subsets in the pathogenesis of RPL by evaluating the number of T cells, associated transcription factors, and miRNAs targeting these transcription factors. The results provide data that may aid the treatment and prevention of RPL.

2. Materials and Methods

2.1. Ethic Approval. The participants were informed about the study and voluntarily agreed to take part. This study complies with the ethical requirements of the Declaration of Helsinki and was approved by the Medical Ethics Committee of Qinhuangdao Maternal and Child Health Care Hospital. Written consent was obtained before conducting the study.

2.2. Inclusion Criteria. Pregnant women aged 18–41 years with a clinical diagnosis of recurrent EPL and no abnormalities in spousal semen quality testing were enrolled in the study. Recurrent EPL referred to two or more abortions before the 12th week of pregnancy [15].

2.3. Exclusion Criteria. Pregnant women with severe chromosomal abnormalities, acquired immune deficiency syndrome, hepatitis C, hepatitis B, and chronic diseases were excluded, in addition to those with a history of long-term continuous medication control, asthma, drug allergies, cervical dysfunction and uterine malformations, smoking and alcohol abuse, tumors, and other malignant diseases. Those younger than 18 years or older than 41 years were also excluded.

2.4. General Data. Fifty patients with recurrent EPL who presented to our hospital between May 2018 and May 2021 and met the inclusion criteria were randomly selected as the EPL group, and another 50 pregnant women with normal pregnancies or normal deliveries were randomly selected as the control group. There was no significant difference ($P > 0.05$) between the two groups in terms of age, nationality, parity, body mass index, or other general data (Table 1).

2.5. Assessment and Detection of Natural Killer (NK) Cell Expression Frequency. The cytotoxicity of NK cells was assessed by flow cytometry using K562 target cells. First, peripheral blood mononuclear cells (PBMCs) were isolated and incubated with prestained K562 target cells and propidium iodide at 37°C and 5% CO_2 for 2 hours. As effector cells, PBMCs were used to kill the target cells, and the dead cells were then permeabilized to propidium iodide.

The PBMCs were first isolated and then washed twice with phosphate-buffered saline. For PBMC staining, trichromatic immunofluorescence analysis was performed on lymphocyte markers using an antibody immunofluorescence assay. The fluorescent dyes used for trichromatic immunofluorescence analysis were isothiocyanate, phycoerythrin, and allophycocyanin, which are anti-CD3 (Abcam, US, cat. no. ab237453), anti-CD16 (Abcam, US, cat. no. ab117117), and anti-CD56 (Abcam, US, cat. no. ab237383) antibodies labeled with fluorescein isothiocyanate. NK cells in peripheral blood were represented by CD3, CD56, and CD16 cells. PBMCs were used in this study when the cellular value and cytotoxicity of NK cells were greater than 14% and 15%, respectively. The frequencies of Th1 and Th2 cells were assessed using flow cytometry fluorescein isothiocyanate- (FITC-) labeled anti-IFN-γ (BioLegend, US, cat. no. 308703) and anti-IL-4-PE (BioLegend, US, cat. no. 355005) and were included in the analysis when the Th1/Th2 ratio was greater than 10.7% [16, 17].

2.6. Measurement of miRNA Expression Levels of T Cell-Related Markers. Total RNA was isolated from PBMCs using RNX-PLUS, and cDNA was synthesized using a reverse transcriptase kit. T cell-associated factors, T-bet, transcription factor GATA-binding protein 3 (GATA3), interferon regulatory factor 4 (IRF4), glucocorticoid-induced tumor necrosis factor (GITR), and tumor necrosis factor receptor superfamily 18 were evaluated using RT-PCR. The primers and reference genes are shown in Table 2. β-Actin was used as the reference gene, and the miRNA level was calculated as the ratio of the target miRNA genes to the reference gene. Relative expression was normalized and presented as the ratio to the relative gene in the control group.

2.7. Evaluation of miRNAs Associated with T Cell Subsets. The miRNAs associated with Treg (miR-106b-93-25, miR-146a, and miR-155) and Th17 (miR-326) cells in PBMCs were evaluated by RT-PCR on a LightCycler 2.0 RT-PCR system. The primers and the reference gene are shown in Table 3. RNU6B was used as the reference gene, and the miRNA level was calculated as the ratio of the target miRNA genes to the reference gene. Relative

TABLE 1: Comparison of general data in the two groups.

	EPL group ($n = 50$)	Control group ($n = 50$)	t/χ^2	P
Age	27.28 ± 3.10	28.35 ± 3.56	1.10	0.75
Body mass index (kg/m^2)	19.87 ± 2.38	20.0 ± 2.58	2.08	0.54
Gravidity			4.04	0.23
2	13 (26)	23 (46)		
3	26 (52)	20 (40)		
≥4	11 (22)	7 (14)		
Parity			3.56	0.28
0	7 (14)	9 (18)		
1	22 (44)	26 (52)		
≥2	21 (42)	15 (30)		

TABLE 2: Primer sequences of target and reference genes.

Genes	Primer	Sequence (5′→3′)
TBX-21 (T-bet)	Forward	GGTGAACGACGGAGAGC
	Reverse	TCGGCATTCTGGTAGGC
GATA-3	Forward	GCCTCAGCCACTCCTAC
	Reverse	CCTGACCGAGTTTCCGTAG
IRF-4	Forward	CGTTCATTGCTCTCCAGTCAC
	Reverse	GCCTTCACGCACCATTCAG
TNFRSF18 (GITR)	Forward	TGGGTCGGGATTCTCAGGTC
	Reverse	TTTCAAGAGCCCACAGCCAG
β-Actin	Forward	GCATGGGTCAGAAGGATTCCT
	Reverse	TCGTCCCAGTTGGTGACG

TABLE 3: Primer sequences of the miRNAs and reference gene.

Genes	Primer	Sequence (5′→3′)
miR-106b	Forward	GGGGCTAAAGTGCTGACAGT
	Reverse	GGAGCAGCAAGTACCCACAG
miR-93	Forward	CTCCAAAGTGCTGTTCGTGC
	Reverse	GGGGCTCGGGAAGTGCTA
miR-25	Forward	GTGTTGAGAGGCGGAGACTT
	Reverse	TGTCAGACCGAGACAAGTGC
miR-146a	Forward	ACTGAATTCCATGGGTTGTGTC
	Reverse	TGACAGAGATATCCCAGCTGAAG
miR-155	Forward	TGCGCTTAATGCTAATTGTGATA
	Reverse	CCAGTGCAGGGTCCGAGGTATT
miR-326	Forward	CATCTGTCTGTTGGGCTGGA
	Reverse	TGGAGGAAGGGCCCAGAG
RNU6B	Forward	CTCGCTTCGGCAGCACA
	Reverse	AAGGCTTCACGAATTTGCGT

expression was normalized and presented as the ratio to the relative gene in the control group.

2.8. Assessment of T Cell Subpopulation Frequencies. Counting of Th17, Treg, exhausted T, and exhausted Treg cell was performed using flow cytometry. The monoclonal antibodies of surface and intracellular antigens used for counting Th17 cells were CD4-FITC (BioLegend, US, cat. no. 357405) and IL-17A-PE (BioLegend, US, cat. no. 506903), and CD4-FITC (BioLegend, US, cat. no. 357405), CD25-PE (BioLegend, US, cat. no. 985802), and CD127-PerCP-Cy5.5 (BioLegend, US, cat. no. 351321) were used for Treg cells; CD8-FITC (BioLegend, US, cat. no. 980908), PD-1-PerCP-Cy5.5 (BioLegend, US, cat. no. 329913), and Tim-3-PE (BioLegend, US, cat. no. 345006) for exhausted T cells; and CD4-FITC (BioLegend, US, cat. no. 357405), CD25-PE (BioLegend, US, cat. no. 985802), and PD1-PerCP-Cy5.5 (BioLegend, US, cat. no. 329913) for exhausted Treg cells [18].

2.9. Statistical Methods. SPSS 22.0 statistical software was used for statistical analysis. Data were expressed as mean ± standard deviation, and Student's t-test or chi-square test were used for between-group comparisons. Count data were expressed as ratios, and the data were processed by a chi-square test. $P < 0.05$ was considered a significant difference.

3. Results

3.1. Expression Levels of T Cell-Related Markers in the Two Groups. The expression levels of T cell subset-related genes in PBMCs in the two groups were compared. The results revealed significant differences in the mRNA expression levels of T-bet, GATA3, IRF4, and GITR ($P < 0.05$) (Figure 1). Compared with the control group, the mRNA expression levels of T-bet and IRF-4 in the PBMCs in the EPL group were significantly upregulated ($P < 0.05$), whereas those of GATA3 and GITR were significantly downregulated ($P < 0.05$).

3.2. Expression Levels of T Cell Subpopulation-Associated miRNAs in the Two Groups. The analysis of Treg cell-related miRNA revealed a significant increase in miR-25, miR-106b, and miR-93 expressions in the EPL group as compared with that in the control group ($P < 0.05$). In addition, the expression of miR-146a and miR-155 in PBMCs in the EPL group was significantly downregulated as compared with than that in the control group
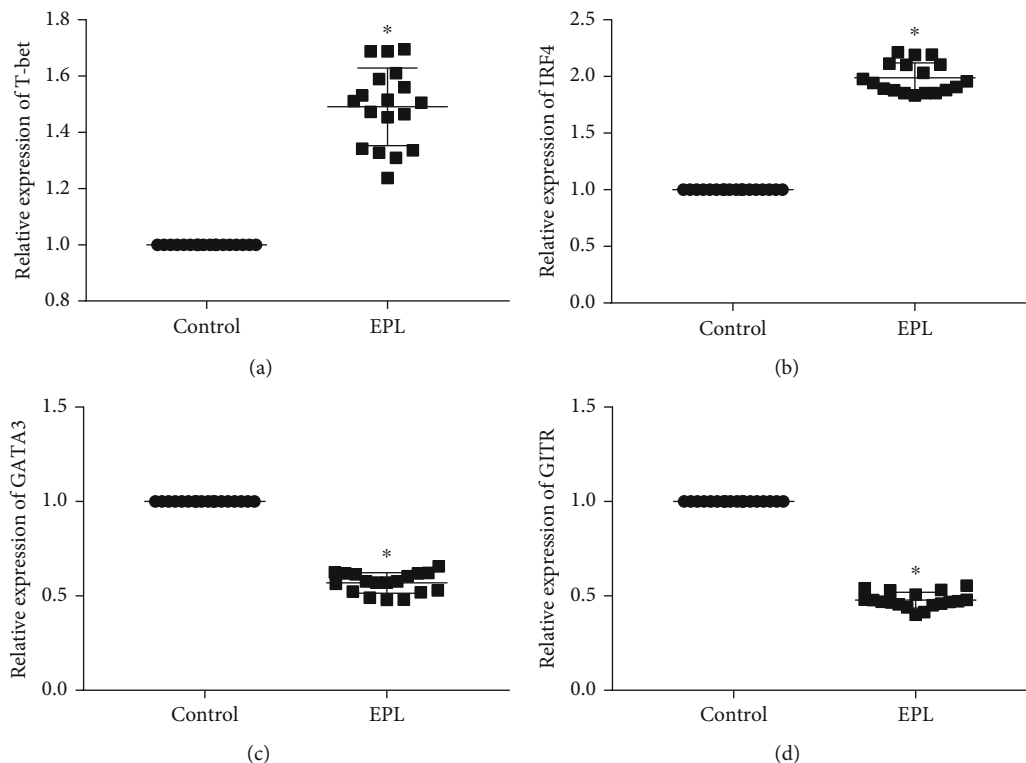
FIGURE 1: Expression of T cell-related markers in PBMCs in the EPL and control groups. (a) T-bet, (b) IRF 4, (c) GATA3, and (d) GITR. * indicates P value was less than 0.05.

($P < 0.05$). However, the expression of miR-326, which regulates the differentiation towards Th17 cells [19], in PBMCs in the EPL group was not significantly different from that in the control group (Figure 2).

3.3. Flow Cytometry Analysis of T Cell Subpopulation Frequencies in the Two Groups.
The results of flow cytometry showed that the frequency of peripheral blood Treg cells and exhausted T cells in the EPL group was significantly lower than that in the control group ($P < 0.05$). And the frequency of Th17 cells and exhausted Treg cells in peripheral blood in the EPL group was significantly increased as compared with than that in the control group ($P < 0.05$) (Figure 3).

4. Discussion

The incidence of EPL in women of normal childbearing age is approximately 1–3%, with the causes primarily linked to chromosomal, endocrine, anatomical, infectious, and immunological abnormalities [6, 7]. However, in most cases, the cause of EPL remains unexplained. In recent years, some studies have investigated various aspects of recurrent EPL, including genes associated with folate metabolism [20], oxidative stress levels, sperm DNA damage [6], congenital uterine malformations in pregnant women, and acquired coagulation dysfunction, all of which have made breakthroughs.

Recurrent EPL may be related to T cell subsets and their associated miRNAs. To shed light on this issue, the present study investigated the expression of T cell subsets and their associated miRNAs in patients with recurrent EPL. Previous studies reported that CD4+, CD25+, and Treg cells were downregulated in peripheral lymphocytes and metaphase lymphocytes of women who had a miscarriage [21, 22]. Research also showed that the frequency of Th17 cells in peripheral blood lymphocytes and metaphase lymphocytes was increased in women with recurrent miscarriages as compared with that in women who had normal pregnancies [23]. In addition, a negative correlation between Th17 and Treg lymphocytes was found in the peripheral blood of these patients [23]. The ratio of Th17/Treg is increased in women with EPL, signifying a proinflammatory response, which may be accompanied by a decrease in the regulatory response, potentially leading to the development of RPL [24]. In this study, the expression frequency of Th17 in the EPL group was higher than that in the control group, whereas the expression of Treg cells showed a decreasing trend compared with the control group, which is consistent with the previous research [24]. As reported previously, miR-155 induces the differentiation of Treg and Th17, as well as IL-17A secretion by Th17 cells, whereas it has no significant effect on the secretion of Treg-related cytokines [25]. In addition, miR-146a has been shown to be essential for the suppressive function of Treg cells, with regulation of the Th1 response controlled by miR-146a expression in Treg cells
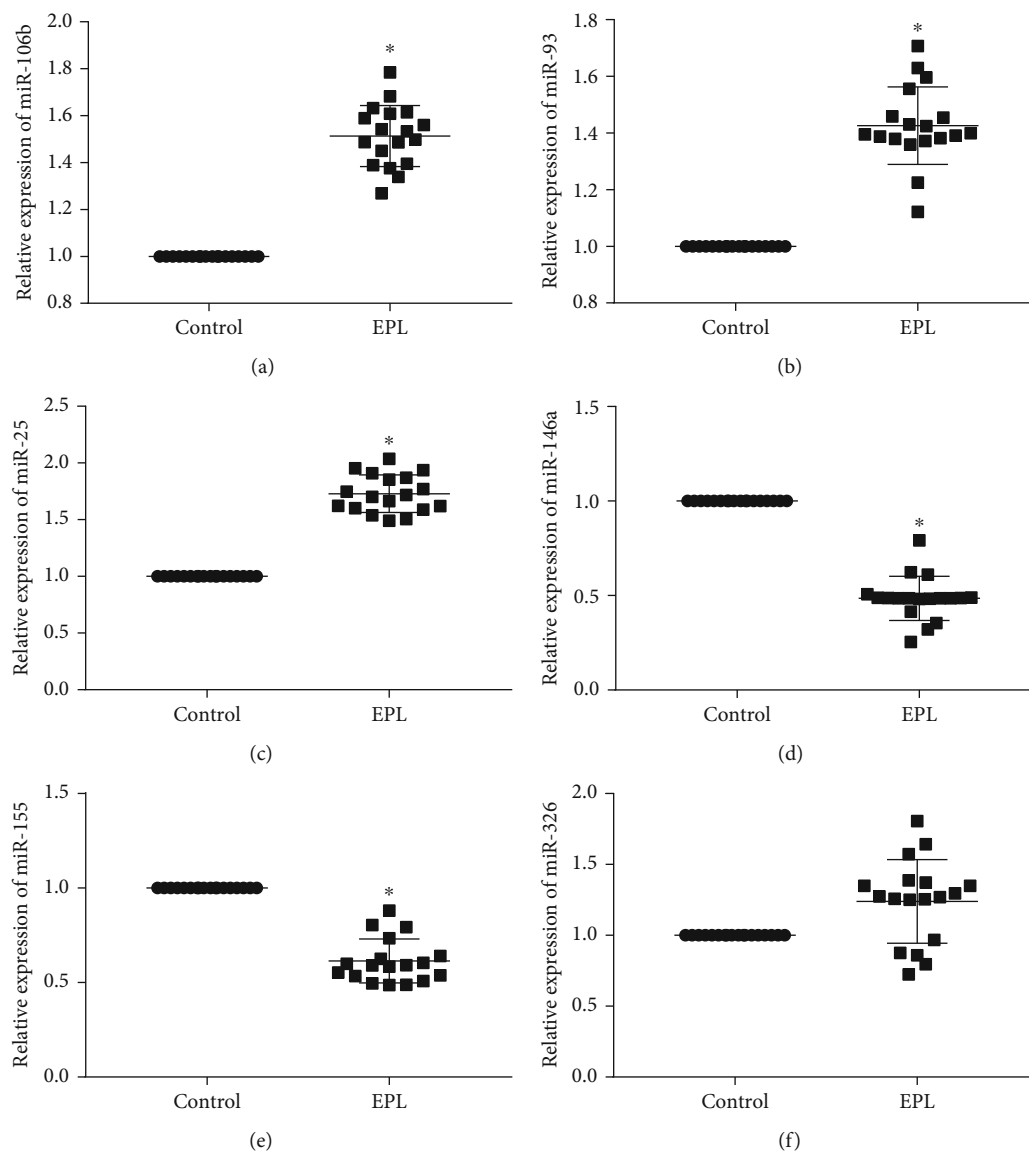
FIGURE 2: Expression of T cell subset-related miRNAs in the two groups. (a) miR-106b, (b) miR-93, (c) miR-25, (d) miR-146a, (e) miR-155, and (f) miR-326. * indicates P value was less than 0.05.

[26]. Furthermore, miR-146a may be able to inhibit the transformation of Treg cells to Th1-like cells. In PBMCs cocultured with colorectal cancer cells, miR-146a increased the number of Treg cells and associated suppressor cytokines, such as transforming growth factor-β (TGF-β) and IL-10 [26, 27]. According to our results, the expression of both miR-155 and miR-146a seems to be reduced in patients with recurrent EPL, which may be related to the reduced number of Treg cells in the patients. Studies have shown that the number of Treg cells decreased in both mouse pregnancy loss model and patients with unexplained recurrent pregnancy loss [28, 29].

The miR-106b-93-25 cluster plays a crucial role in the regulation of the TGF-β signaling pathway, and it is an essential cytokine in the induction of Foxp3 production by Treg cells. Foxp3 is a transcription factor which has

been found to play a critical role in the control of inflammation [30]. Increased expression of miR-106b-25 may disrupt the TGF-β signaling pathway, which plays an important role in maintaining the function and inducing the generation of Treg cells. Our results revealed a decrease in the number of Treg cells and an increase in the transcript level of the miR-106b-93-25 cluster in the peripheral blood of patients in the EPL group. We speculate that there is a definite link between them and that miR-106b-93-25 controls the mechanobiology of Treg cells in women with EPL [31–33].

The results of this study revealed an uncontrolled inflammatory microenvironment in the EPL group, as demonstrated by the increased frequency of Th17 and exhausted Treg cells and increased mRNA expression of T-bet and IRF-4 in peripheral blood. In this study, failure
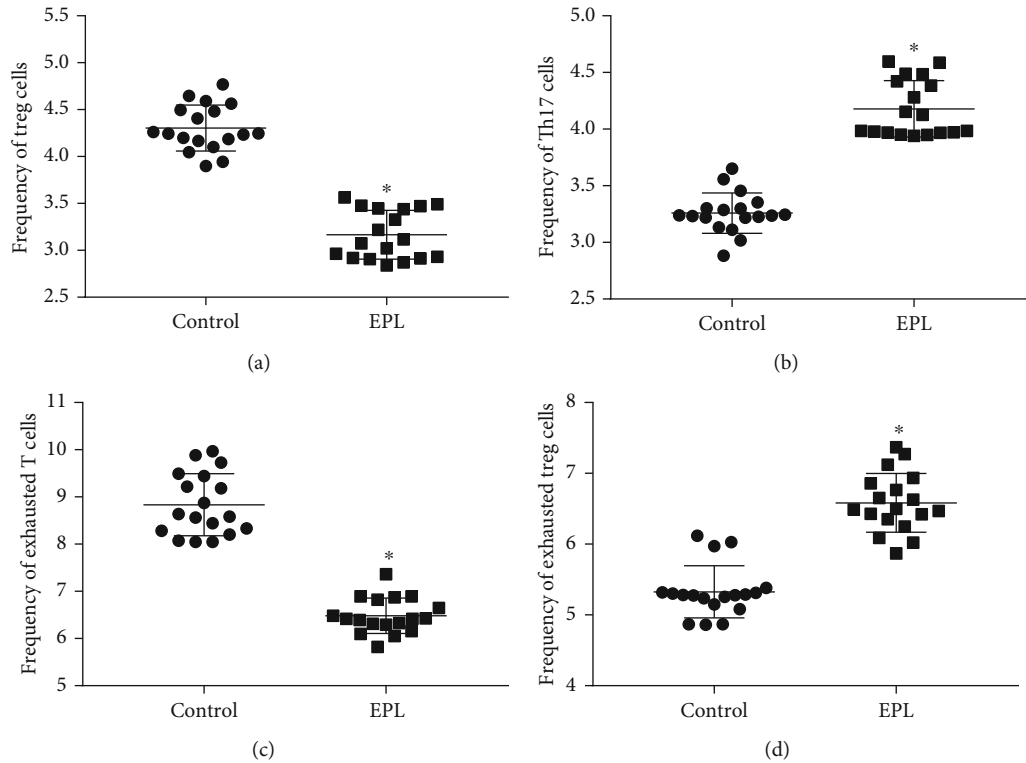
FIGURE 3: Frequency of T cell subsets in the two groups. (a) Treg cells, (b) Th17 cells, (c) exhausted T cells, and (d) exhausted Treg cells. * indicates P value was less than 0.05.

to suppress inflammation was followed by a decrease in the frequencies of Treg and exhausted T cells, as well as a decrease in mRNA expression of GATA3 and GITR. The negative expression of above factors adversely affect the gestational process and may lead to miscarriages. Thus, immunological parameters and their associated epigenetic factors, such as the frequency of Th17 and exhausted Treg cells and expression of T cell-associated factors, may be used as prognostic biomarkers to prevent immune miscarriage in women at high risk.

In conclusion, during pregnancy, regulatory and inhibitory mechanisms control the immune system, possibly via miRNAs. Dysregulation of the immune system may lead to rejection of the embryo and EPL. In this study, we compared T cell-related markers in peripheral blood of patients with recurrent EPL and women with normal pregnancies. The results showed that the expression of T-bet and IRF4 was significantly upregulated, whereas the expression of GATA3 and GITR was significantly downregulated. Among the T cell subpopulation of Treg cell-associated miRNAs, in the EPL group, the expression of miR-106b, miR-93, and miR-25 was upregulated, whereas the expression of miR-146a and miR-155 was downregulated. Compared with the control group, the frequencies of Treg and exhausted T cells were decreased, whereas those of Th17 and exhausted Treg cells were increased in the EPL group. There were significant differences in the expression and frequency of T cell subsets and their related miRNAs in the two groups. Therefore,

immune cells and their associated miRNA can be used as prognostic biomarkers for the treatment of human reproductive disorders in clinical studies.

Data Availability

The data of this manuscript are available from the corresponding author upon request.

Conflicts of Interest

The authors declare no conflict of interest.

Acknowledgments

References

[1] L. Li, J. Liu, S. Qin, and R. Li, "The association of polymorphisms in promoter region of MMP2 and MMP9 with recurrent spontaneous abortion risk in Chinese population," *Medicine*, vol. 97, no. 40, article e12561, 2018.

[2] E. D. Na, I. Jung, D. H. Choi et al., "The risk factors of miscarriage and obstetrical outcomes of intrauterine normal pregnancy following heterotopic pregnancy management," *Medicine*, vol. 97, no. 37, article e12233, 2018.

[3] S. Quenby, I. D. Gallos, R. K. Dhillon-Smith et al., "Miscarriage matters: the epidemiological, physical, psychological, and

economic costs of early pregnancy loss," *Lancet (London, England)*, vol. 397, no. 10285, pp. 1658–1667, 2021.

[4] D. J. Kim, S. K. Lee, J. Y. Kim et al., "Intravenous immunoglobulin G modulates peripheral blood Th17 and Foxp3(+) regulatory T cells in pregnant women with recurrent pregnancy loss," *American journal of reproductive immunology (New York, NY: 1989)*, vol. 71, no. 5, pp. 441–450, 2014.

[5] M. Xie, Y. Li, Y. Z. Meng et al., "Uterine natural killer cells: a rising star in human pregnancy regulation," *Frontiers in Immunology*, vol. 13, article 918550, 2022.

[6] I. Zidi-Jrah, A. Hajlaoui, S. Mougou-Zerelli et al., "Relationship between sperm aneuploidy, sperm DNA integrity, chromatin packaging, traditional semen parameters, and recurrent pregnancy loss," *Fertility and Sterility*, vol. 105, no. 1, pp. 58–64, 2016.

[7] K. J. Sapra, K. S. Joseph, S. Galea, L. M. Bates, G. M. Louis, and C. V. Ananth, "Signs and symptoms of early pregnancy loss," *Reproductive sciences (Thousand Oaks, Calif)*, vol. 24, no. 4, pp. 502–513, 2017.

[8] K. P. Muyayalo, Z. H. Li, G. Mor, and A. H. Liao, "Modulatory effect of intravenous immunoglobulin on Th17/Treg cell balance in women with unexplained recurrent spontaneous abortion," *American journal of reproductive immunology (New York, NY: 1989)*, vol. 80, no. 4, article e13018, 2018.

[9] K. A. Hadfield, S. A. McCracken, A. W. Ashton, T. G. Nguyen, and J. M. Morris, "Regulated suppression of NF-κB throughout pregnancy maintains a favourable cytokine environment necessary for pregnancy success," *Journal of Reproductive Immunology*, vol. 89, no. 1, pp. 1–9, 2011.

[10] S. A. McCracken, K. Hadfield, Z. Rahimi, E. D. Gallery, and J. M. Morris, "NF-κB-regulated suppression of T-bet in T cells represses Th1 immune responses in pregnancy," *European Journal of Immunology*, vol. 37, no. 5, pp. 1386–1396, 2007.

[11] W. Qin, Y. Tang, N. Yang, X. Wei, and J. Wu, "Potential role of circulating microRNAs as a biomarker for unexplained recurrent spontaneous abortion," *Fertility And Sterility*, vol. 105, no. 5, pp. 1247–1254, 2016.

[12] S. Cui, J. Zhang, J. Li et al., "Circulating microRNAs from serum exosomes as potential biomarkers in patients with spontaneous abortion," *American Journal of Translational Research*, vol. 13, no. 5, pp. 4197–4210, 2021.

[13] H. N. Liu, X. M. Tang, X. Q. Wang et al., "MiR-93 inhibits trophoblast cell proliferation and promotes cell apoptosis by targeting BCL2L2 in recurrent spontaneous abortion," *Reproductive sciences (Thousand Oaks, Calif)*, vol. 27, no. 1, pp. 152–162, 2020.

[14] Q. Zhang, P. Tian, and H. Xu, "MicroRNA-155-5p regulates survival of human decidua stromal cells through NF-κB in recurrent miscarriage," *Reproductive Biology*, vol. 21, no. 3, article 100510, 2021.

[15] American College of Obstetricians and Gynecologists, "The American College of Obstetricians and Gynecologists practice bulletin no. 150. Early pregnancy loss," *Obstetrics & Gynecology*, vol. 125, no. 5, pp. 1258–1267, 2015.

[16] S. Abdolmohammadi Vahid, M. Ghaebi, M. Ahmadi et al., "Altered T-cell subpopulations in recurrent pregnancy loss patients with cellular immune abnormalities," *Journal of Cellular Physiology*, vol. 234, no. 4, pp. 4924–4933, 2019.

[17] M. Ahmadi, S. Abdolmohammadi-Vahid, M. Ghaebi et al., "Effect of intravenous immunoglobulin on Th1 and Th2 lymphocytes and improvement of pregnancy outcome in recurrent pregnancy loss (RPL)," *Biomedicine & Pharmacotherapy = Biomedecine & Pharmacotherapie*, vol. 92, pp. 1095–1102, 2017.

[18] M. Ahmadi, S. Abdolmohammadi-Vahid, M. Ghaebi et al., "Regulatory T cells improve pregnancy rate in RIF patients after additional IVIG treatment," *Systems Biology in Reproductive Medicine*, vol. 63, no. 6, pp. 350–359, 2017.

[19] M. Vega-Cárdenas, E. E. Uresti-Rivera, J. D. Cortés-García et al., "Increased levels of adipose tissue-resident Th17 cells in obesity associated with miR-326," *Immunology Letters*, vol. 211, pp. 60–67, 2019.

[20] I. Nowak, A. Bylińska, K. Wilczyńska et al., "The methylenetetrahydrofolate reductase c.c.677 C>T and c.c.1298 A>C polymorphisms in reproductive failures: experience from an RSA and RIF study on a Polish population," *PLoS One*, vol. 12, no. 10, article e0186022, 2017.

[21] L. P. Jin, Q. Y. Chen, T. Zhang, P. F. Guo, and D. J. Li, "The CD4+CD25 bright regulatory T cells and CTLA-4 expression in peripheral and decidual lymphocytes are down-regulated in human miscarriage," *Clinical Immunology*, vol. 133, no. 3, pp. 402–410, 2009.

[22] E. E. Winger and J. L. Reed, "Low circulating CD4(+) CD25(+) Foxp3(+) T regulatory cell levels predict miscarriage risk in newly pregnant women with a history of failure," *American journal of reproductive immunology (New York, NY: 1989)*, vol. 66, no. 4, pp. 320–328, 2011.

[23] W. J. Wang, C. F. Hao, L. Yi et al., "Increased prevalence of T helper 17 (Th17) cells in peripheral blood and decidua in unexplained recurrent spontaneous abortion patients," *Journal of Reproductive Immunology*, vol. 84, no. 2, pp. 164–170, 2010.

[24] S. K. Lee, J. Y. Kim, S. E. Hur et al., "An imbalance in interleukin-17-producing T and Foxp3+ regulatory T cells in women with idiopathic recurrent pregnancy loss," *Human Reproduction (Oxford, England)*, vol. 26, no. 11, pp. 2964–2971, 2011.

[25] R. Yao, Y. L. Ma, W. Liang et al., "MicroRNA-155 modulates Treg and Th17 cells differentiation and Th17 cell function by targeting SOCS1," *PLoS One*, vol. 7, no. 10, article e46082, 2012.

[26] L. F. Lu, M. P. Boldin, A. Chaudhry et al., "Function of miR-146a in controlling Treg cell-mediated regulation of Th1 responses," *Cell*, vol. 142, no. 6, pp. 914–929, 2010.

[27] S. Khorrami, A. Zavaran Hosseini, S. J. Mowla, M. Soleimani, N. Rakhshani, and R. Malekzadeh, "MicroRNA-146a induces immune suppression and drug-resistant colorectal cancer cells," *Tumour biology: the journal of the International Society for Oncodevelopmental Biology and Medicine*, vol. 39, no. 5, p. 1010428317698365, 2017.

[28] A. E. Kedzierska, D. Lorek, A. Slawek, T. Grabowski, and A. Chelmonska-Soyta, "CD91 derived treg epitope modulates regulatory T lymphocyte response, regulates expression of costimulatory molecules on antigen-presenting cells, and rescues pregnancy in mouse pregnancy loss model," *International journal of molecular sciences*, vol. 22, no. 14, p. 7296, 2021.

[29] Z. Zhang, S. Long, Z. Huang, J. Tan, Q. Wu, and O. Huang, "Regulatory effect of daphnetin on the balance of Th17 and Treg cells in the peripheral blood mononuclear cells from patients with unexplained recurrent pregnancy loss," *Central-European Journal Of Immunology*, vol. 45, no. 4, pp. 403–408, 2020.

[30] N. Arpaia, C. Campbell, X. Fan et al., "Metabolites produced by commensal bacteria promote peripheral regulatory T-cell generation," *Nature*, vol. 504, no. 7480, pp. 451–455, 2013.

[31] F. Petrocca, A. Vecchione, and C. M. Croce, "Emerging role of miR-106b-25/miR-17-92 clusters in the control of transforming growth factor beta signaling," *Cancer Research*, vol. 68, no. 20, pp. 8191–8194, 2008.

[32] M. C. Fantini, C. Becker, G. Monteleone, F. Pallone, P. R. Galle, and M. F. Neurath, "Cutting edge: TGF-beta induces a regulatory phenotype in CD4+CD25- T cells through Foxp3 induction and down-regulation of Smad7," *Journal of immunology (Baltimore, Md: 1950)*, vol. 172, no. 9, pp. 5149–5153, 2004.

[33] G. De Santis, M. Ferracin, A. Biondani et al., "Altered miRNA expression in T regulatory cells in course of multiple sclerosis," *Journal of Neuroimmunology*, vol. 226, no. 1-2, pp. 165–171, 2010.

Research Article

Jellyfish Collagen Hydrolysate Alleviates Inflammation and Oxidative Stress and Improves Gut Microbe Composition in High-Fat Diet-Fed Mice

Zhe Lv,[1] Chongyang Zhang [1] ,[1] Wei Song,[2,3] Qingsong Chen,[1] and Yaohui Wang[1]

[1]*Department of Emergency, The First Hospital of Qinhuangdao, Qinhuangdao, China 066000*
[2]*Ministry of Natural Resources (MNR) Key Laboratory of Marine Eco-Environmental Science and Technology, First Institute of Oceanography, Ministry of Natural Resources, Qingdao, China 266061*
[3]*Laboratory of Marine Ecology and Environmental Science, Qingdao National Laboratory for Marine Science and Technology, Qingdao, China 266235*

Correspondence should be addressed to Chongyang Zhang; zhangcy_qhd@163.com

Received 5 June 2022; Revised 17 July 2022; Accepted 22 July 2022; Published 8 August 2022

Academic Editor: Hongmei Jiang

The collagen from jellyfish has many beneficial effects, including antioxidant, anti-inflammatory and immune-modulatory activities. However, whether jellyfish collagen hydrolysate (JCH) has any effects on high-fat diet-induced obesity remains unknown. Consequently, we in the present study orally administrated JCH in high-fat diet-fed mice to explore its effects on body weight gain, inflammatory and oxidative status, and cecum microbe composition. The results showed that oral administration of JCH prevented the body weight gain in high-fat diet-treated mice. Meanwhile, glucose, triglycerides, and total cholesterol level in serum were maintained by JCH administration. Furthermore, JCH administration alleviated oxidative stress by increasing the GSH content and decreasing the level reactive oxygen species in the liver and improved inflammatory response by decreasing the expression of TNF-α, IL-1β, and IL-8 gene in the liver and ileum. Importantly, JCH administration helps recover the alteration of microbiota composition induced by high-fat diet, and the genus *Romboutsia* may critically involve in the beneficial effects of JCH administration. In conclusion, our results indicated that JCH could be potentially used for the prevention and treatment of diet-induced obesity.

1. Introduction

Obesity has become a worldwide problem for decades, and its prevalence causes growing threat to public health. Obese individuals are accompanied by high incidence of chronic diseases, including metabolic syndrome and cancers. Many popular therapies for the treatment of obesity including diet pills are found to have side effects when they are taken for a long period [1]. Consequently, there is an urgent need to explore safe and side-effect free methods for preventing the development of obesity.

Natural agents which have health-promoting effects are promising antiobesity substances and arouse increasing attention in recent years. The jellyfish had been used as a tasty food from ancient China. Recently, the nutritional value of jellyfish has been recognized which makes it popular in other countries. The jellyfish is rich in collagenous protein with no crude fat [2]. The collagen from jellyfish has been proved to exert many beneficial effects, including antioxidant, anti-inflammatory, and immune-modulatory activities and lipid-lowering effect [3–6]. Since obesity is always accompanied by overaccumulation of reactive oxygen species (ROS) and overproduction of inflammatory cytokines [7], these effects of jellyfish collagen suggested that it could be potentially used for preventing and treating obesity. However, there is no report related to the beneficial role of jellyfish collagen on high-fat diet-induced obesity until now.

Dietary fat intake has been proved to the major factor which induces obesity. High-fat diet-induced obesity in rodents has been long used as an appropriate model for

the study of dietary obesity [8]. Consequently, we explored the effects of jellyfish collagen hydrolysate on high-fat-induced body weight gain in mice. Meanwhile, the effects of jellyfish collagen hydrolysate on inflammatory and oxidative status in high-fat diet-fed mice were also explored. Finally, whether jellyfish collagen hydrolysate administration could alter gut microbe composition was studied.

2. Materials and Methods

2.1. Preparation of Jellyfish Collagen Hydrolysate (JCH). Jellyfish (*Nemopilema nomurai*) was washed with distilled water and treated with 0.1 mol/L sodium hydroxide at 4°C for 48 h to remove noncollagenous proteins as previously described [2]. The insoluble fraction was resuspended in sodium phosphate buffer and hydrolyzed with 2% protamex at 50°C for 8 h. The resulting solution was heated at 100°C for 12 min and then centrifuged at 8000 g at 4°C for 8 min. Finally, the supernatant were freeze-dried and stored at -20°C for use.

2.2. Animal Experiment. Male C57BL/6J mice (7 weeks old) were provided by the SLAC Laboratory Animal Central (Shanghai, China). All animals were randomly divided into three groups: mice fed on a low-fat (10 kcal% fat) diet were designated as the control group (Control, $n = 8$), mice fed on a high-fat (45 kcal% fat) diet were designated as the high-fat group (Highfat, $n = 8$), and mice fed on a high-fat diet and orally gavaged with JCH (50 mg/kg body weight once a day) were designated as the JCH administration group (Jellyco, $n = 8$). All diets were provided by Research Diets (Guangzhou, China). The experiment lasted 2 months, and all animals had free access to feed and water. During the treatment, body weight was recorded, and body weight gain was calculated. The experimental protocol was approved by the Protocol Management and Review Committee of the First Institute of Oceanography of China.

2.3. Sample Collection. At the end of the experiment, blood sample was collected from the retroorbital sinus and then centrifuged at 3000 g for 12 min to obtain serum. Liver and ileum tissues were immediately snap-frozen in liquid nitrogen for further analysis. Cecum content were collected and stored at -80°C for the analysis of microbiota composition.

2.4. Determination of Serum Biochemical Indicators and Inflammatory Cytokines. The concentration of serum glucose, triglycerides (TG), total cholesterol (TC), and glutathione (GSH), as well as inflammatory cytokines (TNF-α, IL-1β, and IL-8), was determined by using commercial kits (BYabscience).

2.5. RT-qPCR Analysis. Total RNA was extracted from liver and ileum tissues by using the TRIzol Reagents (Invitrogen) and then was reverse-transcribed into cDNA by using the RevertAid RT Kit (Thermo Scientific). Primers used for RT-qPCR were as follows: TNF-α, forward 5′-CCCACG TCGTAGCAAACCAC-3′, reverse 5′-GCAGCCTTGTC

CCTTGAAGA-3′; IL-1β, forward 5′-TGCCACCTTTT GACAGTGATG-3′, reverse 5′-AAGGTCCACGGGAAAG ACAC-3′; IL-8, forward 5′-TGCATGGACAGTCATCCAC C-3′, reverse 5′-ATGACAGACCACAGAACGGC-3′. Then, qPCR was performed with a total volume of 10 μL assay solution containing 1 μL cDNA, 0.4 μL forward primer, 0.4 μL reverse primer, 3 μL deionized water, 0.2 μL ROX, and 5 μL SYBR Green Mix (Applied Biosystems) as previously described [9].

2.6. Determination of GSH Content and GPX Activity in the Liver and Ileum. The concentration of GSH and GSSG, as well as the activity of GPX in the liver and ileum tissue, was measured by using commercial kits (BYabscience).

2.7. Determination of ROS Level in the Liver. The level of ROS in the liver was determined as previously described [10]. Briefly, fresh liver tissue was embedded in a freezing medium (Sakura) and snap-frozen in methylbutane solution (Sigma) at -80°C. Then, 10 μm sections were stained with dihydroethidium (Sigma-Aldrich) for 25 min at 37°C. Representative pictures were collected under a fluorescence microscopy (Leica). Relative abundance of ROS fluorescence was determined using Image Browser software (Leica).

2.8. Gut Microbe Profiling. DNA from cecum samples was extracted, and the bacterial 16S rDNA gene (V3 + V4 regions) was amplified with specific primers (forward, 5′-ACGGRAGGCWGCAGT-3′; reverse, 5′-TACCAGGGTAT CTAATCCT-3′) by performing PCR reactions. The PCR products were purified, and sequencing libraries were generated and analyzed as previously described [11]. Operational taxonomic units were used to analyze with the RDP classifier algorithm. QIIME was performed for the analysis of α- and β-diversity and principal coordinate analysis.

2.9. Statistical Analysis. All data were analyzed using a one-way ANOVA followed by Student-Newman-Keuls post hoc tests using SPSS 19.0. All data were expressed as means ± SEM, and the results were determined to be significant at $P < 0.05$.

3. Results

3.1. Jellyfish Collagen Hydrolysate Decreased Body Weight Gain and Improved Serum Biochemical Indicators and Inflammatory Cytokine Concentration in High-Fat Diet-Fed Mice. As shown in Figure 1, mice in the Highfat group had significantly higher body weight gain and higher level of glucose, TG, and TC in serum when compared with mice in the Control group, whereas no significant changes in these parameters were observed between mice in the Control and Jellyco group. Mice in the Highfat group had significantly lower GSH content and higher content of IL-1β, TNF-α, and IL-8 in serum when compared with mice in the Control group, whereas no significant changes in the abovementioned parameters were observed between mice in the Control and Jellyco group.
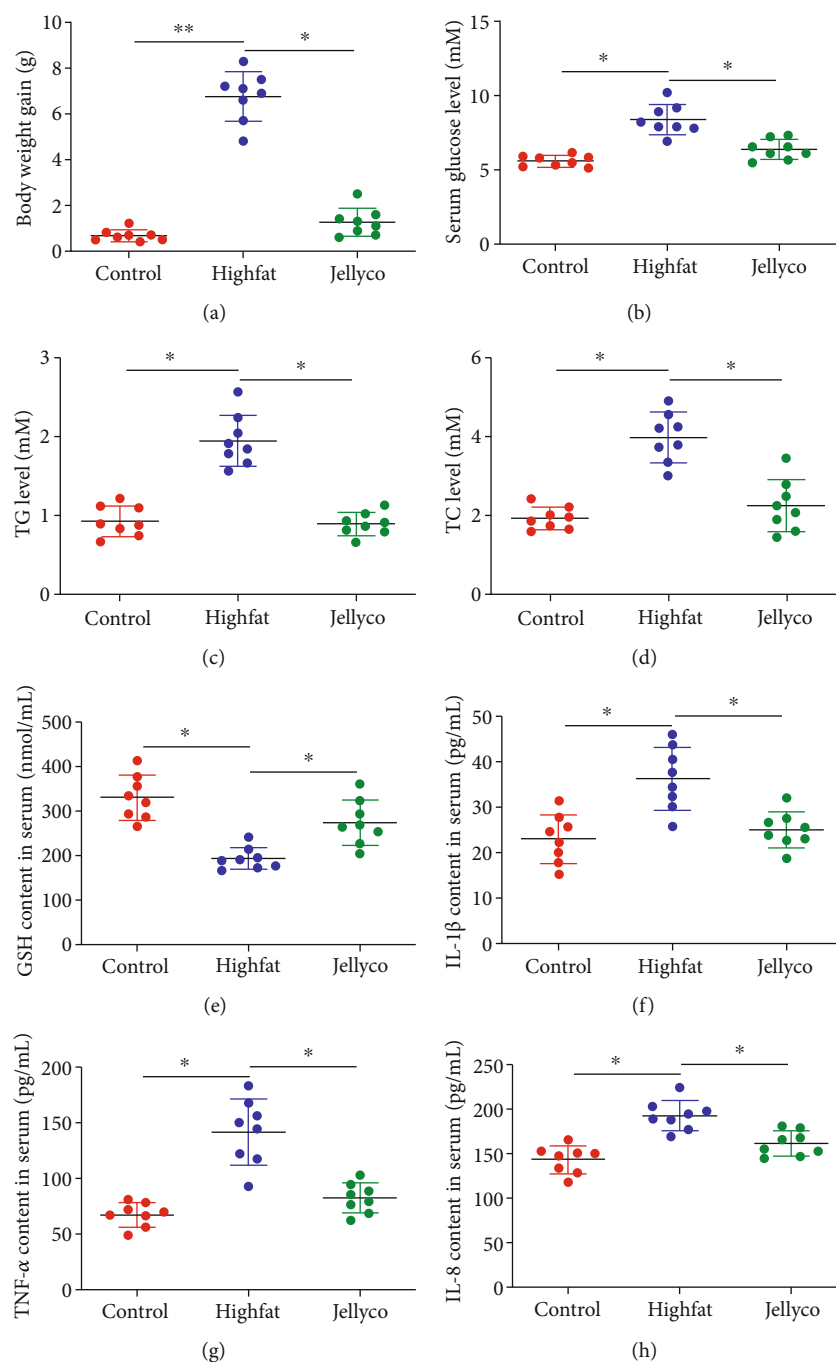
FIGURE 1: Jellyfish collagen hydrolysate decreased body weight gain and improved serum biochemical indicators and inflammatory cytokine concentration in high-fat diet-fed mice: (a) body weight gain, (b) glucose level, (c) TG level, (d) TC level, (e) GSH content, (f) IL-1β content, (g) TNF-α content, and (h) IL-8 content. Data are expressed as means ± SEM, $n = 8$. $^{*}P < 0.05$, $^{**}P < 0.01$.

3.2. Jellyfish Collagen Hydrolysate Alleviated Inflammation and Oxidative Stress in Liver of High-Fat Diet-Fed Mice. As shown in Figure 2, the hepatic gene expression of IL-1β, TNF-α, and IL-8 were significantly increased in mice in the Highfat group than those in the Control group, whereas their expression was significantly decreased in mice in the Jellyco group than those in the Highfat group. Meanwhile, GSH content, the ratio of GSH to GSSG, and GPX activity were significantly decreased in mice in the Highfat group than those in the Control group, whereas these parameters were significantly increased in mice in the Jellyco group than those in the Highfat group.

3.3. Jellyfish Collagen Hydrolysate Prevented Hepatic ROS Accumulation in High-Fat Diet-Fed Mice. As shown in Figure 3, high-fat-diet resulted in the overaccumulation of

(a)

(b)

(c)

(d)

(e)

(f)
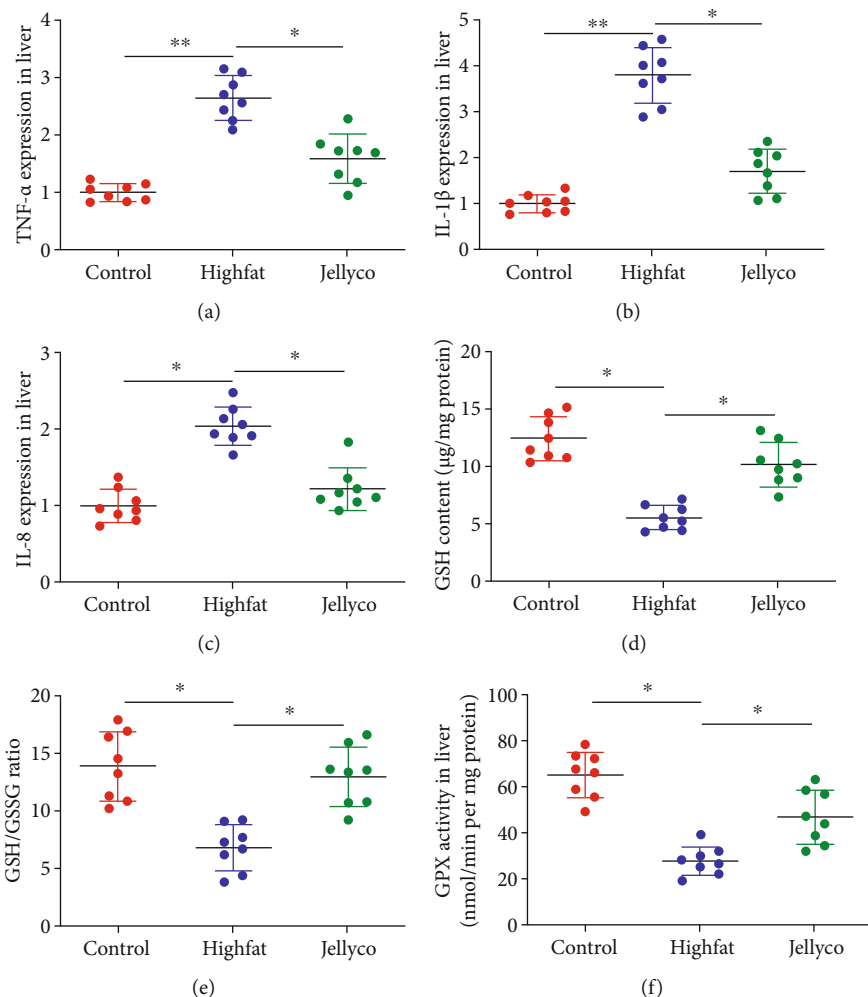
FIGURE 2: Jellyfish collagen hydrolysate alleviated inflammation and oxidative stress in liver of high-fat diet-fed mice. Gene expression of TNF-α (a), IL-1β (b), and IL-8 (c), (d) GSH content, (e) GSH/GSSG ratio, and (f) GPX activity. Data are expressed as means ± SEM, n = 8. $^*P < 0.05$, $^{**}P < 0.01$.
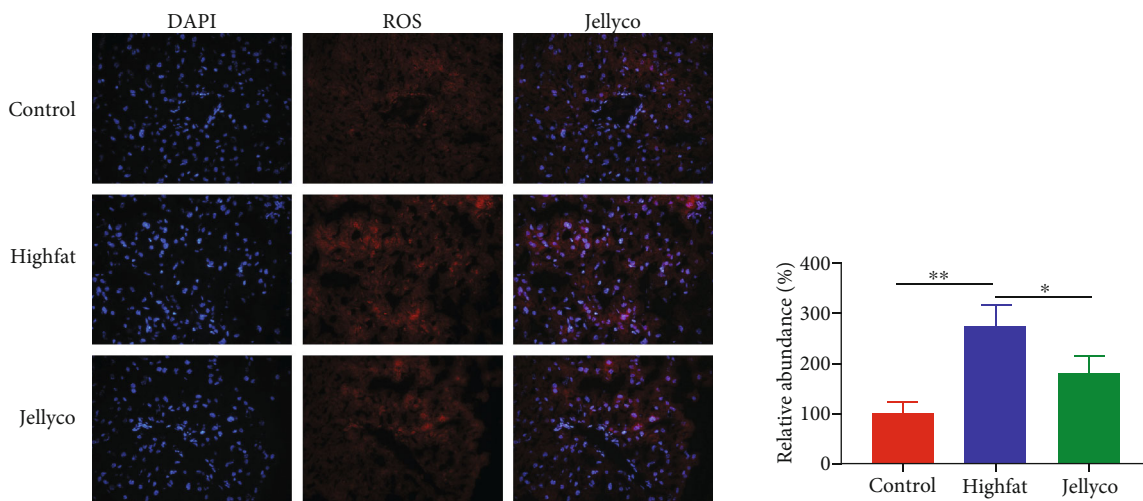
FIGURE 3: Jellyfish collagen hydrolysate prevented hepatic ROS accumulation in high-fat diet-fed mice. Data are expressed as means ± SEM, $n = 3$. $^*P < 0.05$, $^{**}P < 0.01$.
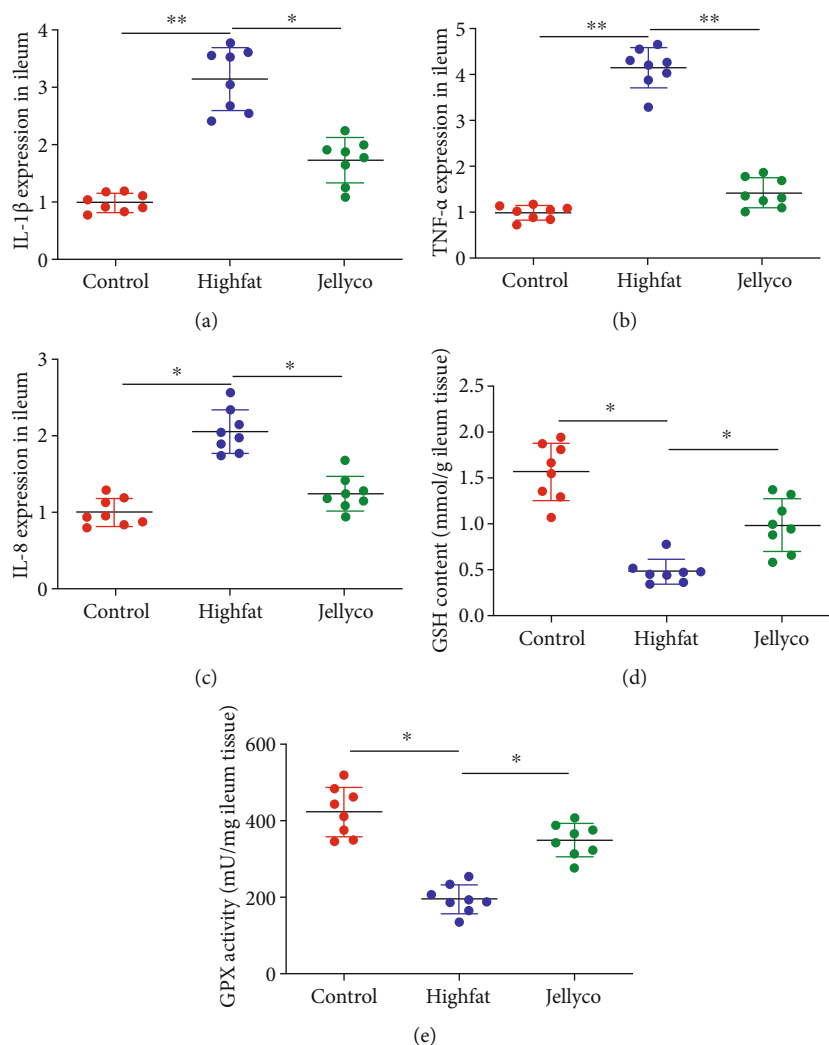
FIGURE 4: Jellyfish collagen hydrolysate alleviated inflammation and oxidative stress in ileum of high-fat diet-fed mice. Gene expression of IL-1β (a), TNF-α (b), and IL-8 (c), (d) GSH content, and (e) GPX activity. Data are expressed as means ± SEM, $n = 8$. $^{*}P < 0.05$, $^{**}P < 0.01$.

ROS in the liver of mice, whereas jellyfish collagen hydrolysate administration significantly decreased hepatic ROS content in mice.

3.4. Jellyfish Collagen Hydrolysate Alleviated Inflammation and Oxidative Stress in Ileum of High-Fat Diet-Fed Mice. As shown in Figure 4, the gene expression of IL-1β, TNF-α, and IL-8 in ileum was significantly increased in mice in the Highfat group than those in the Control group, whereas their expression was significantly decreased in mice in the Jellyco group than those in the Highfat group. GSH content and GPX activity were significantly decreased in mice in the Highfat group than those in the Control group, whereas these parameters were significantly increased in mice in the Jellyco group than those in the Highfat group.

3.5. Jellyfish Collagen Hydrolysate Altered Cecum Microbe Profiling in High-Fat Diet-Fed Mice. No significant difference was observed in α-diversity as indicated by observed species (Figure 5(a)) and Shannon index (Figure 5(b))

among the three treatment groups. The β-diversity as indicated by PCoA based on unweighted UniFrac distance indicated that the overall microbial structure in mice in the Highfat group was clearly separated away from those in mice in the Control and Jellyco group, whereas the microbial structure in mice in the Control group was not separated away from that in mice in the Jellyco group (Figure 5(c)).

Enterobacteriaceae, Clostridiales, Fusobacteriaceae, and Peptostreptococcaceae were the main microbes at the family level (Figure 6(a)). Mice in the Highfat group had lower Clostridiales abundance and higher Fusobacteriaceae abundance when compared with those in the Control and Jellyco groups, whereas microbe abundance in the family level in mice in the Control group was similar to those in mice in the Jellyco group. *Fusobacterium, Romboutsia, Clostridiales, Plesiomonas,* and *Epulopiscium* were the main microbes in the genus level (Figure 6(b)). Notably, the relative abundance of *Romboutsia* was significantly lower in mice in the Highfat group than those in the Control and Jellyco groups (Figure 6(c)).

(a)

(b)

(c)
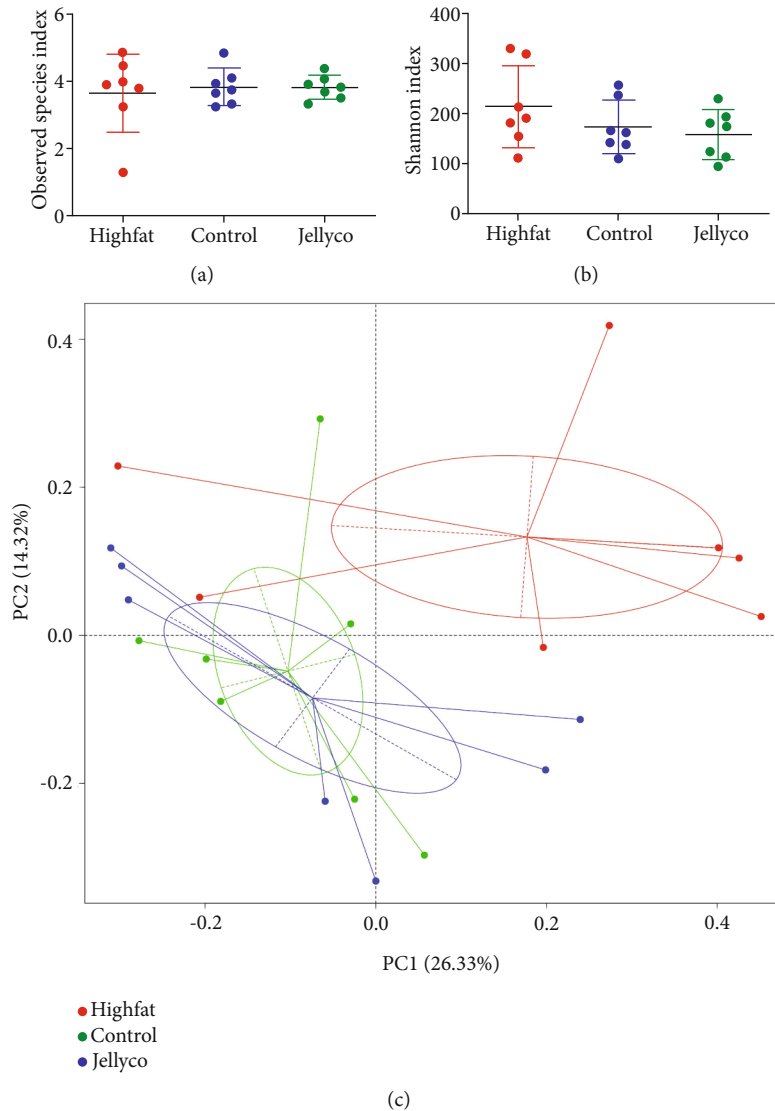
Figure 5: Effects of jellyfish collagen hydrolysate on α- and β-diversity in cecal microbiota in high-fat diet-fed mice: (a) observed species index, (b) Shannon index, and (c) PCoA analysis based on unweighted UniFrac distance. Data are expressed as means $\pm$ SEM, $n = 7$.

4. Discussion

With great biocompatibility and penetrability, collagen and its peptides could be used as bioactive substances. Aquatic animals including jellyfish are excellent source of collagen [12]. Jellyfish collagen was proved to be harmless and exerts widely biological effects on human cells [3]. In the present study, we found that oral administration of JCH prevented the body weight gain in high-fat diet-treated mice. Meanwhile, glucose, TG, and TC level in serum were maintained by JCH administration. Furthermore, JCH administration alleviated oxidative stress and inflammatory response which are often accompanied with obesity. Notably, JCH administration helps recover the alteration of microbiota composition induced by high-fat diet.

Jellyfish is enriched in collagenous protein, which has abundant hydrophobic amino acids. These amino acids have better emulsifying ability and possess strong antioxidant ability [6, 13]. Therefore, JCH was supposed to have higher

antioxidant ability than other protein sources. The antioxidant effects of JCH have been studied both *in vitro* and in *vivo*. Jellyfish collagen peptide, as well as crude protein and protein fractions, showed strong hydroxyl radical- and superoxide anion-scavenging activities *in vitro* [14, 15]. The *in vivo* antioxidant effects of JCH were proved as serum GPX activity, and hepatic SOD activity was increased in aging mice after administration with JCH [2]. In the present study, we found that GSH content, which is the most vital intracellular antioxidant, was significantly increased both in the liver and ileum when the high-fat diet-treated mice were administrated with JCH. Moreover, ROS level in the liver was decreased after JCH administration. These results broaden our knowledge on the antioxidant effects of JCH in different experimental models.

Jellyfish collagen can activate innate and acquired immune response. Specifically, jellyfish collagen enhanced inflammatory cytokine secretion through activating TLR4 and NF-κB signaling pathways [4]. Importantly, collagenase

(a)

(b)

(c)
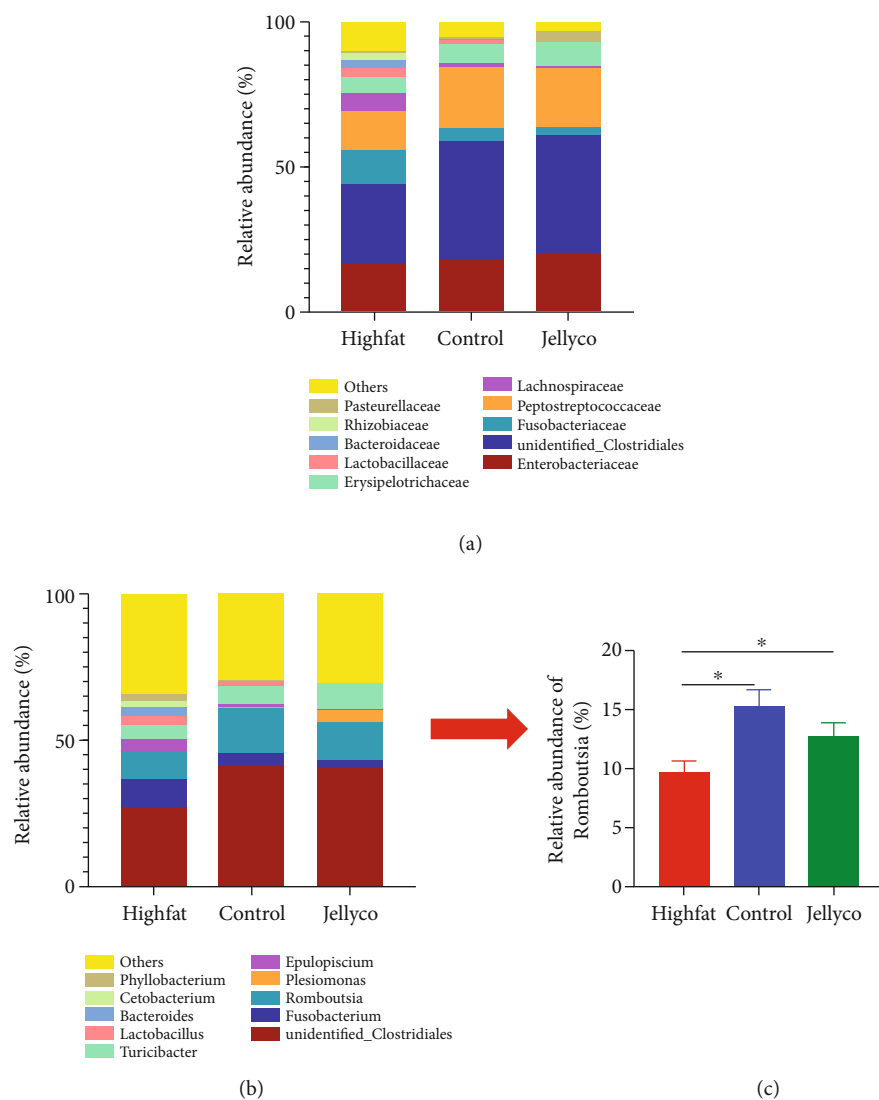
FIGURE 6: Effects of jellyfish collagen hydrolysate on relative abundance of the cecum microbial species in high-fat diet-fed mice. (a)Relative abundance of bacteria classified at a family-level taxonomy. (b) Relative abundance of bacteria classified at a genus-level taxonomy. (c) Relative abundance of *Romboutsia*. Data are expressed as means ± SEM, $n = 7$. *$P < 0.05$.

inhibited the immune-stimulation effects of the extract from jellyfish on human cells, which indicated that collagen is the active substance [16]. However, an *in vivo* study showed that both JC and JCH improved immunity in mice [17]. We further found that JCH administration decreased inflammatory cytokine contents in serum and their expression in both liver and ileum in high-fat diet-induced mice. These results confirmed that JCH had strong anti-inflammation effects; although, the related mechanism needs to be further elucidated.

The intestinal microbiota modulate host energy homeostasis and can be alter by dietary structure such as high-fat diet. Consumption of high-fat diet often led to decreased Bacteroidetes abundance and increased Firmicutes abundance [18]. Additionally, the intestinal microbe diversity was usually decreased in high-fat diet-fed mice [19]. JCH-administrated mice and control mice had the similar microbiota composition which was different from these of high-fat diet-fed mice. As we

known, this is the first study indicating the beneficial effects of JCH on the modulation of gut microbes. Notably, the abundance of *Romboutsia* was decreased by high-fat diet treatment which is in line with previous study [20], whereas its abundance was recovered by JCH administration. The genus *Romboutsia* maintains health of the host and exerts many metabolic capabilities including carbohydrate utilization, metabolic end products, and fermentation of single amino acids [21]. These results suggested that the genus *Romboutsia* may be the major target of JCH. However, how the microbes were involved in the modulation effects of JCH and whether *Romboutsia* plays critical roles remain to be elucidated in the future works.

In conclusion, our results suggested that JCH administration protected mice from high-fat diet-induced obesity and hyperglycemia and hyperlipidemia. Meanwhile, JCH administration helps maintain oxidative and inflammatory status in the liver and intestine of high-fat diet-fed mice. Importantly, JCH administration retrieved cecum microbe

composition, and the genus *Romboutsia* may critically involve in the beneficial effects of JCH. Our results indicated that JCH could be potentially used for the prevention and treatment of obesity.

Data Availability

The data used to support the findings of this study are available from the corresponding author upon request.

Conflicts of Interest

The authors declare no conflicts of interest.

Acknowledgments

References

[1] G. Derosa and P. Maffioli, "Anti-obesity drugs: a review about their effects and their safety," *Expert Opinion on Drug Safety*, vol. 11, no. 3, pp. 459–471, 2012.

[2] J. Ding, Y. Y. Li, J. J. Xu, X. R. Su, X. Gao, and F. P. Yue, "Study on effect of jellyfish collagen hydrolysate on anti-fatigue and anti- oxidation," *Food Hydrocolloids*, vol. 25, no. 5, pp. 1350–1353, 2011.

[3] S. Addad, J. Y. Exposito, C. Faye, S. Ricard-Blum, and C. Lethias, "Isolation, characterization and biological evaluation of jellyfish collagen for use in biomedical applications," *Marine Drugs*, vol. 9, no. 6, pp. 967–983, 2011.

[4] A. B. Putra, K. Nishi, R. Shiraishi, M. Doi, and T. Sugahara, "Jellyfish collagen stimulates production of TNF-α and IL-6 by J774.1 cells through activation of NF-κB and JNK via TLR4 signaling pathway," *Molecular Immunology*, vol. 58, no. 1, pp. 32–37, 2014.

[5] S. Nishimoto, Y. Goto, H. Morishige et al., "Mode of action of the immunostimulatory effect of collagen from jellyfish," *Bioscience, Biotechnology, and Biochemistry*, vol. 72, no. 11, pp. 2806–2814, 2008.

[6] Y. L. Zhuang, X. Zhao, and B. F. Li, "Optimization of antioxidant activity by response surface methodology in hydrolysates of jellyfish (Rhopilema esculentum) umbrella collagen," *Journal of Zhejiang University. Science. B*, vol. 10, no. 8, pp. 572–579, 2009.

[7] X. Zhou, L. He, S. Zuo et al., "Serine prevented high-fat diet-induced oxidative stress by activating AMPK and epigenetically modulating the expression of glutathione synthesis-related genes," *Biochimica et Biophysica Acta - Molecular Basis of Disease*, vol. 1864, no. 2, pp. 488–498, 2018.

[8] N. Hariri and L. Thibault, "High-fat diet-induced obesity in animal models," *Nutrition Research Reviews*, vol. 23, no. 2, pp. 270–299, 2010.

[9] X. Zhou, Y. Liu, L. Zhang, X. Kong, and F. Li, "Serine-to-glycine ratios in low-protein diets regulate intramuscular fat by affecting lipid metabolism and myofiber type transition in the skeletal muscle of growing-finishing pigs," *Animal Nutrition*, vol. 7, no. 2, pp. 384–392, 2021.

[10] X. Zhou, L. He, C. Wu, Y. Zhang, X. Wu, and Y. Yin, "Serine alleviates oxidative stress via supporting glutathione synthesis and methionine cycle in mice," *Molecular Nutrition & Food Research*, vol. 61, no. 11, 2017.

[11] L. He, X. Zhou, Y. Liu, L. Zhou, and F. Li, "Fecal miR-142a-3p from dextran sulfate sodium-challenge recovered mice prevents colitis by promoting the growth of *Lactobacillus reuteri*," *Molecular Therapy*, vol. 30, no. 1, pp. 388–399, 2022.

[12] E. Song, S. Yeon Kim, T. Chun, H. J. Byun, and Y. M. Lee, "Collagen scaffolds derived from a marine source and their biocompatibility," *Biomaterials*, vol. 27, no. 15, pp. 2951–2961, 2006.

[13] N. Rajapakse, E. Mendis, H. G. Byun, and S. K. Kim, "Purification and in vitro antioxidative effects of giant squid muscle peptides on free radical-mediated oxidative systems," *The Journal of Nutritional Biochemistry*, vol. 16, no. 9, pp. 562–569, 2005.

[14] Y. Zhuang, L. Sun, X. Zhao, J. Wang, H. Hou, and B. Li, "Antioxidant and melanogenesis-inhibitory activities of collagen peptide from jellyfish (Rhopilema esculentum)," *Journal of the Science of Food and Agriculture*, vol. 89, no. 10, pp. 1722–1727, 2009.

[15] H. Yu, X. G. Liu, R. E. Xing et al., "In vitro determination of antioxidant activity of proteins from jellyfish Rhopilema esculentum," *Food Chemistry*, vol. 95, no. 1, pp. 123–130, 2006.

[16] T. Sugahara, M. Ueno, Y. Goto et al., "Immunostimulation effect of jellyfish collagen," *Bioscience, Biotechnology, and Biochemistry*, vol. 70, no. 9, pp. 2131–2137, 2006.

[17] J. Fan, Y. Zhuang, and B. Li, "Effects of collagen and collagen hydrolysate from jellyfish umbrella on histological and immunity changes of mice photoaging," *Nutrients*, vol. 5, no. 1, pp. 223–233, 2013.

[18] E. A. Murphy, K. T. Velazquez, and K. M. Herbert, "Influence of high-fat diet on gut microbiota: a driving force for chronic disease risk," *Current Opinion in Clinical Nutrition and Metabolic Care*, vol. 18, no. 5, pp. 515–520, 2015.

[19] M. Zhang and X. J. Yang, "Effects of a high fat diet on intestinal microbiota and gastrointestinal diseases," *World Journal of Gastroenterology*, vol. 22, no. 40, pp. 8905–8909, 2016.

[20] Y. Du, D.-x. Li, D.-y. Lu et al., "*Morus alba* L. water extract changes gut microbiota and fecal metabolome in mice induced by high-fat and high-sucrose diet plus low-dose streptozotocin," *Phytotherapy Research*, vol. 36, no. 3, pp. 1241–1257, 2022.

[21] S. Zhang, G. Zhong, D. Shao et al., "Dietary supplementation with *Bacillus subtilis* promotes growth performance of broilers by altering the dominant microbial community," *Poultry Science*, vol. 100, no. 3, article 100935, 2021.

Research Article

The Gut Microbiota Dysbiosis in Preeclampsia Contributed to Trophoblast Cell Proliferation, Invasion, and Migration via lncRNA BC030099/NF-κB Pathway

Rong Tang,[1] Gong Xiao,[1] Yu Jian,[2] Qiongjing Yuan,[1] Chun Jiang,[2] and Wei Wang [1]

[1]*Department of Nephrology, Xiangya Hospital, Central South University, Changsha, 410078 Hunan, China*
[2]*Department of Obstetrics and Gynecology, Xiangya Hospital, Central South University, Changsha, 410078 Hunan, China*

Correspondence should be addressed to Wei Wang; viviwang66@163.com

Background. Preeclampsia (PE) is the main reason of maternal and perinatal morbidity and mortality. Gut microbiota imbalance in PE patients is accompanied by elevated serum lipopolysaccharide (LPS) levels, but whether it affects the occurrence and development of PE, the underlying mechanism is not clear. This paper intends to investigate the relationship between lncRNA BC030099, inflammation, and gut microbiota in PE. *Methods*. The feces of the patients were collected, and gut microbiota changes were assessed by 16S rRNA sequencing and pathway analysis by PICRUSt. Next, we examined LPS and lncRNA BC030099 levels in feces or placenta of PE patients. Then, we knocked down lncRNA BC030099 in HTR-8/SVneo cells and added the NF-κB pathway inhibitor JSH-23. CCK-8 and Transwell assays were performed to determine cell proliferation, migration, and invasion. Western blot was utilized to evaluate MMP2, MMP9, snail, and E-cadherin, p-IκBα, IκBα, and nuclear NF-κB p65 levels. IL-6, IL-1β, and TNF-α levels were examined by ELISA. *Results*. Gut microbiota was altered in PE patients, and microbial genes associated with LPS biosynthesis were significantly elevated in gut microbiota in the PE group. LPS level in feces and placenta of PE group was significantly elevated. lncRNA BC030099 level in placenta of PE group was also notably promoted. Knockdown of lncRNA BC030099 promoted HTR-8/SVneo cell proliferation, migration, and invasion. Knockdown of lncRNA BC030099 also elevated MMP2, MMP9, and snail levels and repressed E-cadherin level. In addition, lncRNA BC030099 affected NF-κB pathway. Furthermore, NF-κB inhibitor reversed HTR-8/SVneo cell proliferation, invasion, and migration induced by LPS. *Conclusions*. The gut microbiota dysbiosis in PE contributed to HTR-8/SVneo cell proliferation, invasion, and migration via lncRNA BC030099/NF-κB pathway.

1. Introduction

Preeclampsia (PE) is a hypertensive disorder of pregnancy involved in 2% to 8% of pregnancy-related complications worldwide [1]. It is the main reason of maternal and perinatal morbidity and mortality [2]. The etiology and pathogenesis of PE have not been fully clarified. Currently, it is mainly believed to be related to insufficient remodeling of uterine spiral arterioles, excessive activation of inflammatory immunity, and damage to vascular endothelial cells [3]. The clinical treatment measures for PE are limited, focusing on the control of acute hypertension, prevention of PE, and timely delivery, and the only effective treatment

is delivery of the fetus and placenta [4]. Therefore, an indepth understanding of the pathogenesis of PE can provide guidance for clinical prediction and prevention of PE, avoid serious complications in pregnant women, and improve pregnancy outcomes.

Long noncoding RNAs (lncRNAs) are a class of RNA molecules with transcripts > 200 nt, which can regulate target gene expression via epigenetic, transcriptional, and posttranscriptional regulation. It is involved in different biological processes including cell differentiation and proliferation, apoptosis, and necrosis [5, 6]. In addition, abnormal lncRNA expression is associated with disease progress [7]. Therefore, lncRNAs' role in PE pathogenesis has also

attracted much attention. Luo et al. screened lncRNA expression profiles in PE patients' placentas, suggesting abnormal lncRNA expression may be one of the causes of PE [8]. Based on this, Sun et al. detected 5 known uterus-related lncRNAs' expression in 48 PE patients and 24 non-PE healthy subjects and found lncRNA BC030099 expression was significantly facilitated, indicating elevated plasma level of lncRNA BC030099 is related to an accelerated risk of PE and can be used as the potential biomarker to predict the occurrence of PE [9], but whether it is involved in the disease progression of PE and its specific mechanism still need to be further explored.

Gut microbiota is a type of microbial population that inhabits the human gut, with a large number and variety, participating in the metabolism of the human body and maintaining the homeostasis of the human body [10]. Recently, the relationship between gut microbiota changes and pregnancy diseases has received extensive attention. Studies have found that immune tolerance, inflammatory response, abnormal glucose, and lipid metabolism, and oxidative stress caused by gut microbiota imbalance may be involved in PE pathogenesis [11, 12]. The study of gut microbiota provides new targets and ideas for preventing and treating PE. Lipopolysaccharide (LPS), as a product of gut microbiota, can cause inflammation in body and is associated with various disease occurrence and development. Studies have revealed gut microbiota imbalance in PE patients is accompanied by increased serum LPS level [12], but whether it affects the occurrence and development of PE, the underlying mechanism is not clear. Furthermore, accumulative evidence suggests that lncRNAs could affect LPS-induced PE animal or cell models through various signaling pathways. Huang et al. constructed PE rat models induced by LPS and revealed that overexpression of lncRNA Uc.187 could induce PE-like symptoms in a pregnant rat model by affecting the distribution of β-catenin in the cytoplasm and nucleus [13]. Chen et al. used LPS to treat HTR-8/SVneo cells and found that lncRNA KCNQ1OT1 could target the regulation of miR-146a-3p through the CXCL12/CXCR4 pathway in the proliferation, invasion, and migration of HTR-8/SVneo cells [14]. However, the mechanism of lncRNA BC030099 on PE is unclear.

Therefore, based on the above background, this research intends to explore lncRNA BC030099, inflammation, and gut microbiota relationship in PE. Our research may provide new targets for diagnosing and treating PE, as well as new ideas for the study of the pathological mechanism of PE.

2. Materials and Methods

2.1. Collection of Clinical Samples. We collected feces and placental tissue from PE patients in Xiangya Hospital central South University as the PE group ($n = 6$). The healthy subjects during the same period were selected as the control group (C group, $n = 8$). The inclusion criteria of this study were as follows: aged at 25-40 years; gestational weeks from 32 to 39; singleton; no fetal abortion and stillbirth; no history of adverse pregnancy and childbirth; and no history of assisted reproduction; no history of smoking, drinking, and

other drugs. The exclusion criteria were multiple pregnancy; diabetes, chronic hypertension, and kidney disease or other pregnancy complications before pregnancy; antibiotics, glucocorticoids, and immunosuppressants within 1 month before stool collection and other drugs [12]. Fecal samples were collected in stool collection tubes and stored at -80°C until further processing.

2.2. 16S rRNA Sequencing and PICRUSt Pathway Analysis. Fecal samples from healthy subjects ($n = 8$) and PE patients ($n = 6$) were collected to detect changes in microbial diversity. Illumina NovaSeq PE250 was applied for 16S amplicon sequencing to obtain raw data. Sequence data analysis mainly used Qiime 2 (Qiime2-2020.2) and R software (4.0.2). In addition, KEGG pathway analysis was performed by PICRUSt.

2.3. Enzyme Linked Immunosorbent Assay (ELISA). According to LPS (CSB-E09945h, CUSABIO, China), IL-1β (CSB-E08053h, CUSABIO, China), TNF-α (CSB-E04740h, CUSA-BIO, China), and IL-6 (CSB-E04638h, CUSABIO, China) ELISA instructions, we detected LPS level in feces and placental tissues and IL-6, IL-1β, and TNF-α levels in cells. 20 mg of feces and placental tissue was taken, respectively, and the blood stains were washed with $1 \times$ PBS. Feces and placental tissue were cut into small pieces and put into tissue grinder (homogenate tube), 200 μL $1 \times$ PBS was added to make homogenate, then put in -20°C overnight. After repeated freeze-thaw treatment two times to destroy the cell membrane, the tissue homogenate was centrifuged at 5000 g (2-8°C) for 5 min to take the supernatant, which should be detected. For cells, centrifugation was performed at 1000 g (2-8°C) for 15 min, and the supernatant should be immediately detected.

2.4. Cell Treatment. Human trophoblast cell HTR-8/SVneo was purchased from Tongpai (Shanghai, China) Biotechnology Co., Ltd., and culture conditions were as follows: RPMI-1640 medium and 10% fetal bovine serum (FBS). LPS was applied to induce cellular inflammation [15], and in addition, lncRNA BC030099 was knocked down, which are grouped into the si-control, si-con+LPS, si-BC030099, and si-BC030099+LPS groups. In addition, we added 10 μM NF-κB-specific inhibitor JSH-23 (Merck, Germany) [16], grouped as the control, LPS, JSH-23, and LPS+JSH-23 groups. lncRNA BC030099 expression was knocked down. si-BC030099 and negative control si-control were synthesized by Sangon Biotechnology Co., Ltd. (Shanghai, China).

2.5. Quantitative Real-Time PCR (qRT-PCR). Total RNA was extracted using Trizol method, RNA was reverse transcribed into cDNAs using a cDNA reverse transcription kit (#CW2569, Beijing ComWin Biotech, China), and fluorescence quantification was applied by Ultra SYBR Mixture (#CW2601, Beijing ComWin Biotech, China). The relative expression of genes was examined on an PCR instrument (QuantStudio1, Thermo, USA). Using GAPDH as an internal reference, the $2^{-\Delta\Delta Ct}$ method was performed to calculate lncRNA BC030099 level. The primers were as follows: lncRNA BC030099-F: GCCTCCATCCTTTCAGACCC and

lncRNA BC030099-R: GCCCTTGGAAAGTGTCAGGA; GAPDH-F: ACAGCCTCAAGATCATCAGC and GAPDH-R: GGTCATGAGTCCTTCCACGAT.

2.6. Western Blot. Total protein was extracted from cells by RIPA lysis buffer (P0013B, Beyotime, China), followed by protein quantification, mixed with SDS-PAGE loading buffer, and protein was adsorbed on PVDF membrane by gel electrophoresis. MMP2 (10373-2-AP, 1 : 500, Proteintech, USA), MMP9 (ab76003, 1 : 5000, Abcam, UK), snail (13099-1-AP, 1 : 500, Proteintech, USA), and E-cadherin (20874-1-AP, 1 : 1000, Proteintech, USA), IκBα (ab32518, 1 : 500, Abcam, UK), p-IκBα (ab133462, 1 : 10000, Abcam, UK), and nuclear NF-κB p65 (10745-1-AP, 1 : 1000, Proteintech, USA) primary antibodies and β-actin (66009-1-Ig, 1 : 1000, Proteintech, USA) were incubated overnight at 4°C. HRP secondary antibodies were then incubated. Visualization was performed using ECL luminescent fluid (advansta, K-12045-D50, USA). β-actin was used as an internal reference to examine protein levels.

2.7. Cell Counting Kit-8 (CCK-8) Assay. Cells grouped above were digested and counted and seeded in a 96-well plate (5×10^3 cells/well), with $100 \mu L$ per well. After culturing the adherent cells, we followed the above method for the corresponding time and then added $10 \mu L$/well of CCK-8 to each well. After incubation at 37°C and 5% CO_2 for 4 h, the absorbance (450 nm) was analyzed on the Bio-Tek microplate reader (MB-530, HEAES, China).

2.8. Transwell Assays. 1×10^6/mL cells were resuspended in serum-free medium, $100 \mu L$ cell suspension was added into Transwell chamber (#33318035, Corning, USA) upper, and 10% FBS was added into lower chamber and cultured for 48 h. Chamber culture medium was discarded. Cells on upper ventricle were wiped with the wet cotton swab. 4% paraformaldehyde was fixed. Cells were stained with 0.5% crystal violet and eluted with water. Cells on the outer surface of upper chamber were observed under a microscope (Olympus, Japan) and photographed. Detection of cell invasion was performed using Transwell chamber (3428, Corning, USA) with Matrigel Basement Membrane Matrix (354262, BD Biocoat, USA). The other steps were as described above.

2.9. Statistical Analysis. Statistical analysis was performed using Graphpad Prism8.0 statistical software. Measurement data are expressed as the mean ± standard deviation. An unpaired *t*-test was used between groups, and one-way analysis of variance was used for comparison among multiple groups. The correlation of LPS and lncRNA BC030099 in PE placental tissues was calculated by Spearman's correlation analysis. $P < 0.05$ indicated a statistically significant difference.

3. Results

3.1. Gut Microbiota in PE Patients Was Changed, and Key Pathway Targets (LPS) Were Screened. First, we analyzed changes in gut microbiota by 16S rRNA sequencing and pathway analysis by PICRUSt. Figure 1(a) shows the rank abundance curve. Venn diagram showed shared and unique ASVs between groups (Figure 1(b)). Among them, there were 314 ASVs unique to the control group, 184 ASVs unique to PE patients, and 213 ASVs shared by two groups. Relative abundance histogram of the top20 ASVs at genus level further suggested the abundance and composition of microbial communities in each group were different (Figure 1(c)). As shown in Figure 1(d), the relative abundance of the top 20 dominant gut microbiota at phylum level was shown. Furthermore, KEGG showed that microbial genes related to LPS biosynthesis were significantly elevated in gut microbiota in PE group (Figure 1(e)).

3.2. LPS Was Positively Correlated with lncRNA BC030099. Next, we examined LPS level in feces and placenta of PE patients. LPS level in the feces and placenta of PE group were significantly elevated than control group (Figure 2(a)). Furthermore, we used qRT-PCR to evaluate lncRNA BC030099 level in PE patients' placenta. lncRNA BC030099 level in placenta of the PE group was also strikingly elevated than that of the control group (Figure 2(b)). Spearman's correlation analysis showed there was a significant positive correlation between LPS and lncRNA BC030099 expression in placental tissue (Figure 2(c)).

3.3. Knockdown of lncRNA BC030099 Promoted Trophoblast Cell Proliferation, Invasion, and Migration. Next, we knocked down lncRNA BC030099. We found lncRNA BC030099 expression was repressed in the si-BC030099 group compared with the si-control group. This indicated that we successfully knocked down lncRNA BC030099. Compared with the si-BC030099 group, lncRNA BC030099 expression in the si-BC030099+LPS group was facilitated (Figure 3(a)). Cell function experiments revealed compared with the si-control group; the si-BC030099 group had enhanced cell proliferation, migration, and invasion abilities. However, the si-BC030099+LPS group showed reduced cell proliferation, migration, and invasion than the si-BC030099 group (Figures 3(b)–3(d)). The above results indicated knockdown of lncRNA BC030099 promoted trophoblast cell proliferation, invasion, and migration.

3.4. Knockdown of lncRNA BC030099 Elevated MMP2, MMP9, and Snail Levels and Repressed E-Cadherin Level. In addition, Western blot analysis showed that MMP2, MMP9, and snail expressions were increased in the si-BC030099 group compared with the si-control group. But the si-BC030099+LPS group showed decreased expression of MMP2, MMP9, and snail than the si-BC030099 group. The trend of E-cadherin was opposite to that of snail (Figure 4). Collectively, knockdown of lncRNA BC030099 elevated MMP2, MMP9, and snail levels and repressed E-cadherin level.

3.5. lncRNA BC030099 Affected NF-κB Pathway. Next, we examined NF-κB pathway-related protein expression. Compared with the si-control group, the si-con+LPS group showed a decrease in IκBα expression and an increase in p-IκBα and p65 expressions; IκBα expression in the si-
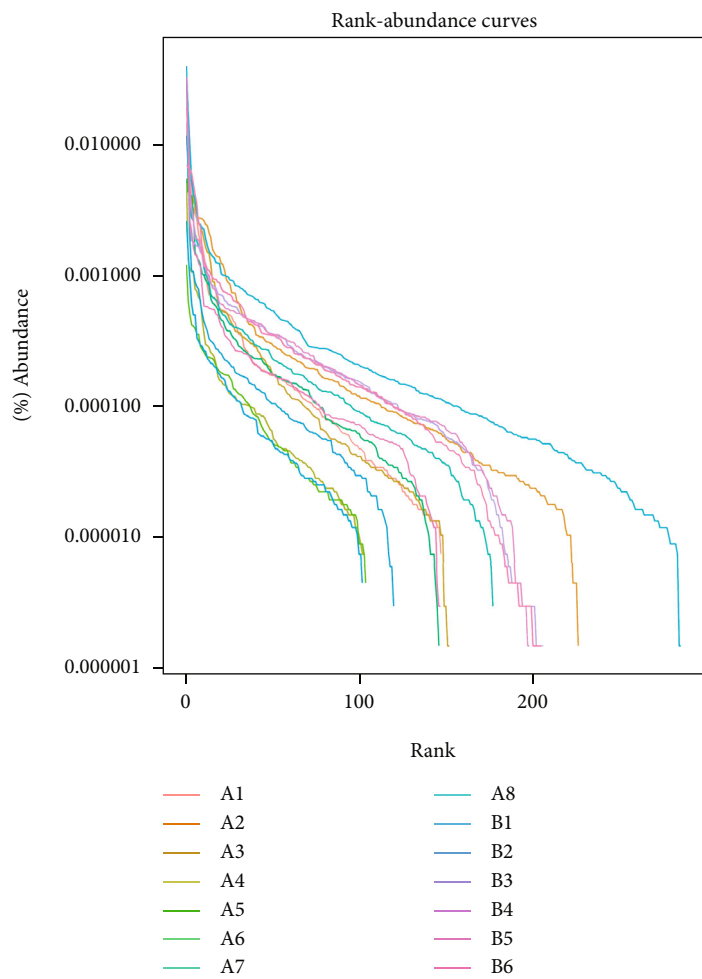
(a)
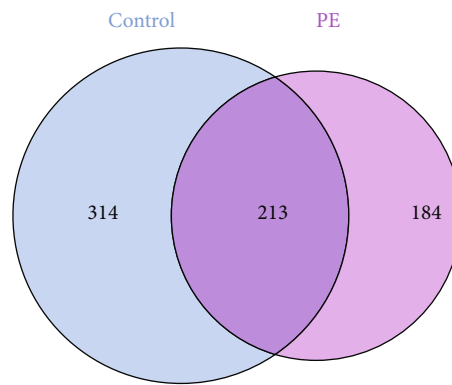
(b)

Figure 1: Continued.

(c)

(d)

Figure 1: Continued.

(e)
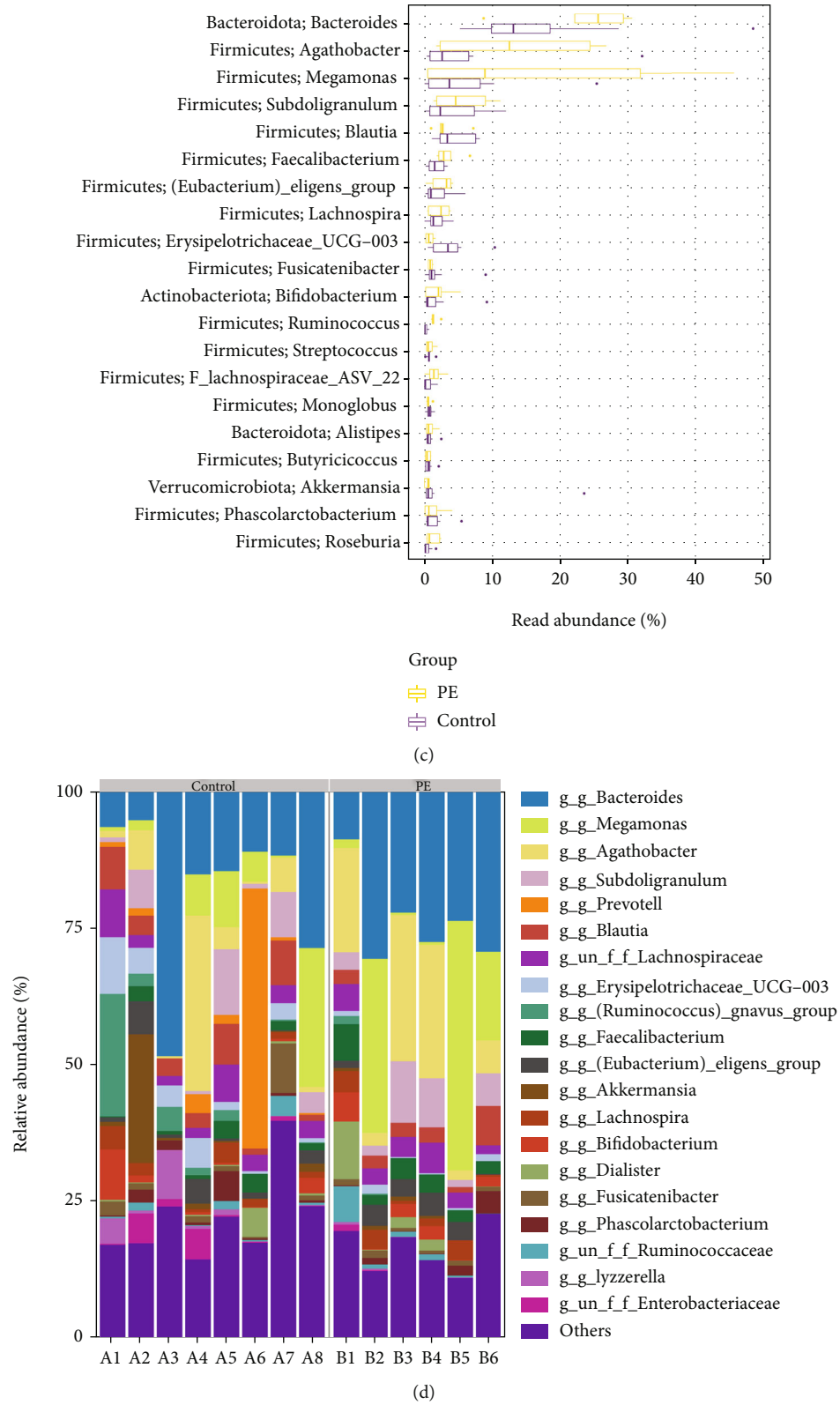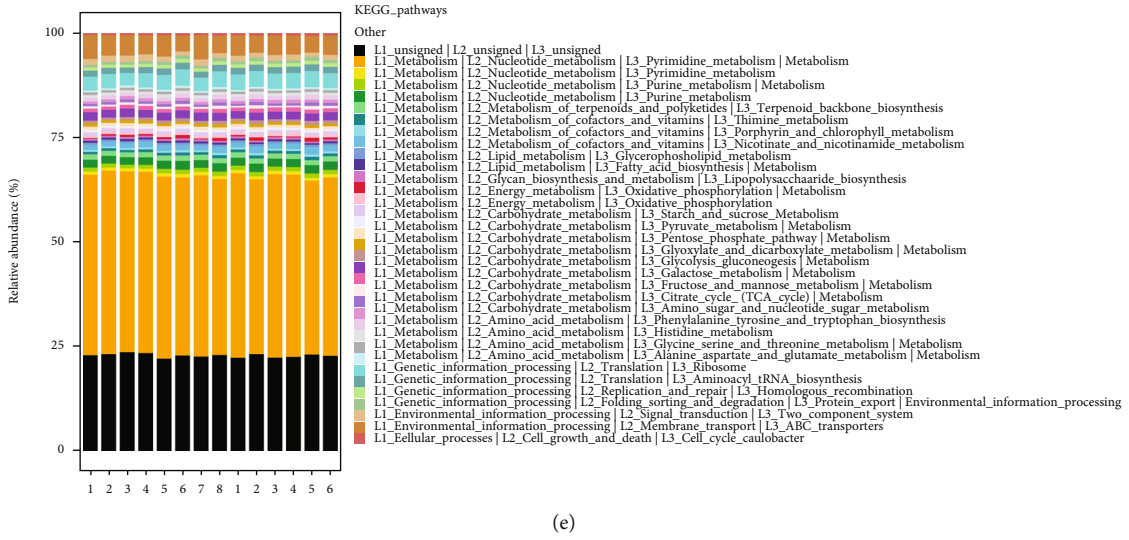
Figure 1: Gut microbiota in PE patients were changed, and key pathway targets (LPS) were screened. (a) Rank abundance curve. (b) Venn diagram. (c) Relative abundance histogram of top 20 ASVs at the genus level. (d) Top 20 dominant gut microbiota with relative abundance at the phylum level. (e) PICRUSt analysis in the KEGG pathway. A: control group; B: PE group.

(a)

(b)

(c)
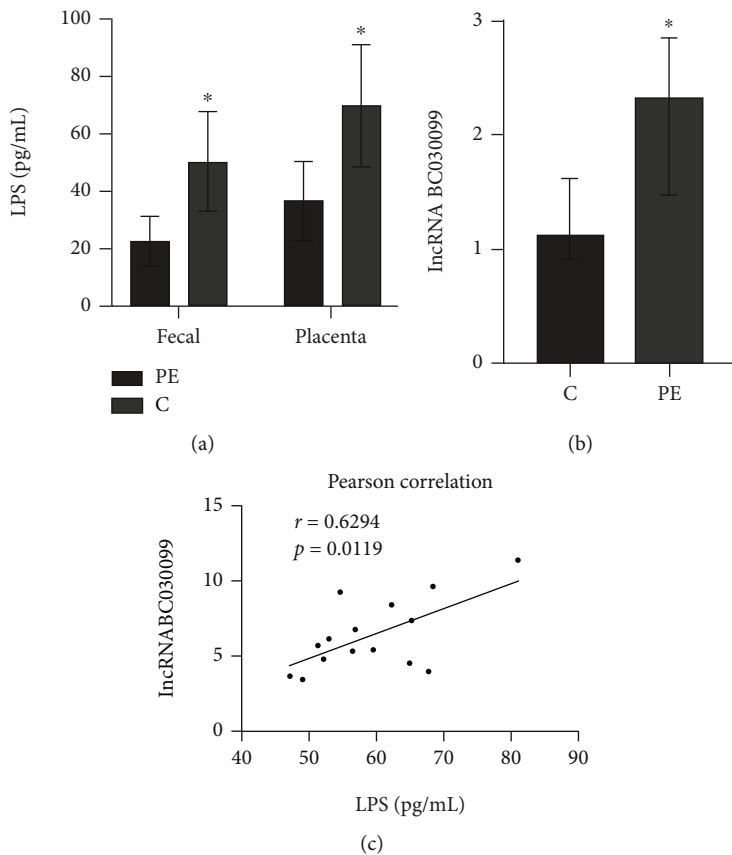
Figure 2: LPS was positively correlated with lncRNA BC030099. (a) LPS level in fecal and placental tissues in PE and control groups. (b) lncRNA BC030099 level in placental tissues in PE and control groups. (c) The correlation of LPS and lncRNA BC030099 in PE placental tissues were evaluated by Spearman's correlation analysis. $^*P < 0.05$ vs. C (control).

BC030099 group was promoted, and p-IκBα and p65 expressions were inhibited. However, the si-BC030099+LPS group had repressed IκBα expression and facilitated p-IκBα and p65 expressions than the si-BC030099 group (Figure 5(a)). In addition, we examined inflammation-related marker expression. Compared with those in the si-control group,

(a)

(b)

(c)

(d)
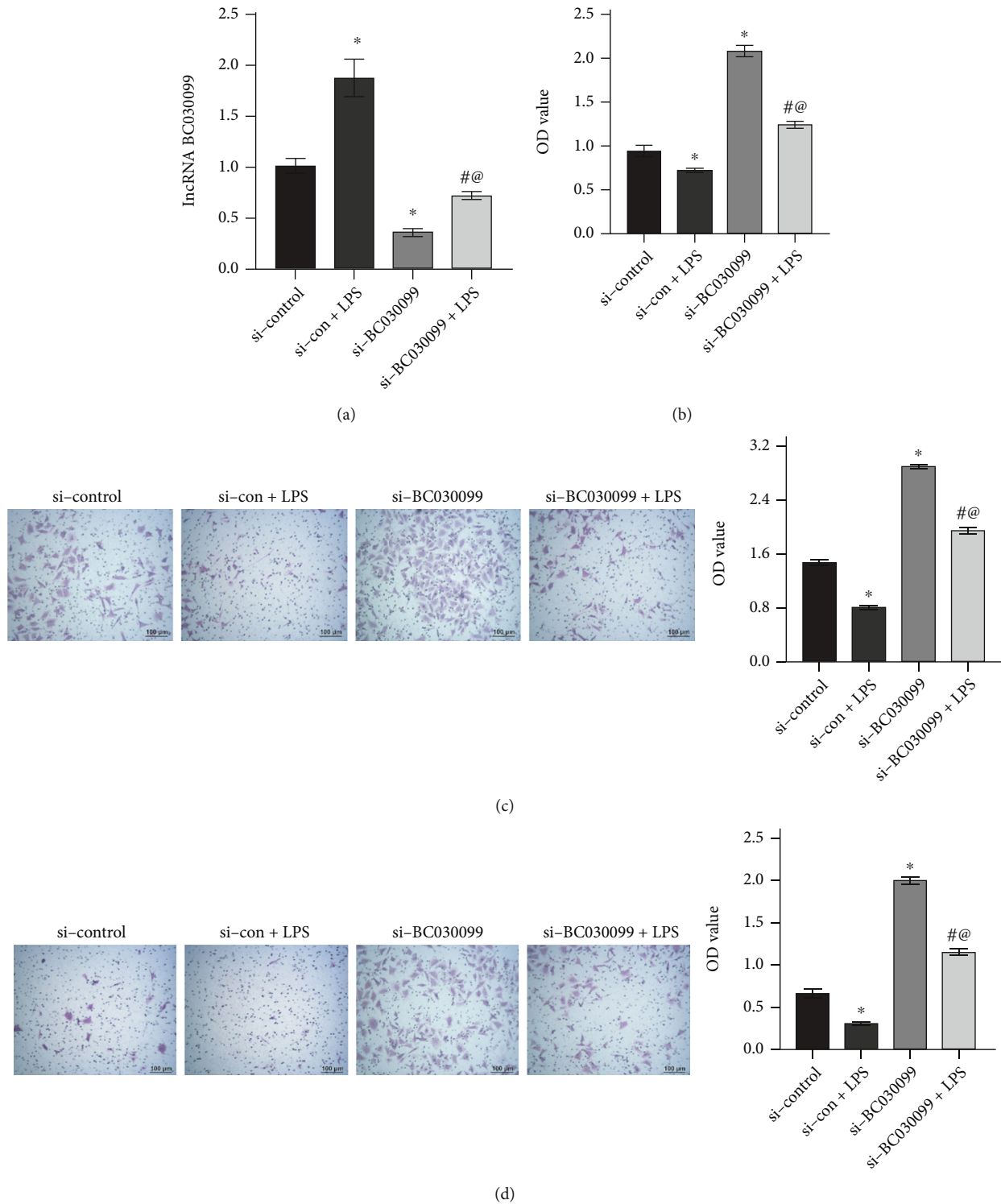
FIGURE 3: Knockdown of lncRNA BC030099 promoted trophoblast cell proliferation, invasion, and migration. (a) lncRNA BC030099 expression in trophoblast cells. (b) CCK-8 assay was utilized to measure HTR-8/SVneo cell proliferation. (c, d) Transwell assays were performed to monitor HTR-8/SVneo cell migration and invasion. Scale bar = 100 μm; $^{*}P < 0.05$ vs. si-control, $^{\#}P < 0.05$ vs. si-con+LPS, and $^{@}P < 0.05$ vs. si-BC030099.

IL-6, IL-1β, and TNF-α levels in the si-con+LPS group were facilitated; IL-6, IL-1β, and TNF-α levels in the si-BC030099 group were repressed. The si-BC030099+LPS group had ele- vated IL-6, IL-1β, and TNF-α levels than the si-BC030099 group (Figure 5(b)). All in all, lncRNA BC030099 affected NF-κB pathway.
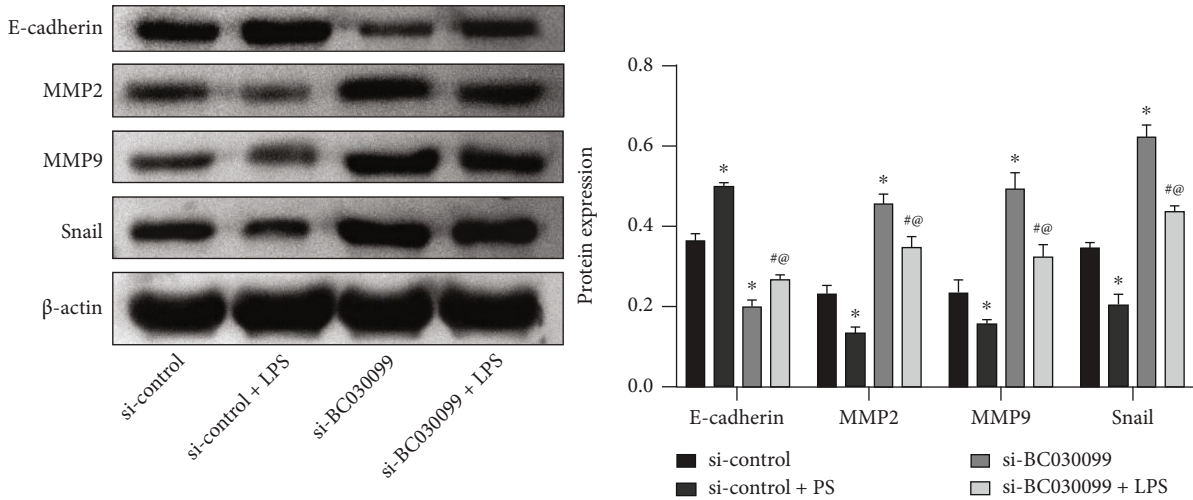
FIGURE 4: Knockdown of lncRNA BC030099 elevated MMP2, MMP9, and snail levels and repressed E-cadherin level. Western blot was utilized to assess MMP2, MMP9, snail, and E-cadherin levels in HTR-8/SVneo cells. $^*P < 0.05$ vs. si-control, $^\#P < 0.05$ vs. si-con+LPS, and $^@P < 0.05$ vs. si-BC030099.
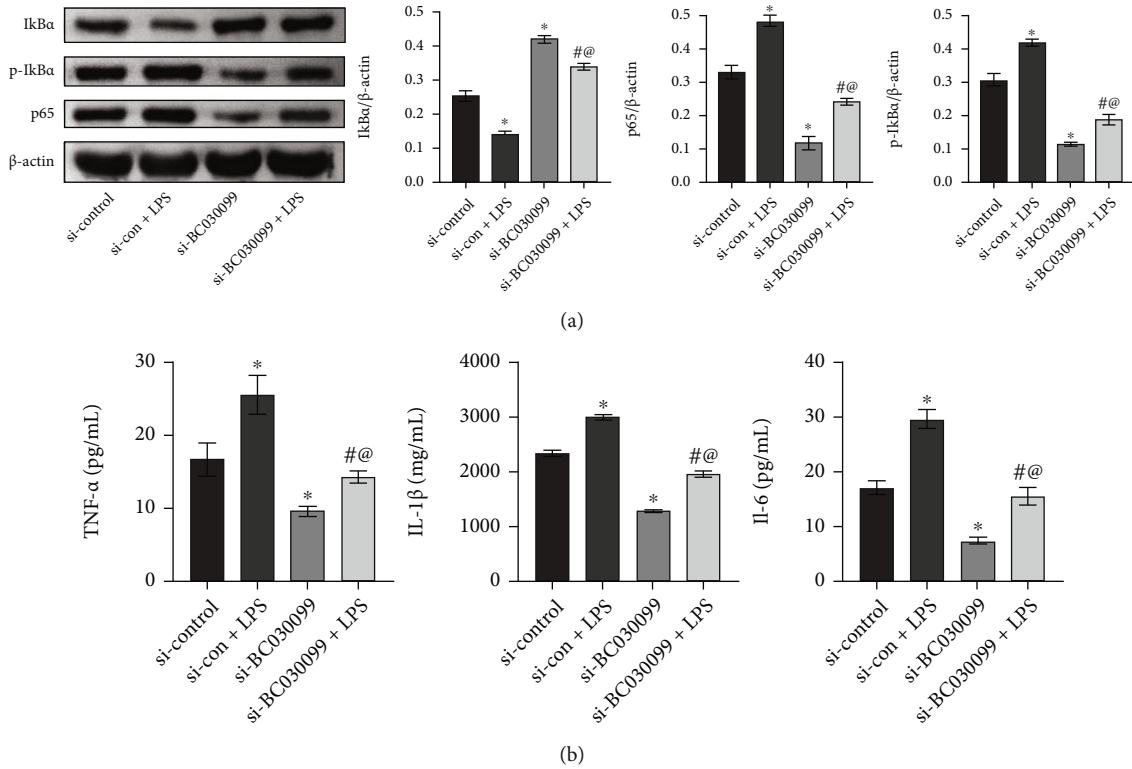
FIGURE 5: lncRNA BC030099 affected NF-κB pathway. (a) Western blot was performed to determine p-IκBα, IκBα, and nuclear NF-κB p65 levels in HTR-8/SVneo cells. (b) IL-6, IL-1β, and TNF-α levels were determined by ELISA. $^*P < 0.05$ vs. si-control, $^\#P < 0.05$ vs. si-con+LPS, and $^@P < 0.05$ vs. si-BC030099.

3.6. NF-κB Inhibitor Reversed Trophoblast Cell Proliferation, Invasion, and Migration Induced by LPS. Finally, we used NF-κB pathway inhibitor JSH-23. IκBα expression was suppressed, and p-IκBα and p65 expressions were facilitated in LPS group than in the control group. However, compared with the LPS group, the LPS+JSH-23 group showed an increase in IκBα expression and a decrease in p-IκBα and p65 expressions (Figure 6(a)). Cell function experiments showed compared with the control group; the LPS group had reduced cell proliferation, migration, and invasion abilities. After adding JSH-23, the LPS+JSH-23 group had enhanced cell proliferation, migration, and invasion abilities
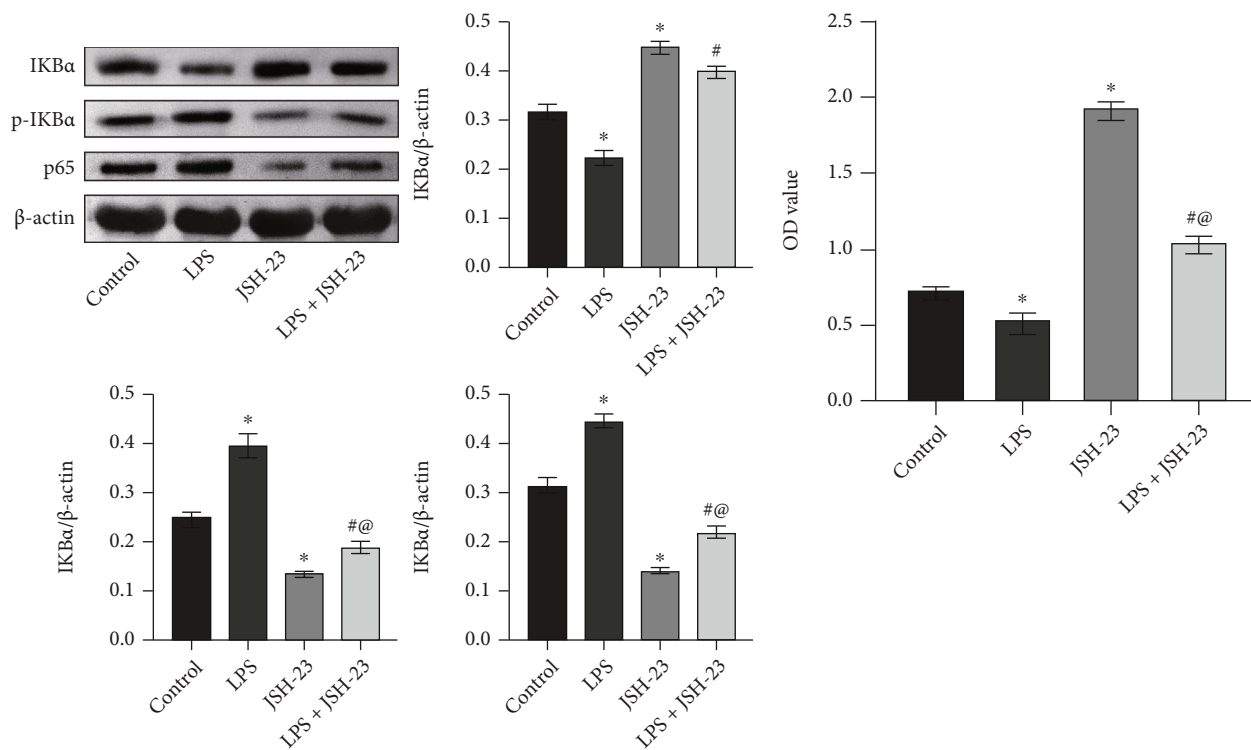
(a)

(b)
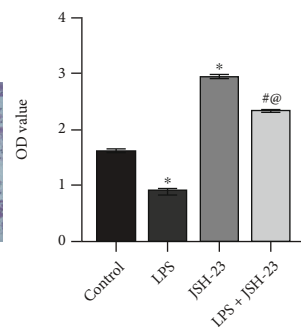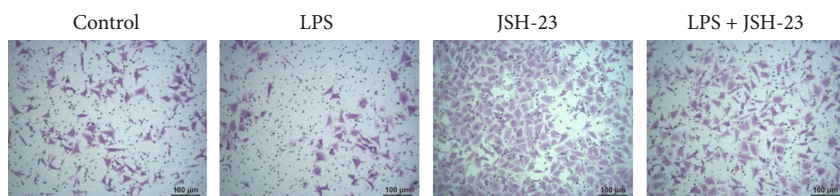
(c)
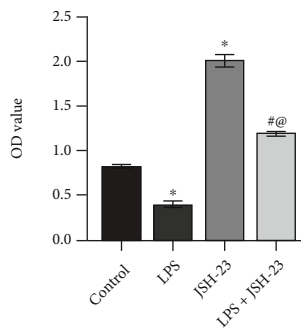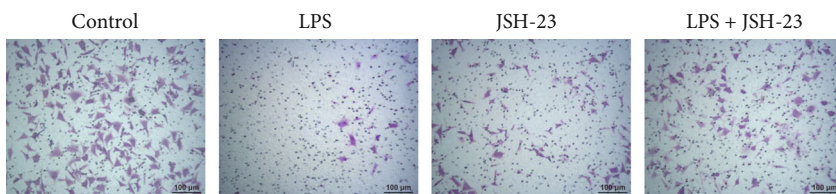
(d)

FIGURE 6: Continued.
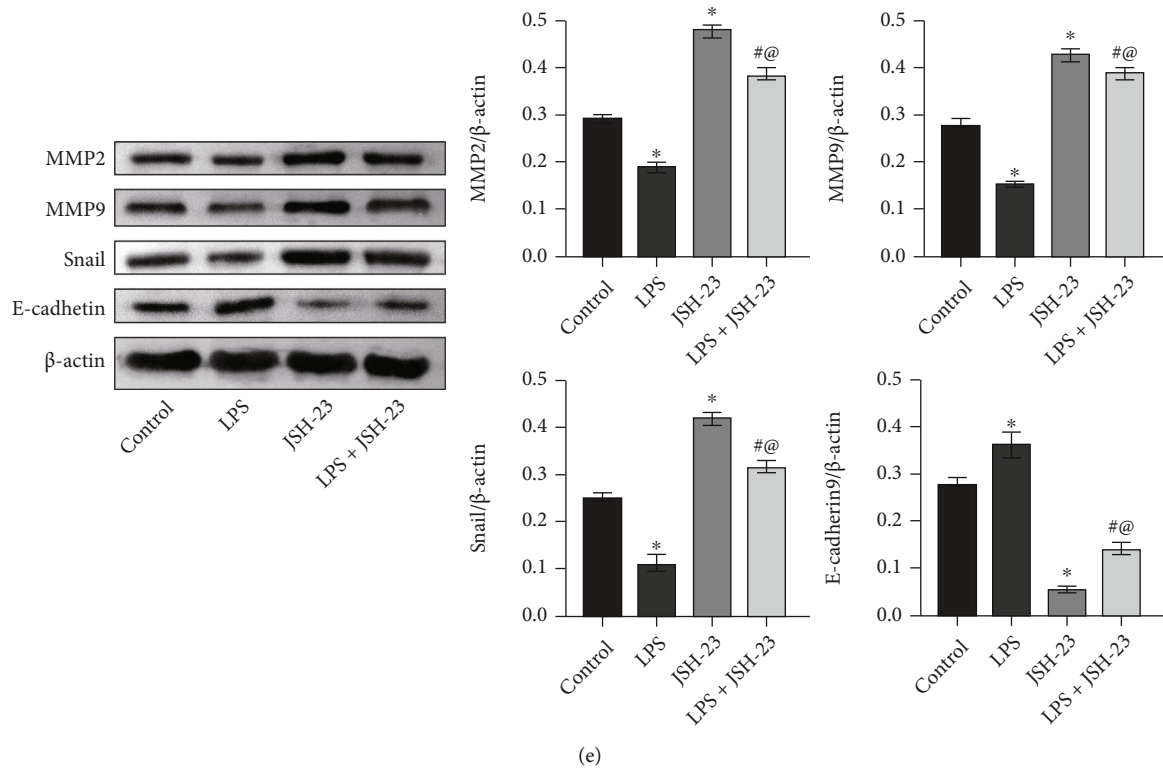
(e)

FIGURE 6: NF-κB inhibitor reversed trophoblast cell proliferation, invasion, and migration induced by LPS. (a) IκBα, p-IκBα, and nucleus NF-κB p65 expressions in trophoblast cells. (b) Cell activity was determined by CCK-8 assay. (c, d) Cell migration and invasion were examined by Transwell assays. (e) Western blot was performed to determine MMP2, MMP9, snail, and E-cadherin levels in trophoblast cells. Scale bar = 100 μm. $^*P < 0.05$ vs. control; $^\#P < 0.05$ vs. LPS.

(Figures 6(b)–6(d)). Then, we used Western blot to detect MMP2, MMP9, snail, and E-cadherin levels. MMP2, MMP9, and snail expressions were suppressed in the LPS group than the control group. After adding JSH-23, MMP2, MMP9, and snail expressions were also repressed in the LPS+JSH-23 group. The trend of E-cadherin was opposite to that of snail (Figure 6(e)). The above results indicated that NF-κB inhibitor reversed trophoblast cell proliferation, invasion, and migration induced by LPS.

4. Discussion

PE is a devastating medical complication of pregnancy that causes severe maternal and fetal morbidity and mortality [17]. PE complicates maternal and child health management and contributes to the majority of adverse pregnancy outcomes, but the mechanisms underlying PE development remain unclear. Studies have shown gut microbiota structure of PE patients has changed significantly, which may be associated with the occurrence and development of disease [18]. However, further studies are needed to understand underlying mechanisms. In this research, we sought to explore lncRNA BC030099, inflammation, and gut microbiota relationship in PE. Our research may contribute to the early diagnosis and targeted monitoring of PE.

Colonization of neonatal gut with beneficial bacteria is essential for mucosal barrier's establishment and mainte-

nance, thereby protecting neonate from intestinal pathogens and local and systemic inflammation [19]. Recent advances show abnormalities in microbiome composition may play a role in various disease pathogenesis including PE [20]. Alterations in gut microbiota composition could alter short-chain fatty acid profile released by bacteria and contribute to hypertension and metabolic syndrome [21]. Chen et al. found that PE patients had repressed bacterial diversity and marked dysbiosis [22]. Our study is consistent with previous studies showing changes in gut microbiota in PE patients. It was reported maternal blood IL-6 levels in PE were positively correlated with Bilophila and Oribacterium, while LPS levels were negatively correlated with Akkermansia [23]. Chang et al. found the abundance of LPS synthesis pathway was significantly elevated in predicted PE patients, while the abundance of the G protein-coupled receptor pathway was observably repressed [11]. We also found that gut microbiota related to LPS biosynthesis were significantly elevated in gut microbiota in the PE group.

lncRNAs are noncoding transcripts, typically over 200 nt in length, that have recently emerged as one of the largest and significantly diverse RNA families [24]. lncRNAs have now become important players in almost all gene functions and regulatory levels [25]. The study showed circulating lncRNA BC030099 level in plasma of PE patients was significantly higher than non-preeclamptic healthy subjects. Elevated plasma lncRNA BC030099 level was related to an

elevated risk of PE and may be considered a novel biomarker [9]. Through validation, we found lncRNA BC030099 level in placenta of the PE group was also markedly elevated. Furthermore, the effects of gut microbiota on host lipid metabolism may be mediated via gut microbiota-produced metabolites including short-chain fatty acids, secondary bile acids, and trimethylamine, as well as proinflammatory bacterial-derived factor LPS [26]. Wang et al.'s studies have shown that patients with PE have gut microbiota imbalance and elevated plasma LPS level [12]. We found LPS levels in the feces and placenta of PE group were significantly facilitated and LPS and lncRNA BC030099 expressions were notably positively correlated. This is the first time we report LPS and lncRNA BC030099 role in PE.

lncRNAs have been shown to participate in different biological processes including cell growth, antiapoptosis, migration, and invasion [27]. Chen et al. reported lncRNA KCNQ1OT1 can regulate miR-146a-3p role in HTR8/SVneo cell proliferation, invasion, and migration through the CXCL12/CXCR4 pathway, which may be involved in PE pathogenesis [14]. Our study also showed knockdown of lncRNA BC030099 promoted HTR-8/SVneo cell proliferation, migration, and invasion. Studies have shown that MMPs are vital mediators of vascular and uterine remodeling and reduced MMP2 and MMP9 expressions is thought to be involved in hypertensive pregnancy and PE [28, 29]. Placental extravillous cell invasion involves cell EMT, and several EMT regulators (including snail and E-cadherin) have been found to play vital roles in PE development [30]. Knockdown of lncRNA CRNDE has been reported to inhibit the proliferation, migration, and invasion of HTR-8/SVneo cells, inhibit the formation of EMT, and reduce the protein expression of MMP2 and MMP9 [31]. Zhou et al. reported that lncRNA SNHG12 promoted trophoblast cell migration and invasion by inducing the progression of EMT [32]. Consistent with their study, we found knockdown of lncRNA BC030099 elevated MMP2, MMP9, and snail levels and repressed E-cadherin level.

NF-κB is a vital transcription factor for inflammation-related protein expression [33]. The NF-κB p65 pathway is associated with PE, and inhibition of NF-κB p65 pathway can ameliorate PE [34]. NF-κB and proinflammatory cytokines have been reported to be associated with trophoblast dysfunction [35], but the underlying mechanisms remain unclear. Vaughan and Walsh reported that placental NF-κB was activated nearly 10-fold in PE. Oxidative stress leads to NF-κB activation in trophoblast-like cells, which is enhanced by TNF-α [36]. We found through cellular experiments that LPS induced the nucleus transition of NF-κB through lncRNA BC030099. Furthermore, NF-κB inhibitor reversed trophoblast cell proliferation, invasion, and migration induced by LPS. This is also the first time that we report the mechanism of action of LPS, lncRNA BC030099 and NF-κB p65 in PE.

In conclusion, we explored the evolution of LPS, lncRNA BC030099, and NF-κB p65 involved in PE progression and its mechanism. We report for the first time that gut microbiota dysbiosis in PE contributed to trophoblast cell proliferation, invasion, and migration through the lncRNA BC030099/NF-κB pathway. This study provides a reference for exploring lncRNA and gut microbiota mechanism in PE.

Data Availability

The data used to support the findings of this study are available from the corresponding author upon request.

Ethical Approval

The study was approved by the Ethics Committee of Xiangya Hospital central South University. The research was conducted according to the World Medical Association Declaration of Helsinki. All the information about the study will be fully explained to the subjects by the researchers.

Consent

All the participants provided informed consent before sampling.

Conflicts of Interest

The authors declare that there is no conflict of interest regarding the publication of this paper.

Authors' Contributions

Rong Tang, Gong Xiao, Qiongjing Yuan, and Wei Wang contributed to the conception and design of the study. Rong Tang and Chun Jiang collected the information. Rong Tang wrote the first draft of the manuscript. Yu Jian is assigned to the contributions to data aggregation, validation, analysis of experimental results, and manuscript editing. Gong Xiao, Qiongjing Yuan, Chun Jiang, and Wei Wang wrote sections of the manuscript. All authors have revised, read, and approved the final version of the manuscript.

Acknowledgments

References

[1] S. Karrar and P. L. Hong, "Preeclampsia," in *StatPearls*, StatPearls Publishing LLC, Treasure Island (FL), 2022.

[2] P. Chaemsaithong, D. S. Sahota, and L. C. Poon, "First trimester preeclampsia screening and prediction," *American journal of obstetrics and gynecology*, vol. 226, no. 2, pp. S1071–S1097.e2, 2022.

[3] E. Jung, R. Romero, L. Yeo et al., "The etiology of preeclampsia," *American journal of obstetrics and gynecology*, vol. 226, no. 2, pp. S844–S866, 2022.

[4] L. C. Chappell, C. A. Cluver, J. Kingdom, and S. Tong, "Preeclampsia," *Lancet*, vol. 398, no. 10297, pp. 341–354, 2021.

[5] L. Chen, J. Wang, J. W. Li, X. W. Zhao, and L. F. Tian, "LncRNA MEG3 inhibits proliferation and promotes apoptosis of osteosarcoma cells through regulating Notch signaling

pathway," *European Review for Medical and Pharmacological Sciences*, vol. 24, no. 2, pp. 581–590, 2020.

[6] I. M. Dykes and C. Emanueli, "Transcriptional and post-transcriptional gene regulation by long non-coding RNA," *Genomics, proteomics & bioinformatics*, vol. 15, no. 3, pp. 177–186, 2017.

[7] Q. Zhang, Z. Wang, X. Cheng, and H. Wu, "lncRNA DANCR promotes the migration an invasion and of trophoblast cells through microRNA-214-5p in preeclampsia," *Bioengineered*, vol. 12, no. 2, pp. 9424–9434, 2021.

[8] X. L. Xiucui Luo, "Long non-coding RNAs serve as diagnostic biomarkers of preeclampsia and modulate migration and invasiveness of trophoblast cells," *Medical Science Monitor*, vol. 24, pp. 84–91, 2018.

[9] Y. Sun, Y. Hou, N. Lv et al., "Circulating lncRNA BC030099 increases in preeclampsia patients," *Molecular Therapy-Nucleic Acids*, vol. 14, pp. 562–566, 2019.

[10] J. Gao, K. Xu, H. Liu et al., "Impact of the gut microbiota on intestinal immunity mediated by tryptophan metabolism," *Frontiers in cellular and infection microbiology*, vol. 8, p. 13, 2018.

[11] Y. Chang, Y. Chen, Q. Zhou et al., "Short-chain fatty acids accompanying changes in the gut microbiome contribute to the development of hypertension in patients with preeclampsia," *Clinical Science (London, England)*, vol. 134, no. 2, pp. 289–302, 2020.

[12] J. Wang, X. Gu, J. Yang, Y. Wei, and Y. Zhao, "Gut microbiota dysbiosis and increased plasma LPS and TMAO levels in patients with preeclampsia," *Frontiers in Cellular and Infection Microbiology*, vol. 9, p. 409, 2019.

[13] J. Huang, Y. Qian, Q. Cheng, J. Yang, H. Ding, and R. Jia, "Overexpression of long noncoding RNA Uc. 187 induces preeclampsia-like symptoms in pregnancy rats," *American Journal of Hypertension*, vol. 33, no. 5, pp. 439–451, 2020.

[14] F. R. Chen, L. M. Zheng, D. C. Wu, H. M. Gong, H. Cen, and W. C. Chen, "Regulatory relationship between lncRNA KCNQ1OT1 and miR-146a-3p in preeclampsia," *Zhonghua Fu Chan Ke Za Zhi*, vol. 55, no. 8, pp. 535–543, 2020.

[15] Y. Zhang, W. Liu, M. Wu et al., "PFKFB3 regulates lipopolysaccharide-induced excessive inflammation and cellular dysfunction in HTR-8/Svneo cells: implications for the role of PFKFB3 in preeclampsia," *Placenta*, vol. 106, pp. 67–78, 2021.

[16] J. Liu, S. S. Lv, Z. Y. Fu, and L. L. Hou, "Baicalein enhances migration and invasion of extravillous trophoblasts via activation of the NF-κB pathway," *Medical Science Monitor*, vol. 24, pp. 2983–2991, 2018.

[17] S. Rana, S. D. Burke, and S. A. Karumanchi, "Imbalances in circulating angiogenic factors in the pathophysiology of preeclampsia and related disorders," *American journal of obstetrics and gynecology*, vol. 226, no. 2, pp. S1019–S1034, 2022.

[18] J. Liu, H. Yang, Z. Yin et al., "Remodeling of the gut microbiota and structural shifts in preeclampsia patients in South China," *European journal of clinical microbiology & infectious diseases: official publication of the European Society of Clinical Microbiology*, vol. 36, no. 4, pp. 713–719, 2017.

[19] K. Sohn and M. A. Underwood, "Prenatal and postnatal administration of prebiotics and probiotics," *Seminars in fetal & neonatal medicine*, vol. 22, no. 5, pp. 284–289, 2017.

[20] J. A. Ishimwe, "Maternal microbiome in preeclampsia pathophysiology and implications on offspring health," *Physiological Reports*, vol. 9, no. 10, article e14875, 2021.

[21] F. Altemani, H. L. Barrett, L. Gomez-Arango et al., "Pregnant women who develop preeclampsia have lower abundance of the butyrate- producer _Coprococcus_ in their gut microbiota," *Pregnancy hypertension*, vol. 23, pp. 211–219, 2021.

[22] X. Chen, P. Li, M. Liu et al., "Gut dysbiosis induces the development of pre-eclampsia through bacterial translocation," *Gut*, vol. 69, no. 3, pp. 513–522, 2020.

[23] L. J. Lv, S. H. Li, S. C. Li et al., "Early-onset preeclampsia is associated with gut microbial alterations in antepartum and postpartum women," *Frontiers in cellular and infection microbiology*, vol. 9, p. 224, 2019.

[24] M. D. Paraskevopoulou and A. G. Hatzigeorgiou, "Analyzing MiRNA–LncRNA interactions," *Methods in molecular biology*, vol. 1402, pp. 271–286, 2016.

[25] X. Qian, J. Zhao, P. Y. Yeung, Q. C. Zhang, and C. K. Kwok, "Revealing lncRNA structures and interactions by sequencing-based approaches," *Trends in biochemical sciences*, vol. 44, no. 1, pp. 33–52, 2019.

[26] M. Schoeler and R. Caesar, "Dietary lipids, gut microbiota and lipid metabolism," *Reviews in endocrine & metabolic disorders*, vol. 20, no. 4, pp. 461–472, 2019.

[27] J. Wang, Z. Su, S. Lu et al., "LncRNA HOXA-AS2 and its molecular mechanisms in human cancer," *Clinica Chimica Acta*, vol. 485, pp. 229–233, 2018.

[28] Y. Zhang and X. Chen, "lnc RNA FOXD2-AS1 affects trophoblast cell proliferation, invasion and migration through targeting mi RNA," *Zygote*, vol. 28, no. 2, pp. 131–138, 2020.

[29] J. Chen and R. A. Khalil, "Matrix metalloproteinases in normal pregnancy and preeclampsia," *Progress in molecular biology and translational science*, vol. 148, pp. 87–165, 2017.

[30] D. Cheng, S. Jiang, J. Chen, J. Li, L. Ao, and Y. Zhang, "The increased lncRNA MIR503HG in preeclampsia modulated trophoblast cell proliferation, invasion, and migration via regulating matrix metalloproteinases and NF-κB signaling," *Disease markers*, vol. 2019, Article ID 4976845, 12 pages, 2019.

[31] H. Zhu and L. Kong, "LncRNA CRNDE regulates trophoblast cell proliferation, invasion, and migration via modulating miR-1277," *American Journal of Translational Research*, vol. 11, no. 9, p. 5905, 2019.

[32] F. Zhou, Y. Sun, Z. Chi, Q. Gao, and H. Wang, "Long noncoding RNA SNHG12 promotes the proliferation, migration, and invasion of trophoblast cells by regulating the epithelial-mesenchymal transition and cell cycle," *The Journal of International Medical Research*, vol. 48, no. 6, article 300060520922339, 2020.

[33] F. Haugen and C. A. Drevon, "Activation of nuclear factor-κB by high molecular weight and globular adiponectin," *Endocrinology*, vol. 148, no. 11, pp. 5478–5486, 2007.

[34] H. Sha, Y. Ma, Y. Tong, J. Zhao, and F. Qin, "Apocynin inhibits placental TLR4/NF-κB signaling pathway and ameliorates preeclampsia-like symptoms in rats," *Pregnancy hypertension*, vol. 22, pp. 210–215, 2020.

[35] A. Yin, Q. Chen, M. Zhong, and B. Jia, "MicroRNA-138 improves LPS-induced trophoblast dysfunction through targeting RELA and NF-κB signaling," *Cell cycle*, vol. 20, no. 5-6, pp. 508–521, 2021.

[36] J. E. Vaughan and S. W. Walsh, "Activation of NF-κB in placentas of women with preeclampsia," *Hypertension in pregnancy*, vol. 31, no. 2, pp. 243–251, 2012.

Research Article

Alpha-Lipoic Acid Promotes Intestinal Epithelial Injury Repair by Regulating MAPK Signaling Pathways

Yu Yang,[1] **Yong Xiao,**[2] **Yue Jiang,**[1] **Jiajun Luo** ⓘ**,**[1] **Jingwen Yuan,**[1] **Junfeng Yan,**[1] **and Qiang Tong** ⓘ[1]

[1]*Department of Gastrointestinal Surgery I Section, Renmin Hospital of Wuhan University, Wuhan 430060, China*
[2]*Department of Gastroenterology, Renmin Hospital of Wuhan University, Wuhan 430060, China*

Correspondence should be addressed to Qiang Tong; qiangtong@whu.edu.cn

Intestinal epithelial cells are an essential barrier in human gastrointestinal tract, and healing of epithelial wound is a key process in many intestinal diseases. α-Lipoic acid (ALA) was shown to have antioxidative and anti-inflammatory effects, which could be helpful in intestinal epithelial injury repair. The effects of ALA in human colonic epithelial cells NCM460 and human colorectal adenocarcinoma cells Caco-2 were studied. ALA significantly promoted NCM460 and Caco-2 migration, increased mucosal tight junction factors ZO-1 and OCLN expression, and ALA accelerated cell injury repair of both cells in wound healing assay. Western blot analysis indicated that ALA inhibited a variety of mitogen-activated protein kinase (MAPK) signaling pathways in the epithelial cells. In conclusion, ALA was beneficial to repair of intestinal epithelial injury by regulating MAPK signaling pathways.

1. Introduction

Intestinal epithelial cells form a selective barrier that separates luminal contents from underlying tissue. Wound healing of intestinal epithelial after injury is a dynamic biological process regulated by a complex network of microenvironments [1]. Studies have shown that a variety of cytokines (such as α-actinin and toll-like receptor [2]), regulatory peptides, and dietary factors [3] modulate intestinal epithelial wound healing. It is worth noting that redox balance is crucial for intestine homeostasis, and overproduction of ROS caused by oxidative upregulation or fluctuant mitochondrial function is related to intestinal epithelial injury [4].

α-Lipoic acid (ALA), a kind of natural dimercaptan antioxidant, is a compound commonly found in mitochondria, which plays an essential role in mitochondrial metabolism [5]. As a cofactor of enzymes, ALA is involved in glucose and lipid metabolism and regulates gene transcription [6]. As a metabolic antioxidant, ALA regulates NF-κB signal transduction and protects against oxidative injury [7]. In addition, ALA can downregulate proinflammatory redox-sensitive signal transduction processes and has a certain anti-inflammatory effect [8]. Based on the above properties, ALA is applied in Alzheimer's disease, diabetic polyneuropathy, and obesity [9]. At present, the application of ALA in the intervention of intestinal damage is increasingly popular. The study of Guven et al. showed that ALA prevented ischemia/reperfusion injury in the rat intestine through scavenging ROS and RNS [10]. In an in vitro Caco-2 cell model, ALA supplementation was proved to enhance epithelial cell proliferation and thus prevented the disruption of intestinal epithelial integrity [11]. In an in vivo experiments on mice, ALA protected the intestine against ulcerative colitis and the associated systemic damage [12].

The present study aims to investigate the effect of ALA on intestinal epithelial injury repair and its mechanism, to provide theoretical basis for clinical treatment.

2. Materials and Methods

2.1. Cell Culture and Reagents. Human colonic epithelial cells NCM460 and human colorectal adenocarcinoma cells Caco-2 were purchased from the American Type Culture Collection (ATCC, Manassas, USA). The cells were cultured in Roswell Park Memorial Institute DMEM/F12 medium supplemented with 10% fetal bovine serum (FBS). Cells were maintained in a 37°C incubator with 5% CO_2. All cell lines tested negative for mycoplasma. Alpha-lipoic acid (ALA) was purchased from Solarbio (Beijing, China). Based on the concentration range of ALA in other studies and the transport of ALA enantiomers in Caco-2 cells [13, 14], and combined with the results of pre-experiments, ALA was dissolved with DMSO and formulated to 50, 150 and 300 μM for formal experiments.

2.2. Wound Healing Assay. Positioning marks were made with a permanent marker at the bottom of the cell culture plates to ensure that the same wound was observed. NCM460 and Caco-2 cells were cultured until 90% confluence in 6-well cell culture plates. Wounds were inflicted on the cell monolayers with 200-μl pipette tips. Then cells were incubated with specific concentration of ALA in serum-free medium. During incubation, the cell migration was observed with an Olympus FluoView™ 300 confocal microscope (Tokyo, Japan). The wound areas were measured with ImageJ software. The remaining wound area was calculated using the following formula: (cell − free area at 12 h or 24 h/ cell − free area at 0 h) × 100%. At least five fields were analyzed in each group.

2.3. Quantitative Real-Time PCR (qRT-PCR). The total RNA was extracted from tissues using TRIzol Reagent (Thermo Fisher, USA) according to the manufacturer's instructions. Then RNA was reverse transcribed to cDNA with 1 μg total RNA, using reverse transcriptase and Oligo dT primers (Takara, Japan). The cDNA was then amplified with specific primers by PCR. The conditions for qRT-PCR were as follows: 95°C for 3 min, followed by 40 cycles of 10 s at 95°C, 10 s at 60°C, and 15 s at 70°C, followed by heating from 65°C to 95°C. Primers for qRT-PCR are listed as follows: ZO-1 forward primer 5′-GAA CGA GGC ATC ATC CCT AA-3′, reverse primer 5′-GAG CGG ACA AAT CCT CTC TG-3′. OCLN forward primer 5′-TTT GTG GGA CAA GGA ACA CA-3′, reverse primer 5′-TCA TTC ACT TTG CCA TTG GA-3′. GAPDH forward primer 5′-GAA GGT GAA GGT CGG AGT C-3′, reverse primer 5′-GAA GAT GGT GAT GGG ATT TC-3′.

2.4. Western Blot. Cells were washed with ice-cold PBS and lysed with RIPA buffer. Samples containing equal quantities of total proteins were resolved on 15% SDS polyacrylamide denaturing gel and transferred to nitrocellulose membranes. After blocking with 5% skim milk in TBST for 1 h, the membranes were incubated overnight at 4°C with the following primary antibodies: AKT (1:1000, Abcam, UK), JNK (1:1000, Abmart, Shanghai, China), and p38 (1:1000, Abmart, Shanghai, China). Goat anti-rabbit IgG secondary antibody (1:5000) (Servicebio, Wuhan, China) was used at room temperature for 1-h incubation. The blot was visualized by using ECL Chemiluminescence Kit (Epizyme, Shanghai, China). Each band was quantified via ImageJ software.

2.5. Statistical Analysis. The results of this study were expressed as mean ± SD values. Student's *t*-test was used to compare the results between the different groups. $P < 0.05$ was considered statistically significant. All analyses were performed using GraphPad Prism version 8 software.

3. Results

3.1. ALA Promoted Epithelial Cell Migration after Injury. Human colonic epithelial cells NCM460 and human colorectal adenocarcinoma cells Caco-2 were cultured in a serum-free medium for 12 h to form a monolayer. Compared with the control cells, the cells treated with ALA showed enhanced injury repair in a dose-dependent manner (Figures 1(a) and 1(b)). As shown in Figures 1(a) and 1(c), the remaining wound area of NCM460 cells that were treated with ALA (150 and 300 μM) were significantly smaller than those of control cells after 12 h and 24 h of incubation ($P < 0.05$). Meanwhile, the remaining wound area of Caco-2 cells that were treated with ALA (50, 150, and 300 μM) were significantly reduced after 12 h of incubation (Figures 1(b) and 1(d)) ($P < 0.05$).

3.2. ALA Increased the Expression of Tight Junction Factor in Intestinal Mucosa. To reveal the effects of ALA on intestinal mucosal tight junction, the expression of ZO-1 and OCLN was measured at the mRNA level. As shown in Figure 2, in NCM460 cells incubated with ALA (150 and 300 μM), the mRNA levels of both ZO-1 and OCLN were much higher than those in the control group ($P < 0.05$), whereas 50 μM ALA had little influence on the expression of ZO-1 and OCLN ($P > 0.05$). ALA significantly increased the expression of ZO-1 and OCLN in the intestinal mucosa epithelial cells at the mRNA level.

3.3. ALA Promoted Intestinal Epithelial Injury Repair through Regulating PI3K/AKT, JNK, and p38 MAPK Signaling Pathways. Previous studies have shown that mitogen-activated protein kinases (MAPK)–related molecules are closely associated with wound healing in many cell lines, including epithelial cells, keratinocytes, and cancer cells [15–17]. To investigate the growth-promoting mechanism of ALA in epithelial cells, we assessed the status of MAPK signaling pathway in ALA-treated NCM460 cells. Western blot indicated that MAPK signaling-related molecules PI3K/AKT, Jun N-terminal kinases (JNK), and p38 were significantly suppressed by the treatment of ALA (Figure 3(a)). High concentrations of ALA suppressed AKT and JNK signaling pathways (Figures 3(b) and 3(c)),

(a)

(b)

(c)

(d)
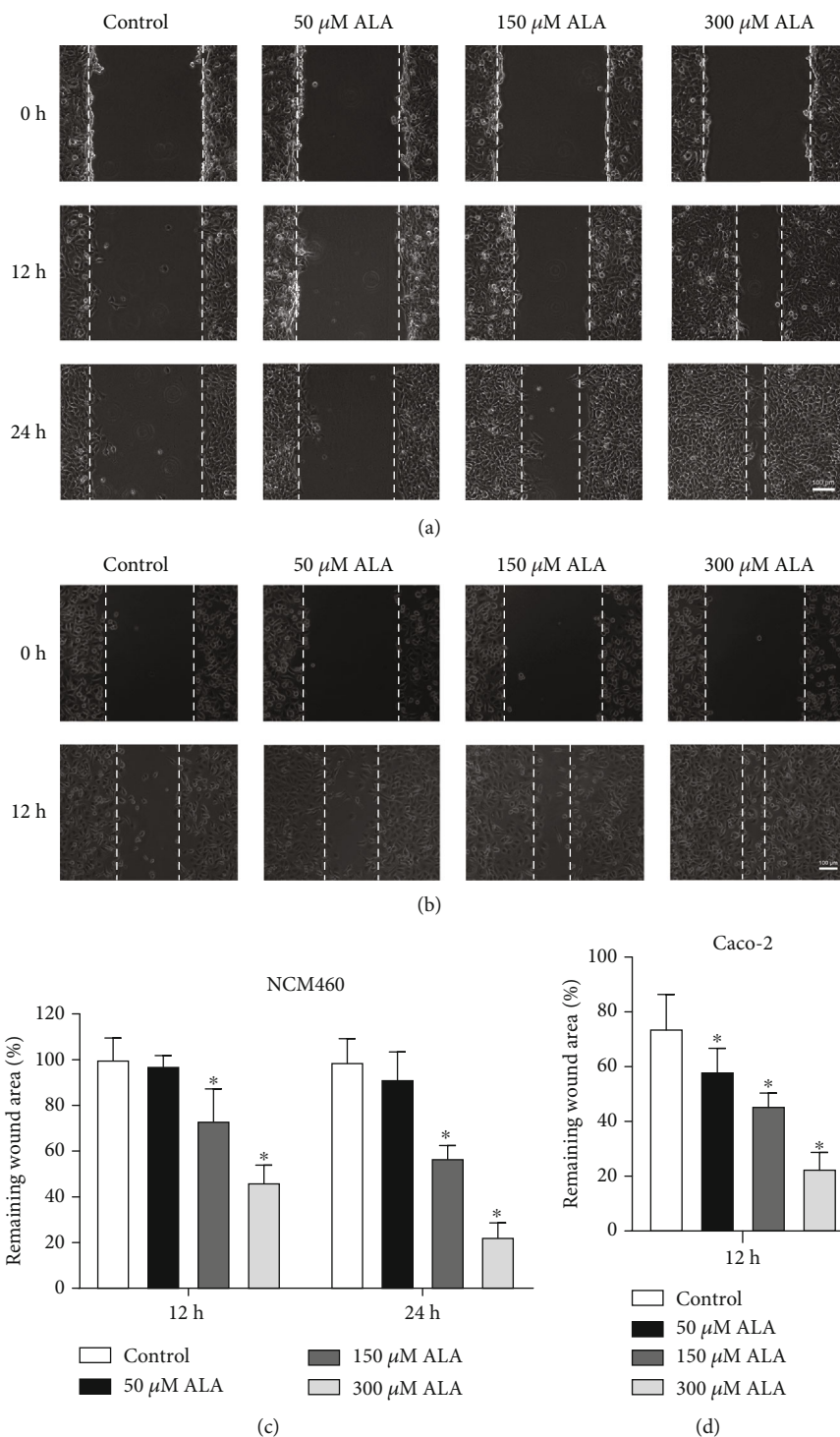
FIGURE 1: Restoration of epithelial cells treated with α-lipoic acid (ALA). (a) Representative images of cell wounds in wound healing assay of ALA (0–300 μM) treated NCM460 cells. Wounds were created on the cell surface with the pipette tips, and then NCM460 cells were treated with ALA (0–300 μM). The remaining wound areas were determined at 12 h and 24 h after wound generation. (b) Representative images of cell wounds in wound healing assay of ALA (0–300 μM) treated Caco-2 cells. Wounds were created, and then Caco-2 cells were treated with ALA (0–300 μM). The remaining wound areas were determined at 12 h after wound generation. (c, d) The remaining wound areas in NCM460 and Caco-2 cells treated with ALA (0-300 μM). Data are presented as mean ± SD values of three duplicates. ∗$P < 0.05$.
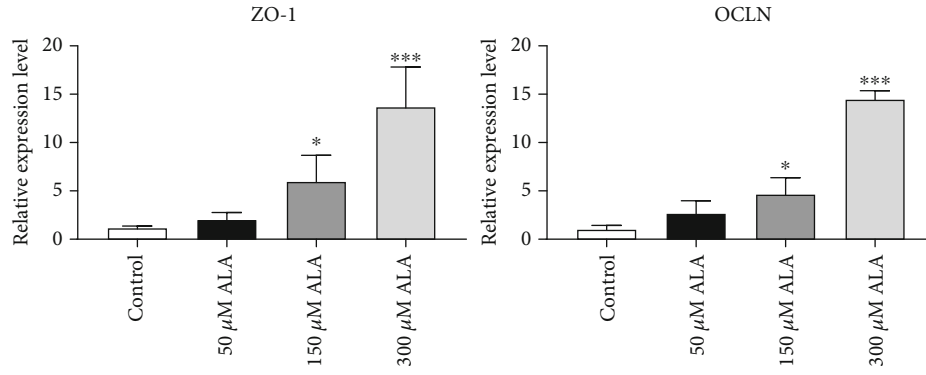
FIGURE 2: Effects of ALA on the mRNA expression of mucosal tight junction factors of NCM460 cells during injury repair. Quantitative real-time PCR analysis of tight junction protein 1 (ZO-1) and occludin (OCLN). $*P < 0.05$ and $***P < 0.0001$.
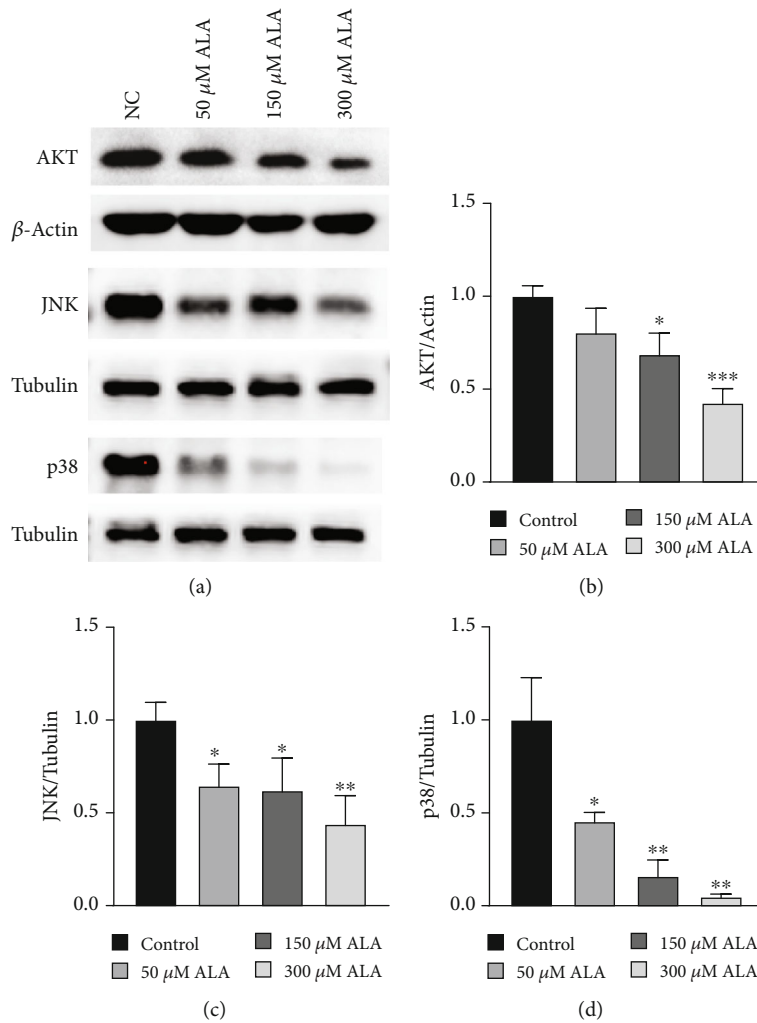
FIGURE 3: ALA suppressed the PI3K/AKT, JNK, and p38 MAPK signaling pathways in NCM460 cells. (a) Western blot showed that the activation of AKT, JNK, and p38 was suppressed by treatment with the ALA in NCM460 cells. (b) Quantified histograms of AKT protein levels normalized by actin. (c) Quantified histograms of JNK protein levels normalized by tubulin. (d) Quantified histograms of p38 protein levels normalized by tubulin. Data represent mean ± SD from at least three independent experiments. $*P < 0.05$, $**P < 0.01$, and $***P < 0.001$ compared to control.

while the inactivation of p38 signaling pathway was observed at lower ALA concentrations (Figure 3(d)).

4. Discussion

Many factors such as inflammation, immunological factors, oxidative stress, medicines, and imbalance of gut microbiota may impair intestinal epithelium function and damage its barrier function [18, 19]. After intestinal epithelium injury, epithelial cells migrate, proliferate and differentiate, and heal gradually [20]. Clinical application of medicine to promote intestinal mucosal wound healing is beneficial to the rehabilitation of patients with various intestinal diseases, including inflammatory bowel diseases (IBD), celiac disease, and intestinal infections [21]. In the present study, we demonstrated that ALA could enhance intestinal injury repair and revealed its mechanism.

Lipoic acid, a powerful antioxidant existed in mitochondria, is absorbed through the gastrointestinal tract in vivo. Vegetables such as spinach, cauliflower, tomatoes, and carrots and meat such as liver are rich in lipoic acid, but food supplementation of lipoic acid is insufficient and slow to take effect. Therefore, ALA is commonly used as a drug or nutritional supplement for a variety of diseases [22].

Existing studies showed that ALA could accelerate mouse cutaneous wound healing [23] or promote human postoperative uterine healing [24]. However, its effect on intestinal epithelial wound healing remains unknown. In this study, we performed wound healing assay on both human colonic epithelial cells (NCM460) and colorectal adenocarcinoma cells (Caco-2). Low concentration of ALA ($50 \mu M$) had no obvious effect on injury repair, while high concentration (150 and $300 \mu M$) of ALA could promote intestinal epithelial injury repair in a concentration-dependent manner (Figures 1(a) and 1(b)). In addition, ALA significantly enhanced epithelial cell migration (Figures 1(c) and 1(d)), which is an important process of wound repair.

Tight junction protein 1 (TJP1, also known as ZO-1), a membrane-associated cytoplasmic protein, plays an important role in cell-cell communication in the intercellular barrier in non-epithelial and epithelial cells [25]. ALA increased ZO-1 expression observed in our present study (Figure 2), which was closely related to proliferation and differentiation of epithelial cells. Occludin (OCLN) is another important tight junction protein in wound healing [26]. Studies have shown that increased OCLN can maintain intestinal barrier function in patients with ulcerative colitis and mice with colitis [27], which is consistent with our finding that ALA increased the expression of OCLN in intestinal epithelial injury repair (Figure 2).

As an antioxidant, the mechanism of ALA is related to its effect on oxidative stress. In a rat experiment, ALA pretreatment significantly reduced oxidative stress and inflammation in the intestine [28]. ALA protected piglet intestinal epithelium cells (IPEC-J2 cells) against H_2O_2 induced injury by scavenging hydroxyl radical [29]. However, the exact mechanism of ALA in intestinal epithelial injury repair process remains unclear.

Mitogen-activated protein kinases (MAPK)–related signaling pathways, including p38, JNK, ERK, and AKT, are involved in numerous cellular responses such us proliferation, differentiation, apoptosis, inflammation, and oxidative stress [30–32]. It has been found that MAPK-related signaling pathways were involved in wound healing. MAPK activation affected the proliferation, migration, and apoptosis of M1-like macrophages and delays the wound healing process after prostate surgery [33]. Glial cell line-derived neurotrophic factor (GDNF) promoted barrier maturation in immature enterocytes cells by inactivation of p38 MAPK signaling [34]. Delbue et al. found that inhibition of the ERK pathway rescued the tight junctional barrier defect in IEC cells [35]. Reactive oxygen species (ROS) is an important and common messenger produced in various environmental stresses and is known to activate many kinds of the MAPKs [36]. ALA may regulate MAPK signaling by eliminating excessive ROS produced after intestinal injury. In our study, we found that the repair of intestinal epithelial injury by ALA may be associated with the inactivation of the PI3K/AKT, JNK, and p38 MAPK signaling pathways (Figure 3), but further verification is needed. The difference in ALA inhibition of AKT, JNK, and p38 may be because they affect angiogenesis and inflammation in different pathways [37]. It has been reported that oxidative stress activates p38 MAPK signaling pathway and leads to a decrease in the expression of TJP [38]; this might be one of the reasons why ALA increased ZO-1 expression in our study.

5. Conclusion

In conclusion, we have demonstrated clearly that ALA increased NCM460 and Caco-2 cells proliferation and migration and increased the expression of tight junction factors ZO-1 and OCLN. Moreover, we found that the positive effect of ALA on intestinal epithelial injury repair may be related to MAPK signaling pathways. Our results provided a theoretical basis for the future development of ALA in treatment of intestinal injury.

Data Availability

The datasets used and analyzed during the current study are available from the corresponding authors on reasonable request.

Conflicts of Interest

There are no conflicts of interest for all the authors.

Authors' Contributions

Yu Yang and Yong Xiao contributed equally to this work.

Acknowledgments

References

[1] M. Iizuka and S. Konno, "Wound healing of intestinal epithelial cells," *World Journal of Gastroenterology*, vol. 17, no. 17, pp. 2161–2171, 2011.

[2] G. Harris, R. Kuo Lee, and W. Chen, "Role of toll-like receptors in health and diseases of gastrointestinal tract," *World Journal of Gastroenterology*, vol. 12, no. 14, pp. 2149–2160, 2006.

[3] A. Andou, T. Hisamatsu, S. Okamoto et al., "Dietary histidine ameliorates murine colitis by inhibition of proinflammatory cytokine production from macrophages," *Gastroenterology*, vol. 136, no. 2, 2009.

[4] G. Aviello and U. G. Knaus, "ROS in gastrointestinal inflammation: rescue or sabotage?," *British Journal of Pharmacology*, vol. 174, no. 12, pp. 1704–1718, 2017.

[5] L. Packer, E. H. Witt, and H. J. Tritschler, "Alpha-lipoic acid as a biological antioxidant," *Free Radical Biology & Medicine*, vol. 19, no. 2, pp. 227–250, 1995.

[6] A. Solmonson and R. J. DeBerardinis, "Lipoic acid metabolism and mitochondrial redox regulation," *The Journal of Biological Chemistry*, vol. 293, no. 20, pp. 7522–7530, 2018.

[7] L. Packer, "α-Lipoic acid: a metabolic antioxidant which regulates NF-κB signal transduction and protects against oxidative injury," *Drug Metabolism Reviews*, vol. 30, no. 2, pp. 245–275, 1998.

[8] A. Maczurek, K. Hager, M. Kenklies et al., "Lipoic acid as an anti-inflammatory and neuroprotective treatment for Alzheimer's disease," *Advanced Drug Delivery Reviews*, vol. 60, no. 13-14, pp. 1463–1470, 2008.

[9] D. Tibullo, G. Li Volti, C. Giallongo et al., "Biochemical and clinical relevance of alpha lipoic acid: antioxidant and anti-inflammatory activity, molecular pathways and therapeutic potential," *Inflammation Research*, vol. 66, no. 11, pp. 947–959, 2017.

[10] A. Guven, T. Tunc, T. Topal et al., "α-Lipoic acid and ebselen prevent ischemia/reperfusion injury in the rat intestine," *Surgery Today*, vol. 38, no. 11, pp. 1029–1035, 2008.

[11] S. Varasteh, J. Fink-Gremmels, J. Garssen, and S. Braber, "α-Lipoic acid prevents the intestinal epithelial monolayer damage under heat stress conditions: model experiments in Caco-2 cells," *European Journal of Nutrition*, vol. 57, no. 4, pp. 1577–1589, 2018.

[12] P. P. Trivedi and G. B. Jena, "Role of α-lipoic acid in dextran sulfate sodium-induced ulcerative colitis in mice: studies on inflammation, oxidative stress, DNA damage and fibrosis," *Food and Chemical Toxicology*, vol. 59, pp. 339–355, 2013.

[13] W. J. Zhang and B. Frei, "α-Lipoic acid inhibits TNF-a-induced NF-κB activation and adhesion molecule expression in human aortic endothelial cells," *The FASEB Journal*, vol. 15, no. 13, pp. 2423–2432, 2001.

[14] R. Uchida, H. Okamoto, N. Ikuta et al., "Investigation of enantioselective membrane permeability of α-lipoic acid in Caco-2 and MDCKII cell," *International Journal of Molecular Sciences*, vol. 17, no. 2, 2016.

[15] J. Lee, H. Jang, S. Park et al., "Platelet-rich plasma activates AKT signaling to promote wound healing in a mouse model of radiation-induced skin injury," *Journal of Translational Medicine*, vol. 17, no. 1, p. 295, 2019.

[16] S. Saika, Y. Okada, T. Miyamoto et al., "Role of p38 MAP kinase in regulation of cell migration and proliferation in healing corneal epithelium," *Investigative Ophthalmology & Visual Science*, vol. 45, no. 1, pp. 100–109, 2004.

[17] E. G. Harper, S. M. Alvares, and W. G. Carter, "Wounding activates p38 map kinase and activation transcription factor 3 in leading keratinocytes," *Journal of Cell Science*, vol. 118, no. 15, pp. 3471–3485, 2005.

[18] A. Bhattacharyya, R. Chattopadhyay, S. Mitra, and S. E. Crowe, "Oxidative stress: an essential factor in the pathogenesis of gastrointestinal mucosal diseases," *Physiological Reviews*, vol. 94, no. 2, pp. 329–354, 2014.

[19] G. A. Weiss and T. Hennet, "Mechanisms and consequences of intestinal dysbiosis," *Cellular and Molecular Life Sciences*, vol. 74, no. 16, pp. 2959–2977, 2017.

[20] A. U. Dignass, "Mechanisms and modulation of intestinal epithelial repair," *Inflammatory Bowel Diseases*, vol. 7, no. 1, pp. 68–77, 2001.

[21] L. Weichselbaum and O. D. Klein, "The intestinal epithelial response to damage," *Science China. Life Sciences*, vol. 61, no. 10, pp. 1205–1211, 2018.

[22] B. Salehi, Y. Berkay Yilmaz, G. Antika et al., "Insights on the use of alpha-lipoic acid for therapeutic purposes," *Biomolecules*, vol. 9, no. 8, 2019.

[23] J. G. Leu, S. A. Chen, H. M. Chen et al., "The effects of gold nanoparticles in wound healing with antioxidant epigallocatechin gallate and α-lipoic acid," *Nanomedicine*, vol. 8, no. 5, pp. 767–775, 2012.

[24] H. Sammour, A. Elkholy, R. Rasheedy, and E. Fadel, "The effect of alpha lipoic acid on uterine wound healing after primary cesarean section: a triple-blind placebo-controlled parallel-group randomized clinical trial," *Archives of Gynecology and Obstetrics*, vol. 299, no. 3, pp. 665–673, 2019.

[25] E.-Y. Lee, J. Y. Yu, A. R. Paek et al., "Targeting TJP1 attenuates cell-cell aggregation and modulates chemosensitivity against doxorubicin in leiomyosarcoma," *Journal of Molecular Medicine (Berlin, Germany)*, vol. 98, no. 5, pp. 761–773, 2020.

[26] T. Volksdorf, J. Heilmann, S. A. Eming et al., "Tight junction proteins claudin-1 and occludin are important for cutaneous wound healing," *The American Journal of Pathology*, vol. 187, no. 6, pp. 1301–1312, 2017.

[27] M. Rawat, M. Nighot, R. Al-Sadi et al., "IL1B increases intestinal tight junction permeability by up-regulation of MIR200C-3p, which degrades occludin mRNA," *Gastroenterology*, vol. 159, no. 4, pp. 1375–1389, 2020.

[28] V. P. Dadhania, D. N. Tripathi, A. Vikram, P. Ramarao, and G. B. Jena, "Intervention of α-lipoic acid ameliorates methotrexate-induced oxidative stress and genotoxicity: a study in rat intestine," *Chemico-Biological Interactions*, vol. 183, no. 1, pp. 85–97, 2010.

[29] X. Cai, X. Chen, X. Wang et al., "Pre-protective effect of lipoic acid on injury induced by H2O2 in IPEC-J2 cells," *Molecular and Cellular Biochemistry*, vol. 378, no. 1-2, pp. 73–81, 2013.

[30] M. Cargnello and P. P. Roux, "Activation and function of the MAPKs and their substrates, the MAPK-activated protein kinases," *Microbiology and Molecular Biology Reviews*, vol. 75, no. 1, pp. 50–83, 2011.

[31] J. Yue and J. M. Lopez, "Understanding MAPK signaling pathways in apoptosis," *International Journal of Molecular Sciences*, vol. 21, no. 7, 2020.

[32] E. F. Wagner and A. R. Nebreda, "Signal integration by JNK and p38 MAPK pathways in cancer development," *Nature Reviews. Cancer*, vol. 9, no. 8, pp. 537–549, 2009.

[33] Z. Deng, F. Shi, Z. Zhou et al., "M1 macrophage mediated increased reactive oxygen species (ROS) influence wound healing via the MAPK signaling in vitro and in vivo," *Toxicology and Applied Pharmacology*, vol. 366, pp. 83–95, 2019.

[34] M. Meir, S. Flemming, N. Burkard et al., "Glial cell line-derived neurotrophic factor promotes barrier maturation and wound healing in intestinal epithelial cells in vitro," *American Journal of Physiology. Gastrointestinal and Liver Physiology*, vol. 309, no. 8, pp. G613–G624, 2015.

[35] D. Delbue, L. Lebenheim, D. Cardoso-Silva et al., "Reprogramming intestinal epithelial cell polarity by Interleukin-22," *Frontiers In Medicine*, vol. 8, p. 656047, 2021.

[36] S. K. Jalmi and A. K. Sinha, "ROS mediated MAPK signaling in abiotic and biotic stress- striking similarities and differences," *Frontiers in Plant Science*, vol. 6, p. 769, 2015.

[37] G. Yu, H. Yu, Q. Yang et al., "Vibrio harveyi infections induce production of proinflammatory cytokines in murine peritoneal macrophages via activation of p 38 MAPK and NF-κB pathways, but reversed by PI3K/AKT pathways," *Developmental and Comparative Immunology*, vol. 127, p. 104292, 2022.

[38] J. Yu, F. Liu, P. Yin et al., "Involvement of oxidative stress and mitogen-activated protein kinase signaling pathways in heat stress-induced injury in the rat small intestine," *Stress*, vol. 16, no. 1, pp. 99–113, 2013.

Research Article

Alterations of the Gut Microbiome in Chinese Zhuang Ethnic Patients with Sepsis

Jieyang Yu [iD],[1,2] Hongping Li [iD],[3] Jingjie Zhao [iD],[4] Yanhua Huang [iD],[5] Chunlei Liu [iD],[2] Pengfei Yang [iD],[2] Dinggui Lu [iD],[6] Jian Song [iD],[1] and Lingzhang Meng [iD][1]

[1]*Center for Systemic Inflammation Research (CSIR), School of Preclinical Medicine, Youjiang Medical University for Nationalities, Baise, Guangxi Province, China*
[2]*Baise Maternal and Child Hospital, Baise, Guangxi Province, China*
[3]*Neonatal Intensive Care Unit, Shenzhen Children's Hospital, Shenzhen, Guangdong Province, China*
[4]*Life Science and Clinical Research Center, The Affiliated Hospital of Youjiang Medical University for Nationalities, Baise, Guangxi Province, China*
[5]*Department of Critical Care Medicine, People's Hospital of Baise, Baise, Guangxi Province, China*
[6]*Trauma Center, Affiliated Hospital of Youjiang Medical University for Nationalities, Baise, Guangxi Province, China*

Correspondence should be addressed to Dinggui Lu; dinggui.lu@ymun.edu.cn, Jian Song; songj@uni-muenster.de, and Lingzhang Meng; lingzhang.meng@ymun.edu.cn

Objectives. Sepsis is characterized as a dysregulated host immune response to infection and has been known to be closely associated with the gut microbiome. This study was aimed at investigating the gut microbial profiles of Zhuang ethnic patients with sepsis. *Method.* Eleven Zhuang ethnic patients with sepsis and 20 healthy individuals (controls) were recruited at the Baise City People's Hospital, China. Their gut microbial community profiles were analyzed by 16S rRNA gene sequencing using the Illumina MiSeq system. *Results.* The gut microbial community of patients with sepsis was significantly altered compared to that of the healthy individuals based on the results of principal coordinate analysis and microbial ecological networks. Additionally, significantly lower microbial alpha diversity was observed in patients with sepsis than in healthy individuals. In particular, the enrichment of *Bilophila*, *Burkholderia*, *Corynebacterium*, and *Porphyromonas*, along with the reduced abundance of a large number of short-chain fatty acid-producing microbes, including *Roseburia*, *Bifidobacterium*, *Faecalibacterium*, *Coprococcus*, *Blautia*, *Clostridium*, *Ruminococcus*, and *Anaerostipe* was observed in patients with sepsis compared to the control group. Moreover, patients with sepsis could be effectively classified based on the abundance of these bacteria using a support vector machine algorithm. *Conclusion.* This study demonstrated significant differences in the gut microbiome between Zhuang ethnic patients with sepsis and healthy individuals. In the future, it is necessary to determine whether such alterations are the cause or consequence of sepsis.

1. Introduction

Sepsis is a life-threatening organ dysfunction syndrome characterized as a dysregulated immune response to infection [1, 2]. It is a major public health problem, as it accounts for a remarkable proportion of deaths of hospitalized patients worldwide, especially those in the intensive care unit [2–4]. Therefore, the pathogenesis of sepsis has attracted wide attention in recent years. Most of the studies

aiming to unravel the etiology of sepsis have focused on the role of the host immune responses [5]. Culture-independent methods such as 16S rRNA and shotgun metagenomic sequencing have revealed that the gut microbiome is crucial for the development and maturation of the host immune system [6]. Some microbes directly regulate host immune homeostasis by enhancing immunoglobulin A production and T-helper-17 cell differentiation [7]. Additionally, some of their products, such as lipopolysaccharides

and short-chain fatty acids (SCFAs), stimulate Toll-like receptor 4- (TLR-4-) positive epithelial cells and dendritic cells [8] and activate the development of regulatory T cells [7].

Increasing evidence supports the existence of a link between the gut microbiome and sepsis [9, 10]. Several studies using preclinical models and on hospitalized patients have reported that the risk of bloodstream infections and critical illness increases when gut microbiome homeostasis is disrupted [11–13]. Zeng et al. found that some gut bacteria can induce the production of protective IgG through the secretion of specific antigens, thereby contributing to the control of systemic infections [14]. Deshmukh et al. demonstrated that the gut microbiome regulates sepsis in neonatal mice by affecting neutrophil homeostasis [15]. Additionally, probiotic supplementation is associated with a reduced risk of sepsis in patients undergoing elective gastrointestinal surgery [16] and also reduces the risk of late-onset sepsis in preterm infants [17]. Finally, it has been reported that fecal microbiota transplantation can restore the innate immune response of patients with sepsis, contribute to pathogen clearance, and regulate SCFA-producing microbes [18, 19].

Altogether, these findings support the association between gut microbiota disruption and the risk of sepsis. This study was aimed at further studying this relationship in a cohort of patients belonging to the Zhuang ethnicity. For this purpose, we investigated the characteristics of the gut microbiota in patients with sepsis using 16S rRNA gene sequencing.

2. Methods

2.1. Study Cohort. All individuals in this study were recruited from Baise City People's Hospital (Guangxi Zhuang Autonomous Region, China) from January to April 2021. All of them provided written informed consent. After excluding the patients who had undergone organ transplantation, long-term immunosuppressive therapy, or developed tumors, a total of 31 individuals were recruited for the analysis. In total, 11 patients were categorized into the sepsis (SEP) group, while 20 healthy individuals who received no antibiotics or probiotics in the last 3 months were categorized as the healthy control (CTRL) group. Sepsis was diagnosed according to the Sepsis 3.0 guidelines (https://rebelem.com/sepsis-3-0). Clinical information was collected and summarized by well-trained clinicians according to standard procedures. The study protocol was approved by the Ethical Committee of Baise City People's Hospital.

2.2. Stool Sample Collection and Sequencing. Stool samples were collected in sterile containers, snap-frozen in dry ice, and stored in the research laboratory at −80°C until further use. The samples of patients with sepsis were collected prior to antibiotic treatment. Total bacterial DNA was extracted from stool samples using the QIAamp Fast DNA Stool Mini Kit (Qiagen, Germany) following the manufacturer's instructions. The V3-V4 region of the 16S rRNA gene was amplified from the extracted DNA using PCR primers 338F (5′-ACTCCTACGGGAGGCAGCAG-3′) and 806R

(5′-GGACTACHVGGGTWTCTAAT-3′). PCR products were mixed at equidensity ratios. Qiagen Gel Extraction Kit was used for purification (Qiagen, Germany). The prepared library was sequenced on an Illumina MiSeq platform with a 300 bp paired-end read mode.

2.3. Gut Microbiota and Statistical Analyses. 16S rRNA gene sequencing analysis, including raw sequence filtering and taxonomic classification, was performed as previously described [20]. The bioinformatic software package QIIME2 (version 2020.11) was used to analyze the 16S rRNA gene sequences [21]. The paired reads were assembled and denoised with the DADA2 package [22] using the "qiime dada2 denoise-paired" command in QIIME2. The command "qiime feature-classifier classify-sklearn" was used to assign sequences to taxonomy against the Greengenes database. Metrics of Shannon's index, Pielou's evenness index, observed feature number, and unweighted and weighted UniFrac distances were calculated using the command "qiime phylogeny align-to-tree-mafft-fasttree" and "qiime diversity core-metrics-phylogenetic" at a sampling depth of 10,000 reads. Metabolic function prediction was performed using PICRUSt2 software [23] with the "qiime picrust2 full-pipeline" command.

Principal coordinate analysis (PCoA) based on unweighted and weighted UniFrac distances was used to estimate differences in the beta diversity, accompanied by permutational multivariate analysis of variance (PERMANOVA) to assess the significance of community dissimilarity using the "vegan" R package. Linear discriminant analysis (LDA) was used to estimate the differentially abundant taxa with the linear discriminate analysis of effect size (LEfSe) software between the two groups ($P < 0.05$) [24]. The microbial ecological network was constructed using SpiecEasi software [25] and visualized using Gephi software. STAMP software was used to investigate the significantly different metabolic pathways between the two groups [26].

Characteristics were summarized as means (± standard deviations) for continuous variables and ratio (%) for categorical variables. Differences in these characteristics were assessed using t-tests and X^2 tests. All analyses were performed using R software (v 3.6.3). The differences were considered statistically significant at $P < 0.05$.

A classification model was built to classify patients with sepsis based on the significantly different genera using a support vector machine (SVM) algorithm with 10-fold cross-validation. The area under the curve (AUC) was calculated to evaluate the model's performance.

3. Results

3.1. Characteristics of Study Participants. A total of 31 Zhuang ethnic individuals were enrolled in this study. All participants were aged between 65 and 98 years. The socio-demographic and clinical characteristics of all the participants are summarized in Table 1. According to the statistical analysis results, there were no significant differences in age or sex between the groups. Compared to the CTRL group, patients with sepsis had higher levels of

Table 1: Demographic and clinical characteristics of the two groups.

Characteristic	SEP ($n = 11$)	Ctrl ($n = 20$)	P value
Age (years)	74.45 ± 10.23	70.35 ± 1.57	0.09
Male/female	7/4	12/8	1
CRP (mg/L)	48.26 ± 61.83	1.98 ± 2.78	<0.01**
IL-6 (pg/mL)	102.18 ± 157.66	27.39 ± 33.42	<0.05*
HBP (ng/mL)	66.17 ± 63.82	8.86 ± 4.36	<0.01**

SEP: Sepsis; Ctrl: Healthy controls; CRP: C-reactive protein; IL-6: Interleukin-6; HBP: Heparin-binding protein.

C-reactive protein (CRP), interleukin- (IL-) 6, and heparin-binding protein (HBP).

3.2. Overall Structure Diversity of Gut Bacterial Communities.

To evaluate the overall characteristics of the gut microbiome, alpha diversity estimators such as observed feature number, Pielou, and Shannon indexes were compared. As shown in Figure 1, the observed feature number of the CTRL group was 105.5 ± 33.57, which was significantly higher than that of the SEP group (68.36 ± 43.49, $P < 0.05$). The Pielou index was also significantly lower in the SEP group (0.59 ± 0.19) than in the CTRL group (0.77 ± 0.09, $P < 0.05$). Moreover, patients with sepsis had a significantly lower value of the Shannon index than that of the healthy individuals (3.48 ± 1.56 versus 5.08 ± 0.96, $P < 0.05$).

PCoA was performed on weighted and unweighted Uni-Frac distances using PERMANOVA. Obvious separations could be observed between SEP and healthy groups both on unweighted ($R^2 = 0.08$, $P = 0.004$, Figure 2(a)) and weighted UniFrac distances ($R^2 = 0.10$, $P = 0.007$, Figure 2(b)).

3.3. Bacterium Analysis of SEP and CTRL Groups.

Gut microbiome communities were dominated by the phyla Actinobacteria, Bacteroidetes, Firmicutes, Fusobacteria, Proteobacteria, Tenericutes, and Verrucomicrobia in both groups (Figure 3(a)). The most abundant genera in both groups were *Alistipes, Bacteroides, Bifidobacterium, Blautia, Collinsella, Coprococcus, Dorea, Enterococcus, Faecalibacterium, Gemmiger, Oscillospira, Phascolarctobacterium, Prevotella, Roseburia, Ruminococcus*, and *Streptococcus* (Figure 3(b)). In the SEP group, the mean relative abundances of *Bifidobacterium* (0.08% versus 3.69%), *Blautia* (3.24% versus 6.91%), *Coprococcus* (1.59% versus 4.98%), *Faecalibacterium* (1.10% versus 4.48%), *Gemmiger* (0.64% versus 2.32%), *Roseburia* (0.25% versus 7.59%), *Ruminococcus* (5.37% versus 11.03%), and *Streptococcus* (2.42% versus 3.53%) were decreased compared to the CTRL group. The mean relative abundances of *Bacteroides* (10.23% versus 6.05%), *Enterococcus* (27.9% versus 0.09%), and *Prevotella* (5.53% versus 2.95%) were comparatively increased in the SEP group.

Furthermore, we used LEfSe software to investigate the significant differences in genera between the individuals with and without sepsis. The results demonstrated that the relative abundance of *Bilophila, Burkholderia, Corynebacterium*, and *Porphyromonas* was higher in the SEP group than in the CTRL group, whereas that of *Roseburia, Oxalobacter,*

Bifidobacterium, Faecalibacterium, Coprococcus, Blautia, Clostridium, Ruminococcus, Gemmiger, Dorea, Paraprevotella, Butyricicoccus, Turicibacter, Anaerostipes, and *SMB53* was lower in the SEP group than in the CTRL group (Figure 3(c)).

Next, to explore the efficacy of classification based on these significantly different genera in the SEP group, we built a classification model using an SVM algorithm with 10-fold cross-validation. The receiver operating characteristic curve of the model is shown in Figure 3(d) and has an AUC of 0.85. After combining with the CRP, IL-6, and HBP levels, the AUC increased to 0.986 (Figure 3(e)).

Additionally, Pearson correlation analysis was performed to evaluate the associations between the differential genera and CRP, HBP, and IL6 levels (Figure 3(f)). The abundance of the genus *Bilophila* was positively correlated with CRP ($R^2 = 0.55$, $P < 0.01$) and HBP ($R^2 = 0.36$, $P = 0.045$) levels; that of *Porphyromonas* was positively correlated with IL-6 level ($R^2 = 0.94$, $P < 0.01$); that of *Bacteroides* was positively correlated with CRP level ($R^2 = 0.40$, $P = 0.026$); and that of *Prevotella* was positively correlated with IL-6 level ($R^2 = 0.85$, $P < 0.01$).

3.4. Functional Alterations between SEP and CTRL Groups.

We analyzed the metabolic pathways in the individuals belonging to both groups. The predicted functions were performed using PICRUSt2 software. The fatty acid elongation pathway was significantly enriched in the gut microbiome of the SEP group compared to that of CTRL. The tricarboxylic acid (TCA) cycle VI, octane oxidation, and L-arginine biosynthesis II (acetyl cycle) were higher in the gut microbiome of the CTRL group (Figure 4(a)).

3.5. Different Microbial Ecological Networks between SEP and CTRL Groups.

Microorganisms in the gut construct a stable ecological network with cooccurrence, competition, and antagonistic relationships. To investigate the microbial network at the genus level, we used the SpiecEasi software. The microbial ecological network of the CTRL group presented 84 nodes and 131 (Figure 4(b)). However, the microbial ecological network of patients with sepsis was simpler, presenting only 80 nodes and 77 edges (Figure 4(c)).

4. Discussion

Sepsis is a major public health issue, with more than one million sepsis-related deaths occurring in China in 2015 (Li et al., 2018). Increasing evidence supports that gut microbial disruption predisposes patients to sepsis, thereby presenting as a potential therapeutic target in sepsis management [2, 10]. As the Zhuang ethnic minority is the largest Chinese minority group, in this study, we aimed to characterize the gut microbiota in patients belonging to the Zhuang ethnicity suffering from sepsis. Using PCoA, we demonstrated that patients with sepsis present a significantly different microbial community and a different microbial ecological network than the healthy individuals. In addition, patients with sepsis had significantly lower microbiome alpha diversity, which is consistent with a previous study
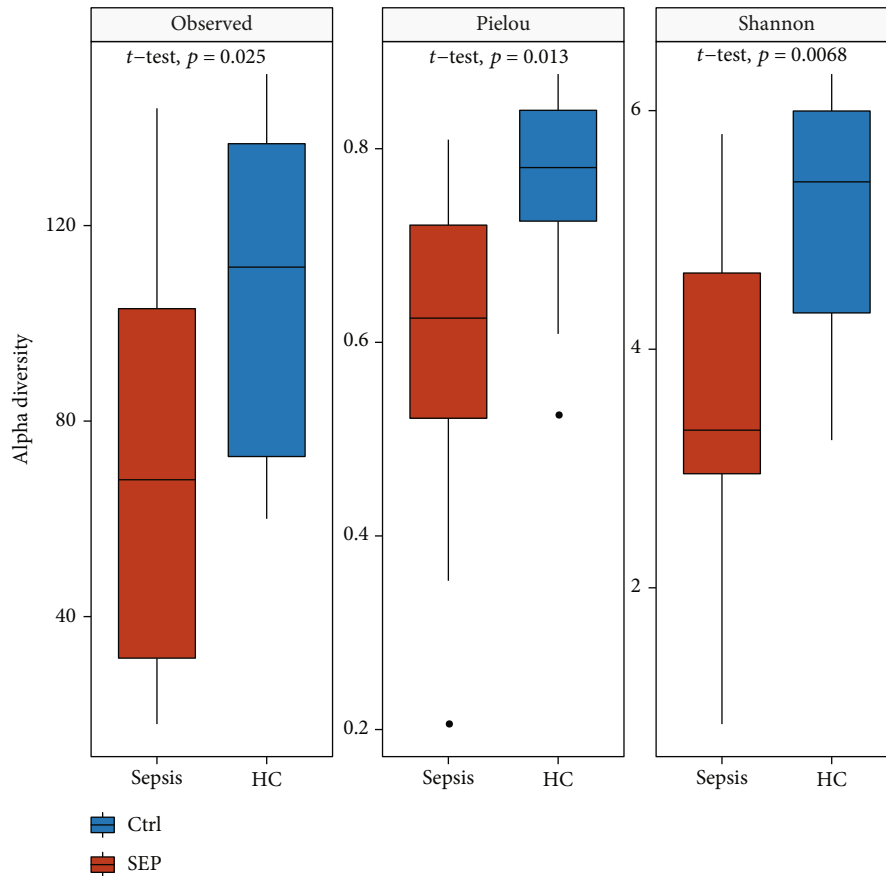
FIGURE 1: Comparisons of alpha diversity indexes between sepsis (SEP) and healthy control (Ctrl) group. Significant lower observed feature number, Pielou, and Shannon indexes were observed in patients with sepsis.

(a)

(b)
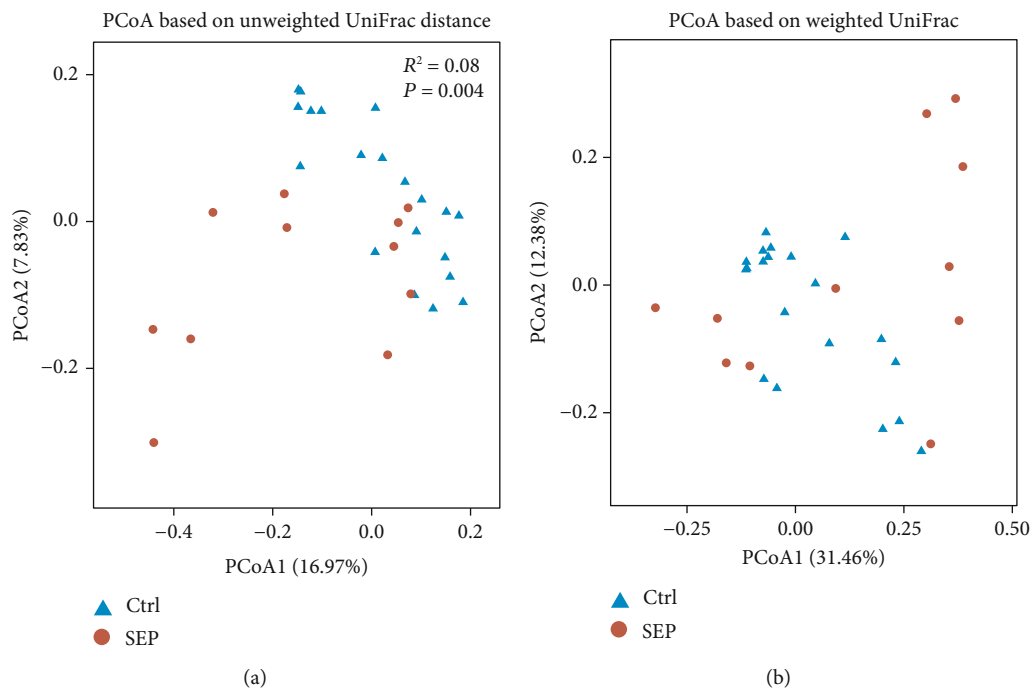
FIGURE 2: Principal coordinate analysis (PCoA) plot based on unweighted and weighted UniFrac distances with PERMANOVA analysis. (a). The PCoA plot based on unweighted UniFrac distance. (b). The PCoA plot based on weighted UniFrac distance.

(a)

(b)

(c)
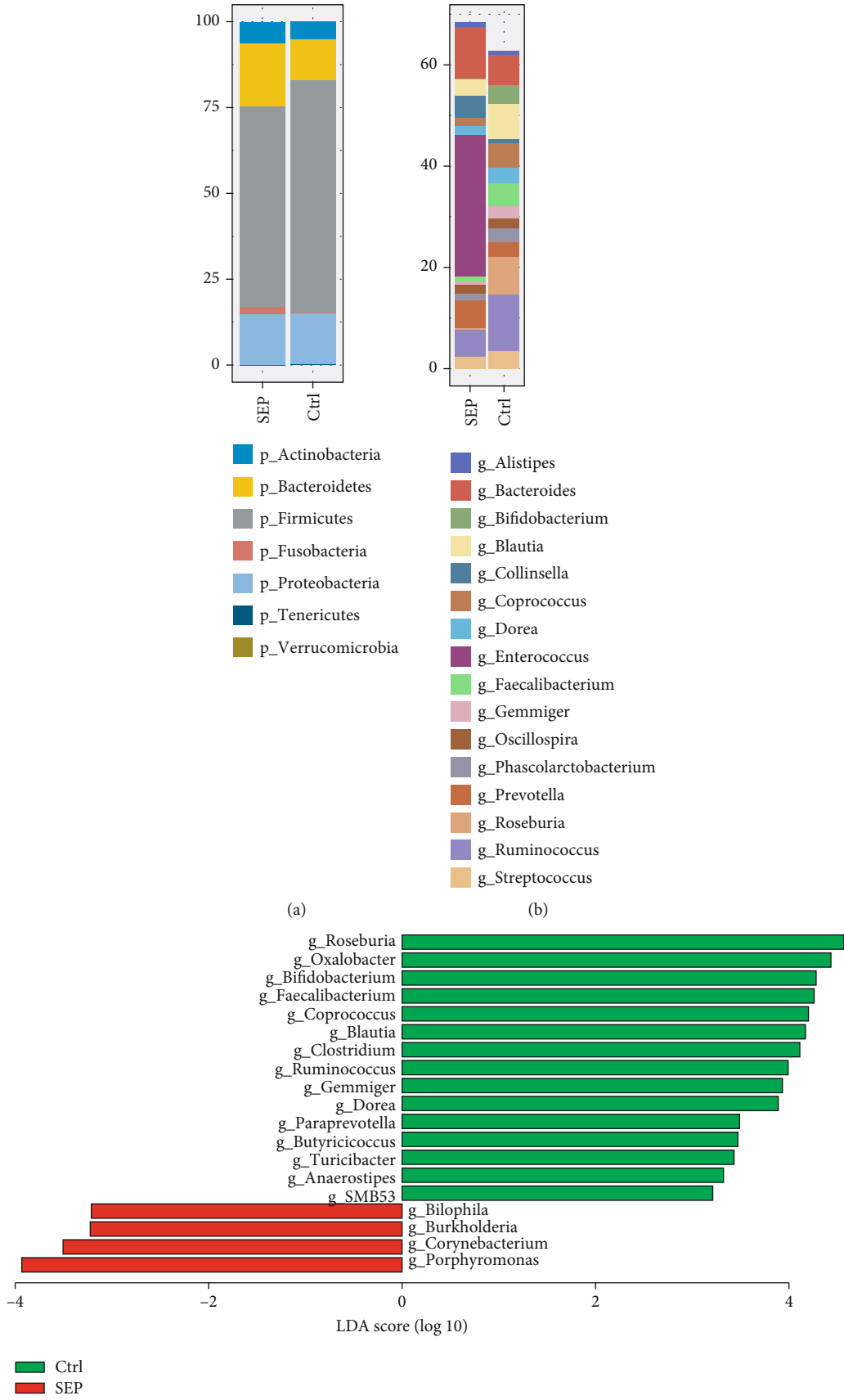
Figure 3: Continued.

(d)

(e)

(f)
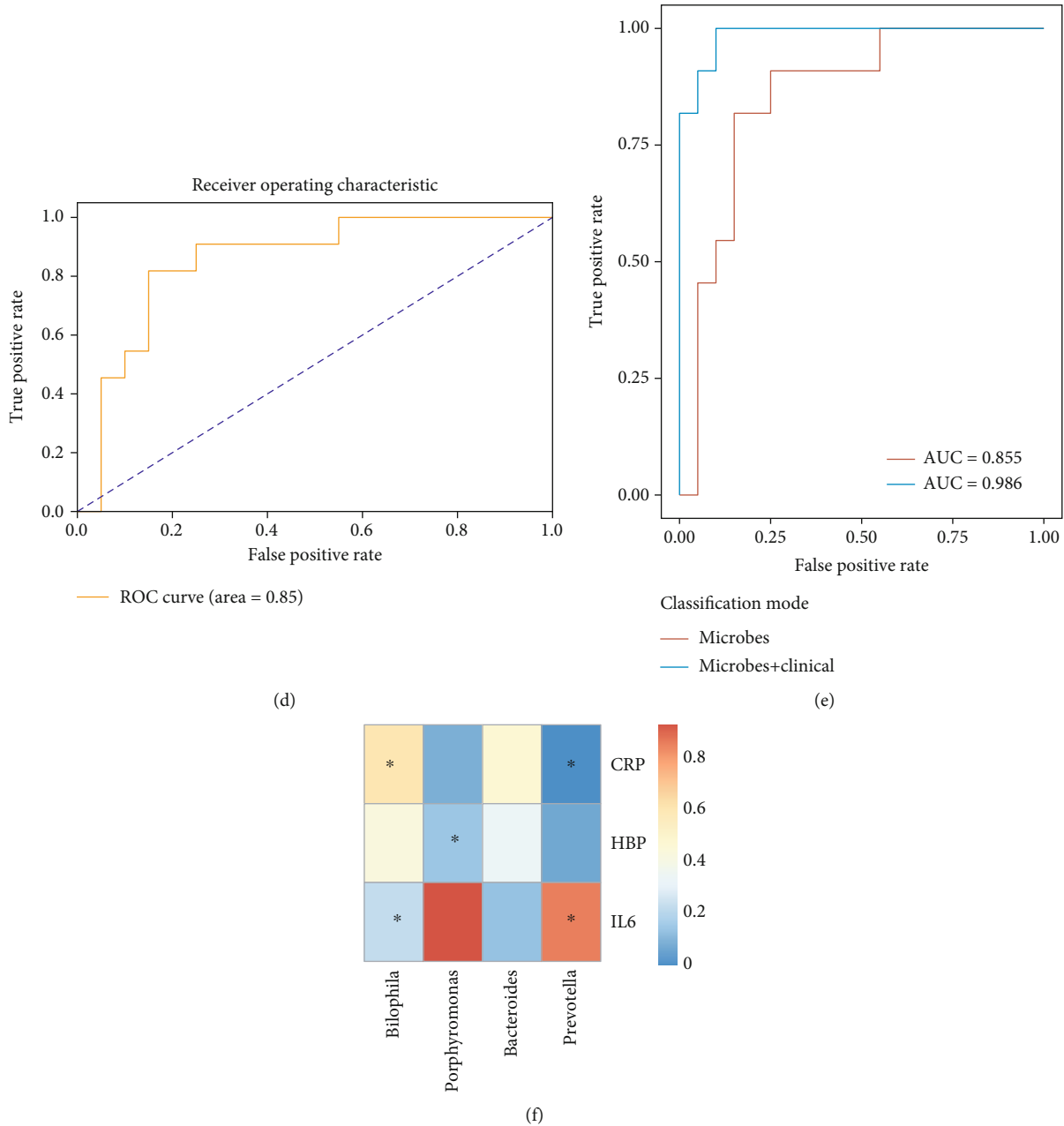
FIGURE 3: Microbial profiles of the gut microbiota in the sepsis (SEP) and healthy control (Ctrl) groups. (a). Relative abundances of the dominant phyla. (b). Relative abundances of the abundant genera. (c). Differences in microbial genera between SEP and Ctrl groups. (d). Receiver operating characteristic curve of the classification mode for sepsis based on different genera using support vector machine algorithm. (e). Receiver operating characteristic curve of the classification mode for sepsis based on different genera in combination of clinical features using support vector machine algorithm. (f). Correlations between some abundant microbes with C-reactive protein (CRP), heparin-binding protein (HBP), and (CRP) and interleukin-6 (IL-6) levels separately.

[27]. Additionally, a previous study reported that enhancing gut microbiome diversity in mice could increase sepsis survival by regulating the immune response [28]. Therefore, increasing the gut microbiome diversity may be beneficial in the treatment of patients with sepsis.

Increases in pathogenic intestinal bacteria and exuberant immune responses are often observed in patients with sepsis [10]. In this study, we observed that the commonly hospital-acquired pathogen *Enterococcus* was relatively frequent in patients with sepsis, which was in accordance with the results of a previous study [29]. Furthermore, compared to the healthy individuals, there were four genera significantly enriched in patients with sepsis, and 15 genera significantly decreased. Based on the abundance of these microbes, patients could be effectively classified as healthy individuals or patients with sepsis using an SVM algorithm. Among the four increased genera, *Bilophila* can produce lipopolysaccharides to stimulate the immune system via TLR-4 [30]. *Porphyromonas gingivalis* can regulate host innate immune signaling and induce inflammation [31]. In this study, the relative

(a)

(b) (c)
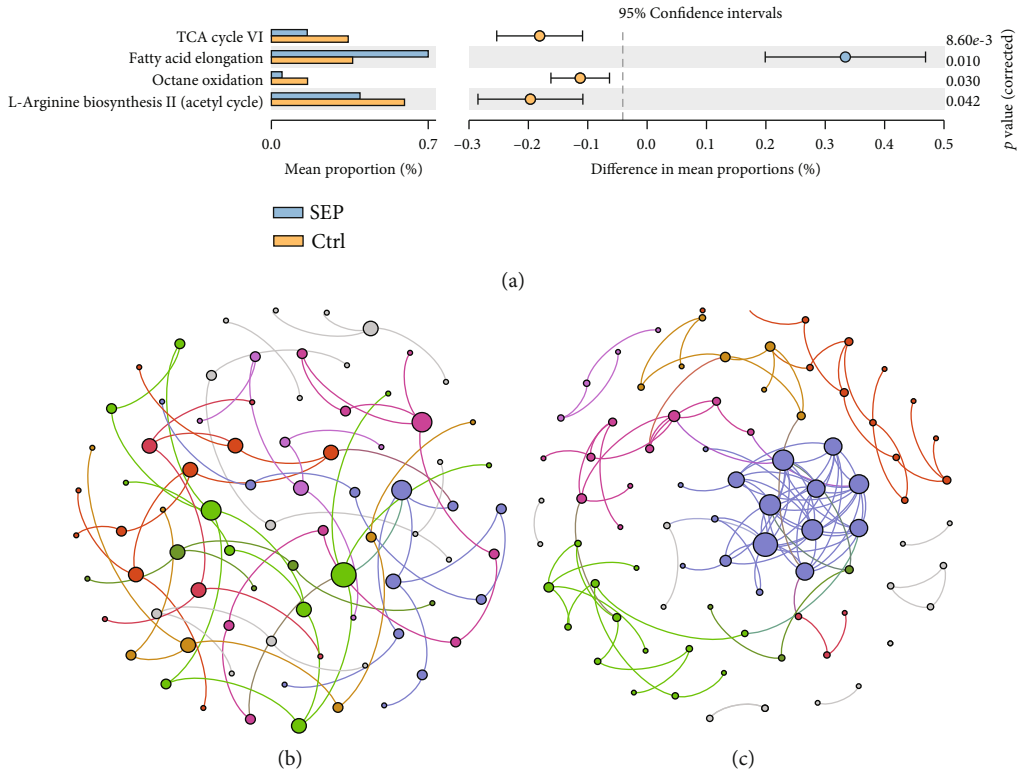
FIGURE 4: Functional metabolic pathways and microbial ecological network in the SEP and Ctrl groups. (a). Significantly different metabolic pathways between SEP and Ctrl groups. (b). Microbial ecological network of the gut microbiome in the patients with sepsis. (c). Microbial ecological network of the gut microbiome in the healthy individuals.

abundance of *Bilophila* was positively correlated with CRP and HBP levels, and the relative abundance of *Porphyromonas* was positively correlated with the IL-6 level. Their relative increase in patients with sepsis might prime the immune system for a robust proinflammatory response. Additionally, among the significantly decreased genera, *Roseburia, Bifidobacterium, Faecalibacterium, Coprococcus, Blautia, Clostridium, Ruminococcus,* and *Anaerostipes* can produce SCFAs [32]. Decreased production of SCFAs can enhance intestinal epithelial cell function [33], activate the development of regulatory T (Treg) cells [34], and decrease nuclear factor kappa B- (NF-κB-) regulated proinflammatory cytokines [35]. Hence, the significant decrease in SCFA-producing bacteria in patients with sepsis observed in this study might have adverse consequences for both gut integrity and systemic immunity.

Since an individual is born, the gut microbiota and host live in symbiotic homeostasis that influences the immune function, including T cell differentiation and activation, cytokine production, and local barrier function [2]. The alterations of the gut microbiome observed in this study might predispose individuals to sepsis by favoring the proliferation of pathogenic bacteria and decreasing the production of SCFAs, which would promote a dysregulated immune response. However, the findings of this study should be considered in light of its limitations, and larger prospective studies should be conducted to confirm this hypothesis. In this study, the sample size was relatively small, and all the individuals in this study were recruited from a single geographic

area without consideration of different demographics. Additionally, the alterations in microbial function and whether such microbial alterations in this study were the causes or consequences of sepsis were not clear. Studies with larger sample sizes, including individuals from different regions, conducting metagenomic and metaproteomic analyses, and experimental studies should be conducted in the future to further answer these questions.

Limitations of this study include, for example, lack of the delineation and the intermodulation between specific bacterium and host immune system; the relationship between gut microbiota and prognosis has not been explored due to limited sample size and the short-term observation period; in addition, this study failed to collect the biopsies from pregnant women which could be important for newborn cases. The above limitations deserve to draw attentions and should be answered in future study.

In conclusion, we identified dysbiosis of the gut microbiome in Zhuang ethnic patients with sepsis. Disruption of the gut microbiome may serve as a potential biomarker for early detection of sepsis risk. Our findings could help improve the understanding of the role of the gut microbiome in sepsis etiology and support preventive strategies based on the modulation of the gut microbiome.

Data Availability

The datasets and code generated and analyzed in this study are available from the corresponding author on request.

Conflicts of Interest

The authors declare that this research was conducted in the absence of any commercial or financial relationships that could be construed as potential conflicts of interest.

Authors' Contributions

LZM, JS, and DGL designed this study. JYY, HPL, and JJZ collected the samples and performed the data analysis for this study. YHH, CLL, and PFY performed the partial analysis for this study. Jieyang Yu, Hongping Li, and Jingjie Zhao contributed equally to this study.

Acknowledgments

References

[1] W. D. Miller, R. Keskey, and J. C. Alverdy, "Sepsis and the microbiome: a vicious cycle," *The Journal of Infectious Diseases*, vol. 223, Supplement_3, pp. S264–S269, 2021.

[2] B. W. Haak and W. J. Wiersinga, "The role of the gut microbiota in sepsis," *The Lancet. Gastroenterology & Hepatology*, vol. 2, no. 2, pp. 135–143, 2017.

[3] C. Rhee, R. Dantes, L. Epstein et al., "Incidence and trends of sepsis in US hospitals using clinical vs claims data, 2009–2014," *JAMA*, vol. 318, no. 13, pp. 1241–1249, 2017.

[4] L. Weng, X.-y. Zeng, P. Yin et al., "Sepsis-related mortality in China: a descriptive analysis," *Intensive Care Medicine*, vol. 44, no. 7, pp. 1071–1080, 2018.

[5] M. Singer, C. S. Deutschman, C. W. Seymour et al., "The third international consensus definitions for sepsis and septic shock (Sepsis-3)," *JAMA*, vol. 315, no. 8, pp. 801–810, 2016.

[6] H. Chung, S. J. Pamp, J. A. Hill et al., "Gut immune maturation depends on colonization with a host-specific microbiota," *Cell*, vol. 149, no. 7, pp. 1578–1593, 2012.

[7] N. Kamada, S. U. Seo, G. Y. Chen, and G. Núñez, "Role of the gut microbiota in immunity and inflammatory disease," *Nature Reviews. Immunology*, vol. 13, no. 5, pp. 321–335, 2013.

[8] E. G. Pamer, "Resurrecting the intestinal microbiota to combat antibiotic-resistant pathogens," *Science*, vol. 352, no. 6285, pp. 535–538, 2016.

[9] J. Baggs, J. A. Jernigan, A. L. Halpin, L. Epstein, K. M. Hatfield, and L. C. McDonald, "Risk of subsequent sepsis within 90 days after a hospital stay by type of antibiotic exposure," *Clinical Infectious Diseases*, vol. 66, no. 7, pp. 1004–1012, 2018.

[10] M. W. Adelman, M. H. Woodworth, C. Langelier et al., "The gut microbiome's role in the development, maintenance, and outcomes of sepsis," *Critical Care*, vol. 24, no. 1, p. 278, 2020.

[11] C. Ubeda, Y. Taur, R. R. Jenq et al., "Vancomycin-resistant enterococcus domination of intestinal microbiota is enabled by antibiotic treatment in mice and precedes bloodstream invasion in humans," *Journal of Clinical Investigation*, vol. 120, no. 12, pp. 4332–4341, 2010.

[12] J. S. Ayres, N. J. Trinidad, and R. E. Vance, "Lethal inflammasome activation by a multidrug-resistant pathobiont upon antibiotic disruption of the microbiota," *Nature Medicine*, vol. 18, no. 5, pp. 799–806, 2012.

[13] H. C. Prescott, R. P. Dickson, M. A. M. Rogers, K. M. Langa, and T. J. Iwashyna, "Hospitalization type and subsequent severe sepsis," *American Journal of Respiratory & Critical Care Medicine*, vol. 192, no. 5, pp. 581–588, 2015.

[14] M. Y. Zeng, D. Cisalpino, S. Varadarajan et al., "Gut microbiota-induced immunoglobulin G controls systemic infection by symbiotic bacteria and pathogens," *Immunity*, vol. 44, no. 3, pp. 647–658, 2016.

[15] H. S. Deshmukh, Y. Liu, O. R. Menkiti et al., "The microbiota regulates neutrophil homeostasis and host resistance to _Escherichia coli_ K1 sepsis in neonatal mice," *Nature Medicine*, vol. 20, no. 5, pp. 524–530, 2014.

[16] S. Arumugam, C. S. M. Lau, and R. S. Chamberlain, "Probiotics and synbiotics decrease postoperative sepsis in elective gastrointestinal surgical patients: a meta-analysis," *Journal of Gastrointestinal Surgery*, vol. 20, no. 6, pp. 1123–1131, 2016.

[17] S. C. Rao, G. K. Athalye-Jape, G. C. Deshpande, K. N. Simmer, and S. K. Patole, "Probiotic supplementation and late-onset sepsis in preterm infants: a meta-analysis," *Pediatrics*, vol. 137, no. 3, article e20153684, 2016.

[18] S. Han, S. Shannahan, and R. Pellish, "Fecal microbiota transplant," *Journal of Intensive Care Medicine*, vol. 31, no. 9, pp. 577–586, 2016.

[19] R. Keskey, J. T. Cone, J. R. DeFazio, and J. C. Alverdy, "The use of fecal microbiota transplant in sepsis," *Translational Research: Journal of Laboratory & Clinical Medicine*, vol. 226, pp. 12–25, 2020.

[20] M. Hall and R. G. Beiko, "16S rRNA gene analysis with QIIME2," in *Methods in Molecular Biology*, Humana Press, New York, NY, 2018.

[21] E. Bolyen, J. R. Rideout, M. R. Dillon et al., "Reproducible, interactive, scalable and extensible microbiome data science using QIIME 2," *Nature Biotechnology*, vol. 37, no. 8, pp. 852–857, 2019.

[22] B. J. Callahan, P. J. McMurdie, M. J. Rosen, A. W. Han, A. J. A. Johnson, and S. P. Holmes, "DADA2: high-resolution sample inference from Illumina amplicon data," *Nature Methods*, vol. 13, no. 7, pp. 581–583, 2016.

[23] G. M. Douglas, V. J. Maffei, J. R. Zaneveld et al., "PICRUSt2 for prediction of metagenome functions," *Nature Biotechnology*, vol. 38, no. 6, pp. 685–688, 2020.

[24] N. Segata, J. Izard, L. Waldron et al., "Metagenomic biomarker discovery and explanation," *Genome Biology*, vol. 12, no. 6, p. R60, 2011.

[25] Z. D. Kurtz, C. L. Müller, E. R. Miraldi, D. R. Littman, M. J. Blaser, and R. A. Bonneau, "Sparse and compositionally robust inference of microbial ecological networks," *PLoS Computational Biology*, vol. 11, no. 5, article e1004226, 2015.

[26] D. H. Parks, G. W. Tyson, P. Hugenholtz, and R. G. Beiko, "STAMP: statistical analysis of taxonomic and functional profiles," *Bioinformatics*, vol. 30, no. 21, pp. 3123-3124, 2014.

[27] Z. Liu, N. Li, H. Fang et al., "Enteric dysbiosis is associated with sepsis in patients," *FASEB Journal*, vol. 33, no. 11, pp. 12299–12310, 2019.

[28] K. T. Fay, N. J. Klingensmith, C. W. Chen et al., "The gut microbiome alters immunophenotype and survival from sepsis," *FASEB Journal*, vol. 33, no. 10, pp. 11258–11269, 2019.

[29] A. Ravi, F. D. Halstead, A. Bamford et al., "Loss of microbial diversity and pathogen domination of the gut microbiota in critically ill patients," *Microbial Genomics*, vol. 5, no. 9, article e000293, 2019.

[30] J. R. Caso, K. S. MacDowell, A. González-Pinto et al., "Gut microbiota, innate immune pathways, and inflammatory control mechanisms in patients with major depressive disorder," *Translational Psychiatry*, vol. 11, no. 1, p. 645, 2021.

[31] K. Y. How, K. P. Song, and K. G. Chan, "Porphyromonas gingivalis: an overview of periodontopathic pathogen below the gum line," *Frontiers in Microbiology*, vol. 7, p. 53, 2016.

[32] Y. Xu, Y. Zhu, X. Li, and B. Sun, "Dynamic balancing of intestinal short-chain fatty acids: the crucial role of bacterial metabolism," *Trends in Food Science & Technology*, vol. 100, pp. 118–130, 2020.

[33] Y. Zhao, F. Chen, W. Wu et al., "GPR43 mediates microbiota metabolite SCFA regulation of antimicrobial peptide expression in intestinal epithelial cells via activation of mTOR and STAT3," *Mucosal Immunology*, vol. 11, no. 3, pp. 752–762, 2018.

[34] Y. Furusawa, Y. Obata, S. Fukuda et al., "Commensal microbe-derived butyrate induces the differentiation of colonic regulatory T cells," *Nature*, vol. 504, no. 7480, pp. 446–450, 2013.

[35] D. Parada Venegas, M. K. De la Fuente, G. Landskron et al., "Short chain fatty acids (SCFAs)-mediated gut epithelial and immune regulation and its relevance for inflammatory bowel diseases," *Frontiers in Immunology*, vol. 10, p. 277, 2019.

Hindawi

Research Article

Overall Structural Alteration of Gut Microbiota and Relationships with Risk Factors in Patients with Metabolic Syndrome Treated with Inulin Alone and with Other Agents: An Open-Label Pilot Study

Ruiping Tian [1] **Jiahui Hong** [1] **Jingjie Zhao** [2] **Dengyuan Zhou** [3] **Yangchen Liu** [3] **Zhenshan Jiao** [4] **Jian Song** [5] **Yu Zhang** [4] **Lingzhang Meng** [5] and **Ming Yu** [1]

[1]*Department of Nutrition and Food Hygiene, School of Public Health, Tianjin Medical University, Tianjin, China*
[2]*Life Science and Clinical Research Center, Affiliated Hospital of Youjiang Medical University for Nationalities, Baise, Guangxi Province, China*
[3]*Department of General Family Medicine, Community Health Service Center of Zhongbei Town, Xiqing District, Tianjin, China*
[4]*Department of Dermatology, Tianjin Academy of Traditional Chinese Medicine Affiliated Hospital, Tianjin, China*
[5]*Center for Systemic Inflammation Research (CSIR), School of Preclinical Medicine, Youjiang Medical University for Nationalities, Baise, Guangxi Province, China*

Correspondence should be addressed to Yu Zhang; niuniuzy7375@aliyun.com, Lingzhang Meng; lingzhang.meng@ymun.edu.cn, and Ming Yu; minnieyu@tmu.edu.cn

Objective. The relative contribution of some products with prebiotic effects, such as inulin, together with medications specific to the human gut microbiome has not been comprehensively studied. The present study determined the potential for manipulating populations in the gut microbiome using inulin alone and combined with other agents in individuals with metabolic syndrome (MetS). The study also assessed whether there is relationship variability in multiple clinical parameters in response to intervention with the changes in the gut milieu. *Participants/Methods*. This single-centre, single-blinded, randomised community-based pilot trial randomly assigned 60 patients (mean age, 46.3 y and male, 43%) with MetS to receive either inulin, inulin+traditional Chinese medicine (TCM), or inulin+metformin for 6 months. Lipid profiles, blood glucose, and uric acid (UA) levels were analysed in venous blood samples collected after overnight fast of 8 h at baseline and at the end of the follow-up period. Microbiota from stool samples were taxonomically analysed using 16S RNA amplicon sequencing, and an integrative analysis was conducted on microbiome and responsiveness data at 6 months. *Results*. The results of 16S rRNA sequencing showed that inulin resulted in a higher proportion of Bacteroides at the endpoint compared with inulin+TCM and inulin+metformin ($p = 0.024$). More Romboutsia ($p = 0.043$), Streptococcus ($p < 0.001$), and Holdemanella ($p = 0.011$) were found in inulin+TCM and inulin+metformin samples. We further identified gut microbiota relationships with lipids, UA, and glucose that impact the development of MetS. *Conclusion*. Among the groups, inulin alone or combined with metformin or TCM altered specific gut microbiota taxa but not the general diversity. Accordingly, we analysed metabolites associated with microbiota that might provide more information about intrinsic differences. Consequently, a reliable method could be developed for treating metabolic syndrome in the future.

1. Introduction

Noncommunicable metabolic syndrome (MetS) is a growing public health concern worldwide. Metabolic syndrome is a constellation of metabolic disorders, characterised by abdominal adiposity, dyslipidaemia, low levels of high-density lipoprotein cholesterol (HDL. C), hypertension, and insulin resistance [1]. Metabolic syndrome directly

affects health *via* the development of cardiovascular and cerebrovascular-related diseases and increases the risk of cancer [2]. While the oral administration of drugs can improve patient outcomes in terms of metabolic indexes, little is known about the status of the gut microbiota in such patients [3].

The human gastrointestinal tract houses hundreds of thousands of bacterial species [4]. Dysbiosis of the gut microbiota and/or structural alterations can trigger diseases and disrupt the epithelial barrier, which elicits an increase in the release of the endotoxin, lipopolysaccharide, from gram-negative bacterial cell walls into the systemic circulation, which triggers proinflammatory cytokine secretion [5]. Hence, many studies of gut microbes have vaulted to prominence [6]. Evidence from studies of humans and other animals has revealed a link between gut microorganisms and various components of MetS [7, 8]. Prebiotics are defined as substrates that are selectively utilised by host microorganisms and confer health benefits [9]. The ILSI Europe Prebiotic Expert Group and Prebiotic Task Force then proposed the concept of prebiotic effects defined as follows: the selective stimulation of growth and/or activity(ies) of one or a limited number of microbial genus(era)/species in the gut microbiota that confer(s) health benefits on the host [10]. Products with a prebiotic effect have thus been assessed in clinical trials in an attempt to improve gut microbial dysbiosis [10]. Moreover, the manipulation of gut microbiota *via* prebiotic interventions has provided evidence that gut microbial modulation helps to improve components or complications of metabolic syndrome [7].

Prebiotics favour the growth of beneficial bacteria, particularly those that produce short-chain fatty acids (SCFAs). Increased SCFAs in the intestine are associated with slowed weight gain, protection against systemic inflammation by increasing the gut barrier function, and improved glucose and lipid metabolism [11]. Inulin, a non-digestible dietary fibre, is a common prebiotic.

Traditional Chinese medicine (TCM) is a form of polypharmacy with a history of thousands of years. Natural medicines and their resulting bioactivities have been considered as therapeutic strategies against diseases [12], including MetS [13]. Some TCMs significantly affect glucose and lipid metabolism by regulating the gut microbiota, particularly bacteria that degrade mucin, have anti-inflammatory properties, produce lipopolysaccharides and SCFAs, or have bile-salt hydrolase activity [14]. The instant medicinal food packet in the present study consisted of *Coptis chinensis*, *Atractylodes macrocephala*, Tangerine peel, Coke malt, medicated leaves (stir-fried), and Hawthorn fruit (charred) according to a specific formula (Supplementary Table 1). *Coptis chinensis* (*Huang-Lian*), a common herb in TCM, is clinically effective in treating dyslipidaemia and hypercholesterolaemia [15]. Hawthorn has also been widely applied to manage hyperlipidaemia and cardiovascular diseases [13]. Medicated leaves improve human immunity through antioxidant and anti-inflammatory activities that lead to regulation of the gut microflora balance [16].

Metformin is linked to the composition of gut microbiota [17], even in healthy humans [18]. It is also applicable to the treatment or prevention of hyperlipidaemia and cardiovascular diseases [19].

The ability of prebiotic mix to regulate microbial communities in the host and benefit from symbiotic relationships among strains to improve their effects have been investigated [20]. Here, a prebiotic mix is simply a combination of products with prebiotic effects that benefit host health. However, to the best of our knowledge, little is known about the effects of inulin when combined with other agents on improving gut microcommunities in individuals with MetS. Overall, we postulated that the prebiotic mix would enhance microbial diversity in the host and take advantage of commensal relationships among organisms to confer more benefits on hosts.

The present study is primarily aimed at determining the influences of these products on gut microbiota structure and composition in patients with MetS. A more complete picture of the microbiota profile might provide greater clarity in terms of prioritising treatment for metabolic disorders and paving the way for further investigation.

2. Methods

2.1. Diagnostic Criteria for MetS. Clinical MetS was diagnosed when at least three of the following five conditions were met: waist circumference ≥ 90 or ≥80 cm in men and women, respectively; blood pressure, 120/80–140/90 mmHg; triglycerides, 150–200 mg/dL; HDL, <40 or <50 mg/dL in men and women, respectively, and fasting glucose 100–125 mg/dL.

2.2. Study Population. Residents of Tianjin for >5 years and aged 35–65 years were included if they had no inflammatory gastrointestinal disease or a history of gastrointestinal surgery within 5 years and had not been prescribed with antibiotics or other medications (proton pump inhibitors and H_2 receptor antagonists) or dietary supplements (probiotics and prebiotics) or antacids that could affect the gut microbiota within 6 weeks before recruitment. They were provided with a pamphlet about the study during a physical examination and asked to participate in if eligible according to the above criteria. Written informed consent to participate was obtained from eligible 60 individuals who indicated an interest and met the inclusion criteria.

2.3. Intervention. All participants were randomly and equally assigned to take oral inulin, inulin+TCM formula, and inulin+metformin ($n = 20$ per group) for 6 months. They were instructed not to change their lifestyle, diet, and usual physical activities during the study and were contacted twice each month for 6 months by telephone or in-home visits to monitor side effects and compliance. None of the participants complained of adverse gastrointestinal reactions. All participants returned empty or remaining allocated packets to verify compliance at the endpoint.

2.4. Data Collection. Information about demographics and physical activity was collected from questionnaires. Physical activity was assessed based on whether the participants exercised daily. Body weight, height, waist circumference, and

blood pressure were measured by on-site nurses. Height and weight were measured using a calibrated height–weight meter. Waist circumference was measured at the level of 0.5–1 cm above the navel using a tape measure. Mean blood pressure was calculated from three reads on the same arm after 5 min of rest in a semiupright position. Fasting plasma samples were also collected at baseline and at the end of the study. Serum glucose, total triglycerides (TGs), high-density lipoprotein (HDL), low-density lipoprotein (LDL), total cholesterol (T-CHOL), and uric acid (UA) were measured using an automated analyser.

Stool samples were collected at the end of the intervention period. The participants were provided with a stool collection kit with instructions about the proper way to collect stool samples. To represent the whole bacterial components/structure, the stools were homogenized vigorously, and one tablespoon of faecal samples was taken and placed in a labelled sterile conical tube, placed in a biohazard bag, delivered to the laboratory on ice, and stored at -80˚C.

2.5. Metagenomic Measures

2.5.1. Extraction of Genomic DNA.
The concentration and purity of total bacterial DNA extracted from stool samples using the CTAB/SDS method (at Novogene Bioinformatics Technology Co. Ltd., Beijing, China) were monitored by electrophoresis on 1% agarose gels. Samples of DNA were then diluted to 1 ng/μL in sterile water.

2.5.2. Amplicon Generation and Purification.
Bacterial genomic DNA was amplified using the specific primers 515F (GTGCCAGCMGCCGCGGTAA) and 806R (GGAC TACHVGGGTWTCTAAT) for the V4 hypervariable regions of the 16S rRNA gene. All polymerase chain reactions (PCR) proceeded in 30 μL volumes containing 15 μL of Phusion® High-Fidelity PCR Master Mix (New England Biolabs Inc., Ipswich, MA, USA), 0.2 μM forward and reverse primers, and approximately 10 ng of template DNA. The cycling conditions comprised 98˚C for 1 min, followed by 30 cycles of 98˚C for 10 s, 50˚C for 30 s, 72˚C for 30 s, and followed by 72˚C for 5 min. The PCR products in an equal volume of 1X loading buffer (containing SYB green) were resolved by 2% agarose gel electrophoresis. Samples with a bright main band at 400–450 bp were mixed at an equal density and purified using Gene JET Gel Extraction Kit (Thermo Fisher Scientific Inc., Waltham, MA, USA).

2.5.3. Metagenomic Sequencing and Analysis.
Sequencing libraries were generated using Illumina TruSeq DNA PCR-Free Library Preparation Kits (Illumina Inc., San Diego, CA, USA) as described by the manufacturer, and index codes were added. The quality of the library was assessed using a Qubit@ 2.0 Fluorometer (Thermo Fisher Scientific Inc.) and an Agilent Bioanalyzer 2100 system. The library was sequenced on an Illumina NovaSeq platform, and 250 bp paired-end reads were generated. The raw 16S rRNA gene sequence reads were quality-filtered, merged, and clustered into operational taxonomic units (OTUs) with ≥97% similarity, and chimeric sequences were identified and removed. Representative sequences of each OTU were

screened for further annotation. The sequencing quality of each sample including the purity of DNA was shown in supplementary table 2.

2.6. In Vitro Assay.
Microplate assay and agar well diffusion assay were performed to test the relationship between herbal formula and specific bacteria.

2.6.1. Microplate Assay.
Inoculum containing 1% Romboutsia, Streptococcus, or Holdemanella was placed in LB medium (Invitrogen, #10855001), in flat-bottom 96-well plates. Meanwhile, equal volume of inulin, inulin+TCM, or inulin+metformin was added into the wells. The growth kinetics was monitored by microplate reader (Tecan Infinite M200) every two hours. Two wavelengths (700 nm and 520 nm) were used to avoid/minimize interference with background signals.

2.6.2. Agar Well Diffusion Assay.
Cream containing inulin, inulin+TCM, or inulin+metformin was, respectively, placed in 6 mm holes on Mueller Hinton Agar plates (Thermal-Fisher, #R01620), and after inoculating Romboutsia, Streptococcus, or Holdemanella, the plates were incubated at 35˚C overnight. Diameters of the clear zones around the holes were measured and compared.

2.7. Statistical Analysis.
All data were statistically analysed using the SPSS software (version 26.0; IBM, Armonk, NY, USA) and are expressed as means ± SD. Continuous and categorical variables for baseline characteristics were analysed using t-tests and χ^2 tests, respectively. Gut microbiota were profiled on an intent-to-treat basis, regardless of whether the participants complied or completed the study. Sequences were analysed using the R software (version 3.5.2). Differences among groups were analysed using the Kruskal–Wallis chi-square test. All values with $p < 0.05$ were deemed significant.

3. Results

3.1. Participant Characteristics.
The baseline characteristics of the 60 participants were similar (Table 1). At the end of the intervention, all participants were included in the analysis.

3.2. Changes in Gut Microbiota.
Among 5,382,635 usable sequences obtained from all samples using the Illumina NovaSeq platform, 3,899,784 were high-quality, yielding an average of 64,996 sequences per sample. The results of the OTU analysis showed that the numbers of bacterial species did not change among the inulin, inulin+TCM, and inulin+metformin groups ($p = 0.133$ and $p = 0.261$, respectively; Figures 1(a) and 1(b)). However, weighted principal coordinate (PCoA), nonmetric multidimensional scaling (NMDS) (Figures 1(c) and 1(d)), and weighted/unweighted UniFrac analyses of the bacterial taxa among the three cohorts revealed significant differences in the gut microbiota composition among the groups ($p = 3.003e − 08$ and $p = 3.928e − 06$; Figures 2(a) and 2(b)). Analysis of group similarities

Table 1: Baseline characteristics of participants ($n = 20$ per group).

	Inulin	Inulin+TCM	Inulin+metformin
Age (y)	42.9 ± 13.6	48.5 ± 11.6	47.4 ± 12.1
Male sex (n %)	8 (40)	8 (40)	10 (50)
BW (kg)	75.2 ± 13.4	71.8 ± 12.8	71.9 ± 6.8
BMI (kg m^{-2})	26.3 ± 2.4	25.8 ± 2.9	26.4 ± 2.4
WC (cm)	91.4 ± 10.2	90.7 ± 8.0	92 ± 5.7
SBP (mmHg)	123.8 ± 10.2	126.7 ± 9.7	123.1 ± 9.8
DBP (mmHg)	86.2 ± 13.4	80.2 ± 6.4	78 ± 6.8
GLU (mmol $^{L-1}$)	5.4 ± 0.5	5.8 ± 1.3	5.5 ± 0.6
TG (mmol $^{L-1}$)	1.2 (0.6)	1.65 (1.19)	1.35 (0.61)
T-CHOL (mmol $^{L-1}$)	4.53 ± 0.8	4.9 ± 1.1	4.47 ± 0.8
HDL (mmol $^{L-1}$)	1.3 ± 0.3	1.3 ± 0.4	1.2 ± 0.3
LDL (mmol $^{L-1}$)	3.2 ± 0.8	3.3 ± 0.9	3.2 ± 0.6
UA (mmol $^{L-1}$)	326.3 ± 86.1	314.5 ± 87.7	317 ± 74.2
PA (yes no.)	15	15	15

(ANOSIM) also indicated significant differences among the three groups ($R = 0.061$, $p = 0.013$, Supplementary Figure 1).

To further confirm manipulation of the gut microbial community in the three groups, predominant bacterial species at the phylum, family, and genus levels were investigated by sequencing and analysing 16S rRNA. Figure 3 shows bar plots of relative abundance at these levels. Consistent with previous findings, Bacteroidetes, Firmicutes, and Proteobacteria were the predominant phyla, followed by Actinobacteria. The abundance of Bacteroidetes at the phylum level was relatively increased ($p < 0.05$) in the inulin than in the other two groups (24.6% vs. 12.4% and 16.7%, respectively), whereas that of Proteobacteria ($p < 0.05$) in the inulin and TCM-treatment arms was 10.1%, 21.2%, and 9.7%, respectively. Firmicutes bacteria did not significantly differ ($p > 0.05$). Bacteroidaceae ($p = 0.024$) and Ruminococcaceae ($p = 0.017$) were the most abundant families in the inulin group, whereas Enterobacteriaceae ($p = 0.017$) and Veillonellaceae ($p = 0.013$) were the most abundant in the inulin TCM group, and Streptococcaceae ($p < 0.001$) was the most abundant in the inulin+metformin group. We analysed the top 15 genera to further evaluate modulation of the microbial community at the genus level. The relative proportion of Bacteroides was higher ($p = 0.024$) in the inulin than in the other two groups, but the abundance of Romboutsia ($p = 0.043$), Streptococcus ($p < 0.001$), and Holdemanella ($p = 0.011$) was greater in inulin+TCM and inulin+metformin samples, respectively.

The differential abundance among the groups was assessed using linear discriminant analysis Effect Size (LEfSe) assays (LDA > 4) (Figures 2(c) and 2(d)). The gut microbiota differed among the groups; Bacteroidetes (phylum), Bacteroidaceae and Ruminococcaceae (families), and Bacteroides (genus) were more abundant in the inulin group. Proteobacteria (phylum), Enterobacteriaceae and Veillonellaceae (families), and Romboutsia (genus) were dominant in the inulin+TCM group. Streptococcaceae (fam-

ily) and Streptococcus and Holdemanella (genera) were significantly elevated in the inulin+metformin group.

Collectively, these results show similar numbers but significant differences in the types of bacteria in the gut microbiota among the three groups.

3.3. Correlations between Bacterial Abundance and MetS Risk Factors. Correlations between the abundance and presence of different bacteria and the clinical parameters of the participants in each group were analysed to identify associations between host responsiveness and bacterial abundance. Figure 4 summarises the results, which are detailed in the Supplementary Figure 1.

Several associations were significant in the inulin group (Figure 4).

Among the bacterial abundance that significantly and positively correlated with clinical parameters, HDL levels were closely associated with the abundance of *Bacteroidetes* ($r = 0.522$, $p = 0.018$), Bacteroidaceae ($r = 0.485$, $p = 0.03$), and *Bacteroides* ($r = 0.485$, $p = 0.03$). Some bacteria negatively correlated with the clinical parameters in the inulin group. For example, the abundance of *Actinobacteria* correlated negatively with T-CHOL ($r = -0.594$, $p = 0.005$) and LDL ($r = -0.554$, $p = 0.011$), whereas UA correlated positively ($r = 0.457$, $p = 0.043$). Similarly, the *Firmicutes* abundance significantly and negatively correlated with HDL ($r = -0.522$, $p = 0.018$).

Figure 4 shows the correlations between bacterial abundance and clinical parameters in the inulin+TCM group. Correlations between Romboutsia and HDL and between Veillonellaceae and WC were negative ($r = -0.644$, $p = 0.002$ and $r = -0.505$, $p = 0.023$, respectively).

Fewer significant correlations were found between bacterial abundance and clinical parameters in patients with MetS in the inulin+metformin than in the other two groups (Figure 4).

4. Discussion

This prospective study analysed the characteristics of the gut microbiota and their associations with risk factors in patients with MetS treated with various formulations. Little is known about these characteristics and correlations; therefore, the specific bacteria produced and the effects of interventions on the microbiota need to be understood to develop a basis for further investigation of optimal treatments for MetS.

The LEfSe results showed that the Ruminococcaceae family and the Bacteroides genus were more abundant in the inulin group. The Ruminococcaceae family plays an important role in dietary fibre degradation and is involved in the production of SCFAs that provide energy for the colonic epithelium and systemic nutrients [21]. SCFAs affect glucose homeostasis, lipid metabolism, regulation of the immune system, and the inflammatory response [22]. However, we did not identify associations between SCFAs and MetS traits, which might be partly due to a dietary imbalance.
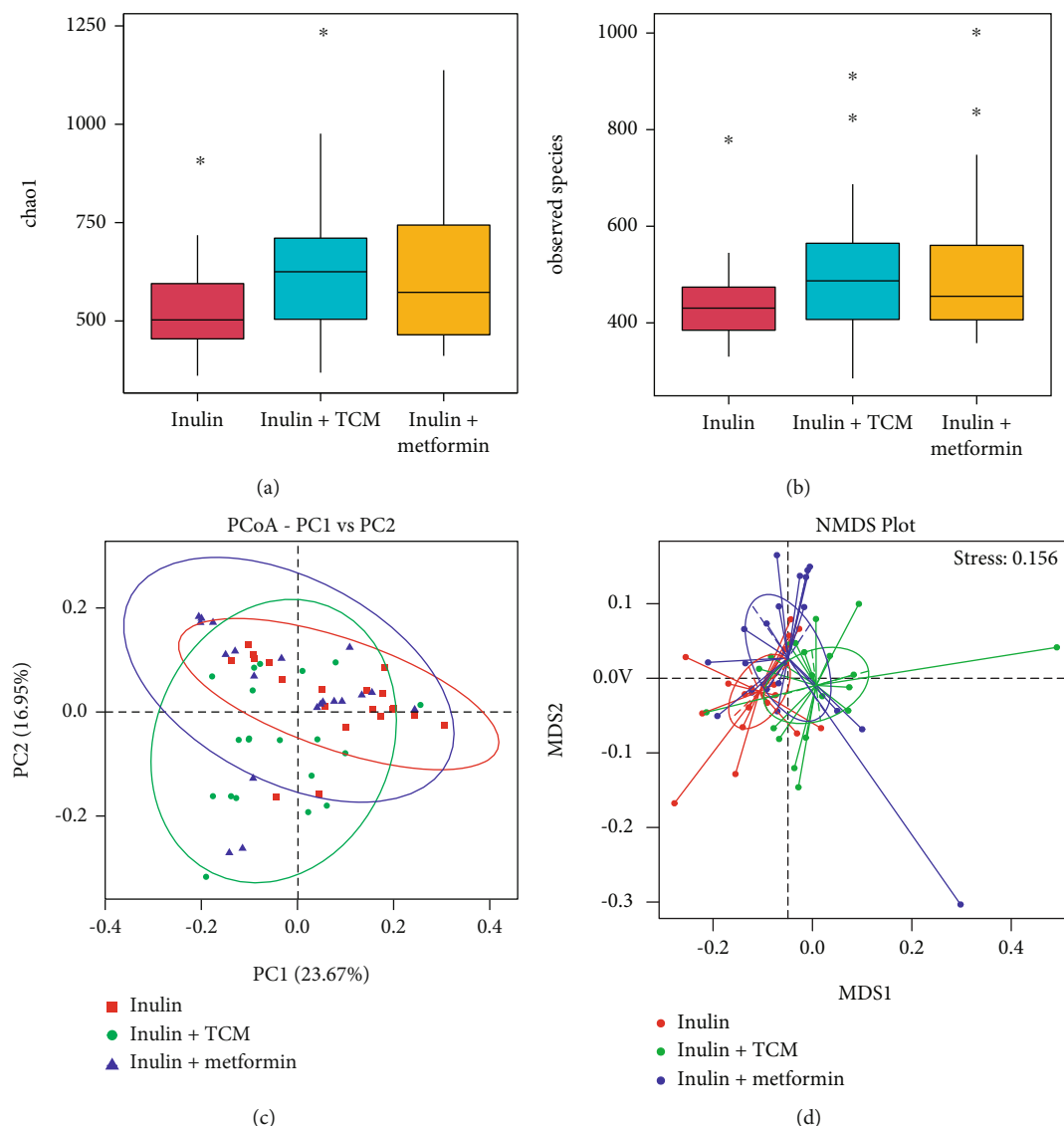
FIGURE 1: Shifts in enteric bacterial composition after 6 months of intervention. (a, b) Numbers of species and Chao1 diversity indices of intestinal bacteria assessed by 16S rRNA high-throughput sequencing significant differ (Kruskal–Wallis χ^2 test; $n = 20$ per group). (c, d) PCoA and NMDS analyses of intestinal bacterial composition profiles. NMDS: nonmetric multidimensional; PCoA: principal coordinate analysis.

The genus Bacteroides comprises gram-negative, obligate anaerobic, nonmotile, nonspore forming rods that are among the most prevalent components of the human intestinal microbiota and important degraders of polysaccharides in the human intestine [23]. Microorganisms in the colon can decompose "resistant" polysaccharides that are not metabolised during transit through the small intestine. Polysaccharide derivatives with an appropriately modified structure can improve the immunological activity of polysaccharides. They can actively enhance immune cells and regulate the immune function [24]. For example, sulfated polysaccharides can improve the role of polysaccharides in macrophage phagocytosis and promote the secretion of IL-6, IL-1β, and other interleukins by macrophages [25].

Higher proportions of the Enterobacteriaceae and Veillonellaceae families and the Romboutsia genus were associ-

ated with inulin+TCM. Some diseases are associated with a significantly higher abundance of Enterobacteriaceae and Veillonellaceae [26, 27]. Furthermore, both taxa were typically found together [26]. An increase in Enterobacteriaceae in gut-associated microbial populations is a microbial signature of epithelial dysfunction [28]. The abundance of Veillonellaceae is inversely associated with changes in the glucose response and IL-6 levels after prebiotic intake [29]. Romboutsia, an obesity biomarker, correlates positively and significantly with indicators of body weight (including waistline and body mass index), serum lipids (LDL, TGs, and T-CHOL), and UA in humans [30]. The genus Romboutsia also correlates positively with HDL in rodent models [31].

Streptococcus and Holdemanella genera were relatively more abundant in the inulin+metformin group. Streptococcus might increase levels of folate production and serum

(a)

(b)

(c)

(d)
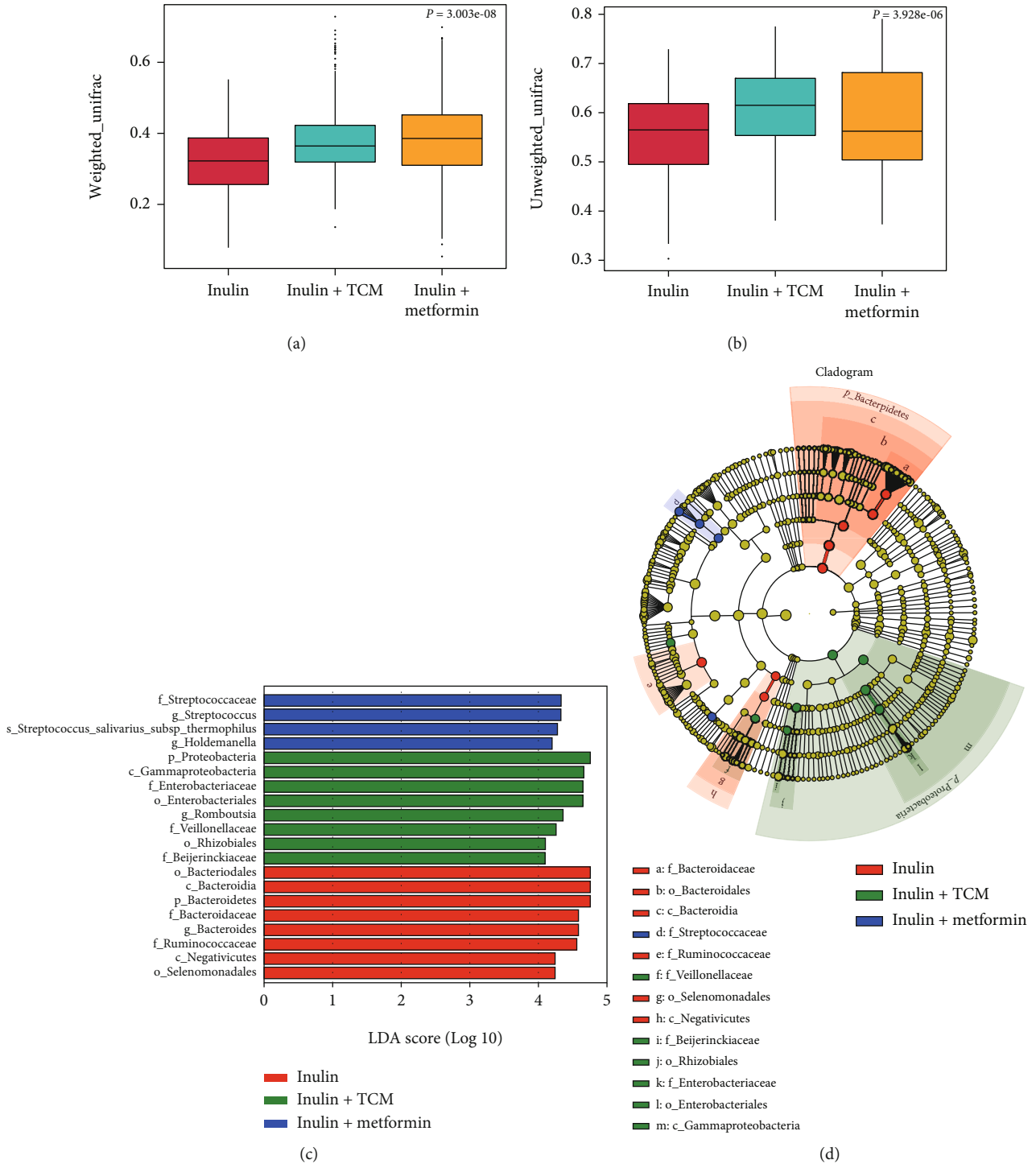
FIGURE 2: Comparison of β diversity among intestinal bacteria using weighted/unweighted UniFrac and LEfSe analyses after 6 months of intervention. (a, b) Weighted/unweighted UniFrac analysis of β diversity shows significant differences among intestinal bacteria ($n = 20$ per group; Kruskal–Wallis χ^2 test). (c, d) Results of LEfSe assays show differences in gut bacteria abundance among groups and effect size of each differentially abundant bacterial taxa ($n = 20$ per group; significantly different, Wilcoxon rank sum tests).

folate concentrations *via* the upregulation of folate-mediated one-carbon metabolism and fatty acid oxidation pathways. This would result in rapid and dramatic reductions in liver fat and other cardiometabolic risk factors [32]. However, Streptococcus has been linked to the development of multi-

ple metabolic disorders, including atherosclerotic cardiovascular disease [33, 34]. A relationship between Holdemanella and sex-specific fat distribution has been identified. The Holdemanella genus is associated positively and negatively with android fat ratios in males and females, respectively
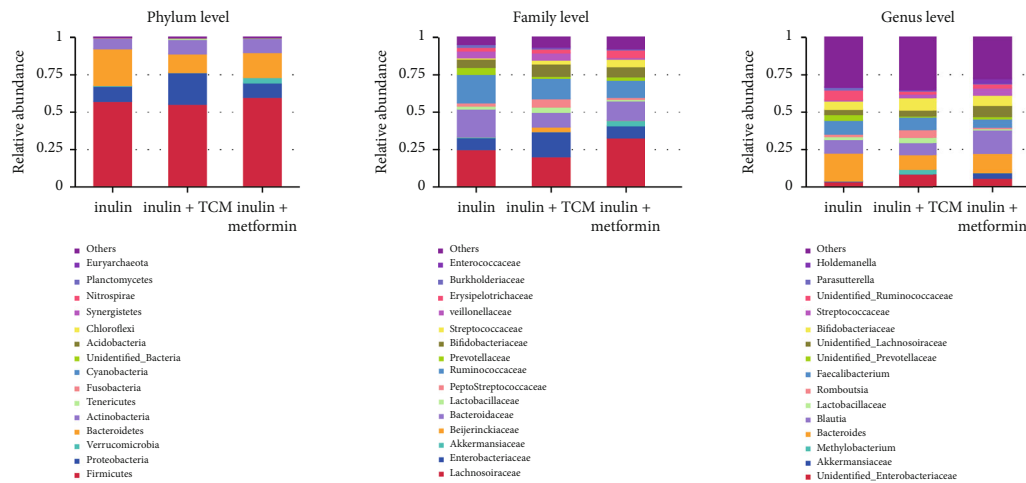
FIGURE 3: Relative abundance of bacterial taxa in the top 15 at phylum, family, and genus levels in patients with MetS treated with inulin, inulin+TCM, or inulin+metformin ($n = 20$ each) for 6 months. MetS: metabolic syndrome; TCM: traditional Chinese medicine.
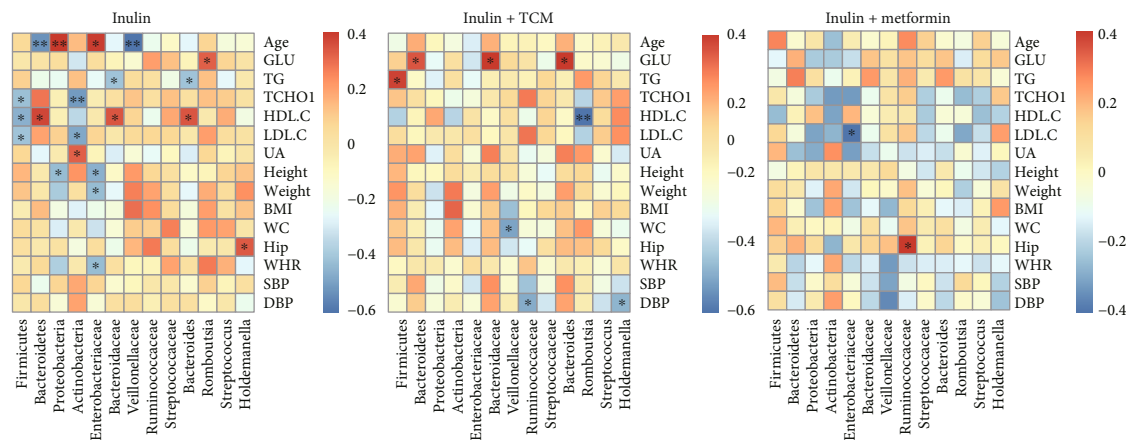
FIGURE 4: Heatmaps of correlations between species abundance (columns) and clinical parameters (rows) in patients with metabolic syndrome. Red and blue shades: positive and negative correlations, respectively. BMI: body mass index; DBP: diastolic blood pressure; GLU: glucose; HDL. C: high-density lipoprotein cholesterol; Hip: hip circumference; LDL. C: low-density lipoprotein cholesterol; SBP: systolic blood pressure; TCHO1: total cholesterol; TG: triglyceride; UA: uric acid; WC: waist circumference; WHR: waist to hip ratio (circumference). *Statistically significant correlations.

[35]. Metformin is responsible for most of the gut microbiota changes and metabolic improvements linked to prebiotic intervention [36].

This study has some limitations. The magnitude of the effects of the interventions remains uncertain because the study cohort was extremely small to rule out the possibility of chance findings. A wash-out period was not applied, and therefore, previous gut bacterial features might have impacted outcomes. Larger studies are needed to confirm structural alterations after discrepant interventions. Changes could be determined in experimental animals after controlling for the environmental system. In terms of taxa, we did not obtain more information about the bacterial species that are more closely associated with physiological roles. Interplay might occur between diet/lifestyle and the gut microbiome and among microbiomes. The association between gut bacteria and corresponding metabolites was not analysed.

Interestingly, our *in vitro* study showed that density of Romboutsia, Streptococcus, and Holdemanella was not altered by the herbal formula used in this study, by microplate assay and agar well diffusion (supplementary figure 2). This indicated the herbal needs to be digested, either the intermediate products or by-products induced the alteration of gut microbiota. It would be necessary to clarify the exact product(s) in future study.

In summary, information is insufficient to conclude the effects of distinct interventions on MetS risk factors. Whether ingredients in the prebiotic mix act alone or in combination to modulate the gut microbiome remains unclear. Further studies are needed to be conducted to clarify the molecular mechanism that determine the effects of the prebiotic mix on the human gut microbiome. However, metabolites derived from microbiota might facilitate better characterisation of the relationship between microbiota and risk for MetS. The metabolic benefits associated with

microbial alterations requires further investigation, as they will provide insight into the roles of microbial metabolites as potential candidate biomarkers in individuals with metabolic syndrome.

Data Availability

The raw sequencing data and code generated or analysed in this study are available from the corresponding author upon reasonable request.

Conflicts of Interest

The authors declare that this research was conducted in the absence of any commercial or financial relationships that could be construed as a potential conflicts of interest.

Authors' Contributions

Ming Yu, Lingzhang Meng, and Yu Zhang designed this study. Jian Song helped design this study. Ruiping Tian, Jiahui Hong, and Jingjie Zhao collected biopsies and performed sequencing. Jingjie Zhao and Ruiping Tian performed data analysis. Dengyuan Zhou, Yangchen Liu, and Zhenshan Jiao performed partial data analysis. Jian Song performed partial data analysis and composed this manuscript. Ruiping Tian, Jiahui Hong, and Jingjie Zhao contributed equally to this study. Yu Zhang revised this manuscript.

Acknowledgments

Supplementary Materials

Supplementary 1. Supplementary Table 1: the composition of herbal formula. The table described the composition of the herbal formula, including the quantity information of each component.

Supplementary 2. Supplementary Table 2: the sequencing quality of each sample. The sequencing quality of each sample was tested and was provided for further conformation.

Supplementary 3. Supplementary Figure 1: analysis of similarities (ANOSIM) indicated that the difference among groups was significant ($R = 0.061$, $p = 0.013$). The violin plots showed the similarity analysis of gut microbiota among different groups.

Supplementary 4. Supplementary Figure 2: *In vitro* assay exhibited that specific bacterium was not altered. (A) Microplate assay showed that Romboutsia, Streptococcus, and Holdemanella were not altered by different treatments. Data represents similar results acquired from 5 repeated experiments. NS: no significant. Each group contained 8 samples. (B) Agar well diffusion assay showed Romboutsia, Streptococcus, and Holdemanella were not altered by different treatments. Data represents similar results acquired from 5 repeated experiments. NS: no significant. Each group contained 8 samples.

References

[1] S. Castro-Barquero, A. M. Ruiz-León, M. Sierra-Pérez, R. Estruch, and R. Casas, "Dietary strategies for metabolic syndrome: a comprehensive review," *Nutrients*, vol. 12, no. 10, p. 2983, 2020.

[2] F. Bishehsari, R. M. Voigt, and A. Keshavarzian, "Circadian rhythms and the gut microbiota: from the metabolic syndrome to cancer," *Nature Reviews. Endocrinology*, vol. 16, no. 12, pp. 731–739, 2020.

[3] M. Wutthi-i, S. Ch, and S. Ya, "Gut microbiota profiles of treated metabolic syndrome patients and their relationship with metabolic health," *Scientific reports*, vol. 10, no. 1, 2020.

[4] M. Shuai, L. S. Y. Zuo, Z. Miao et al., "Multi-omics analyses reveal relationships among dairy consumption, gut microbiota and cardiometabolic health," *eBioMedicine*, vol. 66, article 103284, 2021.

[5] S. Balducci, M. Sacchetti, J. Haxhi et al., "Physical exercise as therapy for type 2 diabetes mellitus," *Diabetes/Metabolism Research and Reviews*, vol. 30, no. S1, pp. 13–23, 2014.

[6] Y. Zhang, Y. Gu, H. Ren et al., "Gut microbiome-related effects of berberine and probiotics on type 2 diabetes (the PREMOTE study)," *Nature Communications*, vol. 11, no. 1, pp. 1–12, 2020.

[7] M. Mazidi, P. Rezaie, A. Pascal, M. Ghayour, and G. A. Ferns, "Gut microbiome and metabolic syndrome," *Diabetes and Metabolic Syndrome: Clinical Research & Reviews*, vol. 10, no. 2, pp. S150–S157, 2016.

[8] C. Haro, S. Garcia-Carpintero, J. F. Alcala-Diaz et al., "The gut microbial community in metabolic syndrome patients is modified by diet," *The Journal of Nutritional Biochemistry*, vol. 27, pp. 27–31, 2016.

[9] J. Rodriguez, S. Hiel, A. M. Neyrinck et al., "Discovery of the gut microbial signature driving the efficacy of prebiotic intervention in obese patients," *Gut*, vol. 69, no. 11, pp. 1975–1987, 2020.

[10] R. Uauy, "Foreword," *The British Journal of Nutrition*, vol. 101, no. S2, p. S1, 2009.

[11] S. O'Connor, S. Chouinard-Castonguay, C. Gagnon, and I. Rudkowska, "Prebiotics in the management of components of the metabolic syndrome," *Maturitas*, vol. 104, pp. 11–18, 2017.

[12] X. Zhao, P. K. Oduro, W. Tong, Y. Wang, X. Gao, and Q. Wang, "Therapeutic potential of natural products against atherosclerosis: targeting on gut microbiota," *Pharmacological Research*, vol. 163, article 105362, 2021.

[13] S. Dehghani, S. Mehri, and H. Hosseinzadeh, "The effects of Crataegus pinnatifida (Chinese Hawthorn) on metabolic syndrome: a review," *Iranian Journal of Basic Medical Sciences*, vol. 22, no. 5, pp. 460–468, 2019.

[14] H. Y. Zhang, J. X. Tian, F. M. Lian et al., "Therapeutic mechanisms of traditional Chinese medicine to improve metabolic diseases via the gut microbiota," *Biomedicine & Pharmacotherapy*, vol. 133, article 110857, 2021.

[15] X. Zhang, Y. Zhao, J. Xu et al., "Modulation of gut microbiota by berberine and metformin during the treatment of high-fat diet-induced obesity in rats," *Scientific Reports*, vol. 5, no. 1, pp. 1–10, 2015.

[16] X. Fu, Q. Wang, H. Kuang, and J. Pinghui, "Mechanism of Chinese medicinal-medicated leaven for preventing and treating gastrointestinal tract diseases," *Digestion*, vol. 101, no. 6, pp. 659–666, 2020.

[17] K. Forslund, F. Hildebrand, T. Nielsen, and G. Falony, "Disentangling type 2 diabetes and metformin treatment signatures in the human gut microbiota," *Nature*, vol. 528, no. 7581, pp. 262–266, 2015.

[18] T. Bryrup, C. W. Thomsen, T. Kern et al., "Metformin-induced changes of the gut microbiota in healthy young men: results of a non-blinded, one-armed intervention study," *Diabetologia*, vol. 62, no. 6, pp. 1024–1035, 2019.

[19] O. Label and C. Trial, "Structural alteration of gut microbiota during the amelioration of human type 2 diabetes with hyperlipidemia by metformin and a traditional Chinese herbal formula," *mBio*, vol. 9, pp. 1–12, 2018.

[20] T. T. T. Tran, F. J. Cousin, D. B. Lynch et al., "Prebiotic supplementation in frail older people affects specific gut microbiota taxa but not global diversity," *Microbiome*, vol. 7, no. 1, pp. 1–17, 2019.

[21] S. Hooda, B. M. V. Boler, M. C. R. Serao et al., "454 pyrosequencing reveals a shift in fecal microbiota of healthy adult men consuming polydextrose or soluble corn fiber," *The Journal of Nutrition*, vol. 142, no. 7, pp. 1259–1265, 2012.

[22] D. J. Morrison and T. Preston, "Formation of short chain fatty acids by the gut microbiota and their impact on human metabolism," *Gut Microbes*, vol. 7, no. 3, pp. 189–200, 2016.

[23] D. Ryan, L. Jenniches, S. Reichardt, L. Barquist, and A. J. Westermann, "A high-resolution transcriptome map identifies small RNA regulation of metabolism in the gut microbe Bacteroides thetaiotaomicron," *Nature Communications*, vol. 11, no. 1, p. 3557, 2020.

[24] F. Chen and G. Huang, "Preparation and immunological activity of polysaccharides and their derivatives," *International Journal of Biological Macromolecules*, vol. 112, pp. 211–216, 2018.

[25] J. Jiang, F. Y. Meng, Z. He et al., "Sulfated modification of longan polysaccharide and its immunomodulatory and antitumor activity in vitro," *International Journal of Biological Macromolecules*, vol. 67, pp. 323–329, 2014.

[26] D. Gevers, S. Kugathasan, L. A. Denson et al., "The treatment-naïve microbiome in new-onset Crohn's disease," *Cell Host & Microbe*, vol. 15, pp. 382–392, 2014.

[27] W. M. P. Genta Kakiyama, "Modulation of the fecal bile acid profile by gut microbiota in cirrhosis," *Journal of Hepatology*, vol. 58, no. 5, pp. 949–955, 2013.

[28] M. X. Byndloss, E. E. Olsan, F. Rivera-Chávez et al., "Microbiota-activated PPAR-γ-signaling inhibits dysbiotic Enterobacteriaceae expansion," *Science*, vol. 357, no. 6351, pp. 570–575, 2017.

[29] C. Pedersen, E. Gallagher, F. Horton et al., "Host-microbiome interactions in human type 2 diabetes following prebiotic fibre (galacto-oligosaccharide) intake," *The British Journal of Nutrition*, vol. 116, no. 11, pp. 1869–1877, 2016.

[30] Q. Zeng, D. Li, Y. He et al., "Discrepant gut microbiota markers for the classification of obesity-related metabolic abnormalities," *Scientific Reports*, vol. 9, no. 1, pp. 1–10, 2019.

[31] B. Zheng, T. Wang, H. Wang, L. Chen, and Z. Zhou, "Studies on nutritional intervention of rice starch- oleic acid complex (resistant starch type V) in rats fed by high-fat diet," *Carbohydrate Polymers*, vol. 246, article 116637, 2020.

[32] A. Mardinoglu, H. Wu, E. Bjornson et al., "An integrated understanding of the rapid metabolic benefits of a carbohydrate-restricted diet on hepatic steatosis in humans," *Cell Metabolism*, vol. 27, no. 3, pp. 559–571.e5, 2018.

[33] R. B. Jones, T. L. Alderete, J. S. Kim, J. Millstein, F. D. Gilliland, and M. I. Goran, "High intake of dietary fructose in overweight/obese teenagers associated with depletion of Eubacterium and Streptococcus in gut microbiome," *Gut Microbes*, vol. 10, no. 6, pp. 712–719, 2019.

[34] Z. Jie, H. Xia, S. L. Zhong et al., "The gut microbiome in atherosclerotic cardiovascular disease," *Nature Communications*, vol. 8, no. 1, pp. 1–11, 2017.

[35] Y. Min, X. Ma, K. Sankaran et al., "Sex-specific association between gut microbiome and fat distribution," *Nature Communications*, vol. 10, no. 1, pp. 1–9, 2019.

[36] S. Hiel, M. A. Gianfrancesco, J. Rodriguez et al., "Link between gut microbiota and health outcomes in inulin -treated obese patients: lessons from the Food4Gut multicenter randomized placebo-controlled trial," *Clinical Nutrition*, vol. 39, no. 12, pp. 3618–3628, 2020.

Research Article

Transcriptome Sequencing and Bioinformatics Analysis of Ovarian Tissues from Pomacea canaliculata in Guangdong and Hunan

Jing Liu[1], **Jian Li**,[2] **Zhi Wang**[3], **and Hua Yang**[2]

[1]*College of Resources and Environment, Hunan Agriculture University, Changsha, Hunan 410128, China*
[2]*College of Bioscience and Biotechnology, Hunan Agriculture University, Changsha, Hunan 410128, China*
[3]*College of Life Sciences, Hunan Normal University, Changsha, Hunan 410081, China*

Correspondence should be addressed to Zhi Wang; wangzhispider@hotmail.com and Hua Yang; yhua7710@126.com

In this study, the fecundity of Pomacea canaliculata was studied by collecting egg masses from Guangdong and Hunan using field egg collection and indoor propagation. Through high-throughput RNA sequencing (RNA-seq), we analyzed the ovarian tissue of the snails in Guangdong (G_O) and those in Hunan (H_O) using comparative analysis of transcription. Moreover, we used bioinformatics methods to screen the key pathways and genes that affect the fecundity of snails from the two locations. *Results.* The results showed that the absolute fecundity and weight-relative fecundity of Pomacea canaliculata in Guangdong were significantly higher than those in Hunan. We found 1,546 differential genes through differential gene screening (528 genes upregulated in snails from Guangdong and 1018 in snails from Hunan). The ribosomal signaling pathway and *rpl23a*, *uba52* are critical pathways and essential genes that affect the fecundity of snails. *Conclusions.* The 27 differential genes in the ribosome signaling pathway, collected from H_O, were all downregulated. As a result, ovarian tissue protein synthesis is impaired, which is an important mechanism that affects snails' ability to reproduce.

1. Introduction

Invasive species are one of the main threats to biodiversity. Many freshwater snails are likely to damage the function or structure of the ecosystem [1]. However, only one type of snail is listed as one of the world's 100 most invasive species by the International Union for Conservation of Nature [2]. Pomacea canaliculata, also known as apple snails, is native to the Amazon River Basin. In the early 1980s, people introduced it into China and other Asian countries as a high-protein food for commercial purposes. However, they were discarded in large quantities due to their unpalatable taste and poor market sales. Eventually, they settled in the natural environment. The snails seriously endanger aquatic crops, such as rice, and xerophyte crops, such as vegetables near waters, causing considerable losses to the agricultural economy and a severe threat to ecological security.

The level of biological individual fecundity reflects the adaptation characteristics of species or populations to environmental changes, which directly affects the replenishment and proliferation of populations [3]. The vital fecundity of the snails provides favorable conditions for the formation of invasion hazards [4]. A female apple snail can lay 50–800 eggs at a time. On average, each female apple snail can lay 13,764 eggs in its lifetime and reproduce 6,070 young apple snails [5]. The feeding ratio of female snails is higher than that of male snails, so more energy is introduced into the female snail population. When food is limited, female snails use more energy for reproduction. Only if the food supply is reduced above 50% will the fecundity of the snails decrease and be partially compensated for by the increased hatching survival rate [6]. In the long-term restriction of 80% of the food supply, snails can still mature, mate, and lay viable eggs [7]. In addition, the number of female snails

in the snail population tends to be more than that of male snails [5], and female snails can lay eggs multiple times after mating once [8]. These reproductive characteristics of Pomacea canaliculata enable them to quickly adapt to the environment they invade where they dominate.

This study investigated Pomacea canaliculata samples from Guangdong and Hunan. Their reproductive characteristics were studied using field survey sampling and laboratory spawning. The differentially expressed genes were enriched and analyzed based on the ovarian transcriptome data, and genes related to reproduction were screened. Research on the fecundity of snails can help clarify the law of population growth and reproductive strategies, which might provide a specific theoretical reference for predicting its spread and provide scientific guidance for the prevention and control of apple snails.

2. Materials and Methods

2.1. Experimental Materials. The *P*. canaliculata used in this research were collected from the field. The *P*. canaliculata in Guangdong were collected in rice fields in Gaoyao District, Zhaoqing City, Guangdong Province. In contrast, the P. canaliculata in Hunan were collected from ponds in Furong District, Changsha City, Hunan Province. The two snail breeds were separately reared in aquariums at room temperature according to sex (i.e., male and female). The water in the box was tap water aired outdoors for two days and fed with cabbage. The experiment was reviewed and approved by the Ethics Committee of Hunan Agricultural University, and it followed all the principles of care and use of laboratory animals.

2.2. Determination of the Reproductive Ability of Snails

2.2.1. Determination of the Reproductive Ability of Snails in the Field. In October 2020, we randomly collected 30 complete egg masses of snails from the collection sites of snails in Guangdong and Hunan. To avoid damaging the collected samples, we took them out together with the attachments of the snail egg masses and brought them back to the laboratory. We then soaked them in a 2% sodium hydroxide solution until the eggs were separated from the attachments, which helped us count the number of eggs.

2.2.2. Determination of the Reproductive Ability of Snails under Laboratory Conditions. Using a plastic bucket (D24 cm ∗ H60 cm) as the experimental container, we put the snails from Guangdong and Hunan together for single-pair mating. First, we selected snails with normal vitality and no damage to their body surfaces. Then, we absorbed the water on their body surfaces using gauze and measured their mass (W, g). Finally, we placed male and the female pair in the experimental barrel for single-pair mating. Each mating group had three repetitions. The experiment lasted one month. We used cabbage as bait, changed the water every two days, kept the water temperature in the biochemical incubator at $25 \pm 1°$C, and covered the bucket's mouth with gauze to prevent the snails from escaping. We also observed the living conditions of snails every day and

recorded the date and number of spawning eggs. When the surface of the egg mass became hard while the connection between it and the attachment was still wet, we gently peel it off with a small blade. We then soaked it in a 2% sodium hydroxide solution until the egg pieces were entirely dispersed, allowing us to count the number of egg particles.

2.3. RNA Extraction and Transcriptome Sequencing. This study took female apple snails for transcriptome sequencing from that had completed spawning. After dissection of the snail, the ovarian tissue was rapidly excised, snap-frozen in liquid nitrogen, and stored at -80°C for RNA extraction. We named snails in Guangdong G_O and snails in Hunan H_O. We generated three biological replicates of snails in each area. The total RNA was extracted with an RNA extraction kit, and an Agilent 2100 bioanalyzer detected the quality and concentration of the total RNA. Novogene Co., Ltd. constructed the sequencing library, and transcriptome paired-end sequencing was performed using the Illumina HiSeq2500 platform.

2.4. Screening Differential Genes. We obtained clean reads by removing the sequences containing linkers and low-quality sequences from the original sequence data. The reference genomes were downloaded from the NCBI database and aligned with the Tophat software. The DESeq2 R software was used to screen for differential expression of genes, and differential genes were defined as FDR < 0.05 and FC > 2.

2.5. GO Function Annotation of Differential Genes and Enrichment Analysis of the KEGG Pathway. The study also used the Cytoscape plug-in ClueGo + Cluepedia to analyze the differential genes GO (gene ontology) and KEGG (Kyoto encyclopedia of genes and genomes). The analysis parameter setting adopts the software default setting, the network specificity selection is medium, and the result is displayed when $p < 0.05$.

2.6. Analysis of the Protein Interaction Network of Differential Genes. The study used the STRING online analysis software for the protein-protein interaction network analysis of differential genes. In order to make the related protein interaction network closer to the real functional state, only the nodes with interaction score greater than 0.9 were retained, and the nodes with failed gene symbol identification were deleted. The protein interaction network was visualized using the Cytoscape software, and the network topology was analyzed using the CytoHubba plug-in to screen out hub genes.

2.7. Statistical Analysis. We processed the data using the Microsoft Excel 2016 software, and the results were expressed as Mean ± Standard Deviation. Moreover, we also used the SPSS 26 and a one-way analysis of variance (ANOVA) to analyze the differences between groups ($p < 0.05$). The calculation formula is absolute fecundity = eggs/egg mass; relative weight fecundity = eggs/weight.

TABLE 1: Absolute fecundity of Pomacea canaliculata in Guangdong and Hunan.

Area	Absolute fecundity (eggs/egg mass)	Range
Guangdong	282.34 ± 125.92^a	69-799
Hunan	163.52 ± 80.87^b	54-340

TABLE 2: Relative fecundity of Pomacea canaliculata in Guangdong and Hunan.

Area	Weight (g)	Egg masses	Eggs	Relative weight fecundity (eggs/weight)
Guangdong	23.92 ± 2.22^a	3.67 ± 1.15^a	653.33 ± 60.12^a	27.59 ± 4.67^a
Hunan	27.51 ± 18.36^a	1.67 ± 0.58^a	246.33 ± 20.55^b	11.80 ± 6.80^b

TABLE 3: Comparison results of clean reads and reference genomes.

Sample number	Total reads	Clean bases/ G	Mapped ratio/%	Uniq mapped reads	Uniq mapped ratio/%
G_O1	55420990	8.31	85.91	46567375	84.02
G_O2	48191858	7.23	85.34	40141606	83.3
G_O3	49830396	7.47	84.77	41284342	82.85
H_O1	54695332	8.2	81.06	43277495	79.12
H_O2	53698116	8.05	80.51	41838227	77.91
H_O3	50923560	7.64	83.9	41248544	81.0
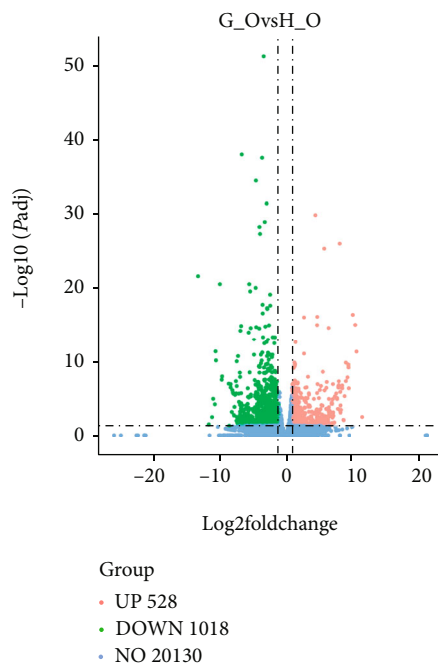
FIGURE 1: Volcano plot of differentially expressed genes. The red dots in the volcano map indicate upregulated genes, green dots indicate downregulated genes, and blue dots indicate indifferent genes.

3. Results

3.1. Comparison of the Reproductive Ability of Snails. The experimental results conducted on snails from Guangdong and Hunan are shown in Table 1. The results show significant differences in the absolute fecundity of Pomacea canaliculata in Guangdong and Hunan. In addition, there is no significant difference in the number of egg-laying snails in Guangdong and Hunan. However, there were substantial differences in the number of eggs and relative weight and fecundity (see Table 2).

The same letter indicates that the difference is not significant, and the different letter suggests that the difference is significant ($p < 0.05$).

The exact number and letters in the same column indicate that the difference is insignificant, and different letters indicate a significant difference ($p < 0.05$).

3.2. Assessing Sequencing Data Quality. After processing the sequencing data, we obtained 312,760,252 clean reads. Based on the data, the clean bases of each sample were above 7.23 Gb, while the mapped ratio was above 80%. The comparison ratio with the reference genome was between 80.51% and 85.91%, and the unique comparison ratio was higher than 77.91% (see Table 3).

3.3. Screening of Differentially Expressed Genes. Comparing G_O and H_O through differential expression analysis, 1,546 differentially expressed genes were obtained. Compared with H_O, there were 528 genes upregulated and 1018 genes downregulated in G_O. From the volcano map of differentially expressed genes from G_O vs. H_O (Figure 1), we can quickly see that the farther the deviation from 0 is for the x-axis, the more significant the considerable difference in expression. For the y-axis, the larger the value, the smaller the probability of false positives, and the more reliable the result.

3.4. Differential Gene GO Function Enrichment and KEGG Pathway Analysis. The 66 GO entries in 5 KEGG channels are divided into 12 groups and connected by 144 edges. The most important terms include GO:0005507 copper ion binding ($p = 0.00764$, enrichment number 7), dre00480 Glutathione metabolism ($p = 0.01249$, enrichment number 7), GO:1901564 organonitrogen compound metabolic process
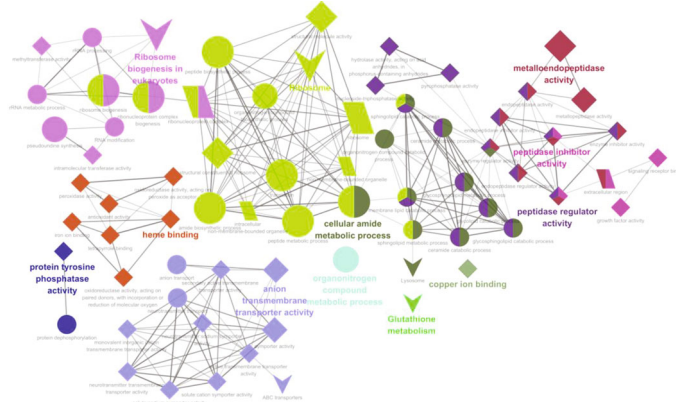
FIGURE 2: Network of enriched GO terms and KEGG pathways. The circle represents BP, the diamond represents MF, the quadrilateral represents CC, and the arrow represents the pathway. Based on the kappa score level (≥0.1), the term is used as a functional grouping network of connecting nodes. For each group, the size of the nodes indicates their importance, and the largest node size represents the most critical path.
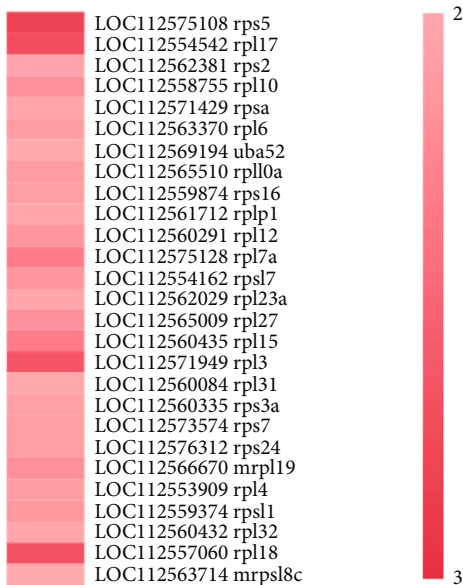
FIGURE 3: Expression profile of differentially expressed genes annotated with ribosomal signaling pathways. The bar's color represents the fold of upregulation of the corresponding gene. The darker the color, the larger the value, indicating that the fold of the gene is upregulated.

FIGURE 4: Protein-protein interaction network of differentially expressed genes. Each node represents the protein corresponding to the differentially expressed gene (green means downregulation, while red means upregulation). The edges represent the interactions between the proteins.

13), dre03010 Ribosome ($p = 1.51 \times 10^{-9}$, enrichment number 27) (See Figure 2). Among the three marked pathways, dre03010 Ribosome has the highest degree of enrichment. Note that the 27 differential genes in the ribosomal pathway are all upregulated. Their expression levels were upregulated by at least two times and the most upregulated by 2.8 times (see Figure 3).

3.5. Analysis of the Protein Interaction Network. Based on the STRING online database and Cytoscape software, we have drawn a protein-protein interaction network diagram that includes 112 differential genes (24 downregulated and 88 up-regulated) and 608 protein-protein interaction networks, as shown in Figure 4. The larger the node, the more interactive the relationship with other nodes. As shown in Figure 4, mrto4, rpl23a, uba52, and rpl3 are the most prominent nodes. To identify potential hub genes in the network, the Cytoscape plug-in, CytoHubba, used six algorithms to calculate and screen the protein–protein interaction network and select the top 10 genes of each algorithm (Table 4). The results of all topological measurements have a relatively high degree of overlap. We used the Venn diagram to intersect the results obtained by the six algorithms and finally screen

($p = 0.002356$, enrichment number 49), and GO:0004725 protein tyrosine phosphatase activity ($p = 0.01875$, enrichment number 9),

GO:0030414 peptidase inhibitor activity ($p = 0.00693$, enrichment number 13), GO:0020037 heme-binding ($p = 0.01557$, enrichment number 22), dre03008 ribosome biogenesis in eukaryotes ($p = 2.07 \times 10^{-7}$, enrichment number 17), GO:0004222 metalloendopeptidase activity ($p = 0.00018$, enrichment number 16), GO:0043603 cellular amide metabolic process ($p = 0.00001$, enrichment number 33), GO:0008509 anion transmembrane transporter activity ($p = 0.00380$, enrichment number 10), GO:0061134 peptidase regulator activity ($p = 0.00693$, enrichment number

TABLE 4: Top 10 hub genes obtained by different algorithms.

Gene	Degree	Gene	Closeness	Gene	MCC	Gene	Betweenness	Gene	Stress	Gene	MNC
mrto4	39	mrto4	56.83333	rpl23a	9.223e13	mrto4	1351.4171	mrto4	11736	mrto4	39
rpl23a	32	rpl23a	51.25	rps11	9.223e13	nhp2l1a	867.04406	nsa2	4822	rpl23a	31
uba52	30	uba52	50.83333	rpl15	9.223e13	uba52	735.93096	fbl	3334.0	rpl3	30
rpl3	30	rpl3	50.25	rpl18	9.223e13	nsa2	480.52399	rpl23a	3232.0	rps11	29
rps11	29	rps11	49.91667	rpl3	9.223e13	dkc1	388.92945	nhp2l1a	2786.0	rpl15	28
rpl15	28	nsa2	49.75	rpl4	9.223e13	fbl	365.27046	uba52	2644.0	rps2	28
rpl4	28	rpl15	49.41667	rpl10a	9.223e13	nop56	331.98893	nop56	2312.0	uba52	28
rps2	28	rpl4	48.75	rps2	9.223e13	rpl23a	327.47269	pes	2286.0	rpl4	28
rpsa	27	rpl2	48.75	uba52	9.223e13	gnb2l1	302.95149	dkc1	2178.0	rpl10a	27
rps7	27	rpl10a	48.25	rpl31	9.223e13	pes	164.6678	rpl3	2074.0	rpl18	27
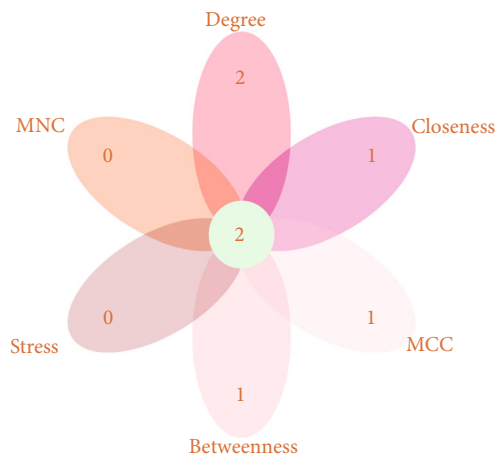
FIGURE 5: Venn diagram of hub genes obtained using different algorithms. The number marked in the center represents the number of hub genes obtained by the intersection of the six algorithms.

out uba52 and rpl23a, as shown in Figure 5. These two genes have a more robust interaction relationship than other genes in the entire protein–protein interaction network. They may play a more critical role in the reproduction process than other genes.

4. Discussion

P. canaliculata was introduced into Guangdong for breeding in the early 1980s [9]. Then, in the early 1990s, they were introduced across multiple provinces and cities, with the distribution area gradually extending to Hunan and other places. The reproduction of apple snails is affected by temperature [10, 11]. The suitable temperature for breeding and hatching is 22-32°C, and the eggs usually cannot hatch after the temperature is lower than 15°C. Since the annual average temperature in Guangdong Province is about 19-24°C, and the average temperature in January is about 16-19°C, apple snails can reproduce in Guangdong three generations a year [8]. Meanwhile, since the annual average temperature in Hunan Province is 16-18.5°C, and the average temperature in January is about 4-7°C, apple snails cannot reproduce for three generations a year in Hunan because of low temperature. Apple snails consume energy to adapt to a low-temperature environment, so their energy for reproduction is reduced, which means their fecundity is lower than that of apple snails in Guangdong.

The reproductive characteristics of apple snails show huge differences between populations, partly due to phenotypic plasticity and partly due to genetic variation [12, 13]. The reproduction of snails is a complex process involving many genes. In this study, 1,546 genes were identified by analyzing G_O and H_O. The results of the KEGG enrichment analysis based on differential genes and protein interaction network analysis showed that the ribosomal pathways of rpl23a and uba52 and two ribosomal-related pivot genes are essential pathways and key genes that affect the reproductive ability of apple snails.

Ribosomes are important sites for protein synthesis. The ribosomes of eukaryotes are composed of 60S large subunits and 40S small subunits. A 60S large subunit consists of three rRNA molecules (25SrRNA, 5.8SrRNA, and 5SrRNA) and 46 proteins, while the 40S small subunit includes one rRNA (18SrRNA) and 33 proteins [14–16]. Ribosomal Protein (RP) is a collective term for all proteins forming ribosomes. It is widely distributed in various tissues and forms ribosomes together with ribonucleic acid. It plays a vital role in protein biosynthesis. Many ribosomal proteins form ribosomes, participate in protein biosynthesis, and have functions independent of protein biosynthesis. Studies have shown that ribosomes are closely related to cell growth, differentiation, and embryonic development [17, 18]. In this experimental study, the differential genes involved in the ribosomal signaling pathway in the H_O were all downregulated, 23 of which were ribosomal protein genes. The downregulation of ribosomal protein genes will reduce the production of corresponding ribosomal proteins, thereby reducing the number of ribosomes in the cell. This fact indicates that the ovaries of apple snails in Hunan Province, due to the downregulation of differential gene expression, affect the protein biosynthesis of ovarian tissues, thereby affecting the normal physiological functions of the ovaries and showing poor reproductive ability.

The *rpl23a* (ribosomal protein l23a) gene encodes a ribosomal protein, which is a component of the 60S subunit. As an indispensable part of eukaryotic ribosomes, the *rpl23a* gene can improve the catalytic ability of rRNA to synthesize proteins [19], and it plays a vital role in protein synthesis, folding, and arrangement [20]. *Uba52* (ubiquitin a-52 residue ribosomal protein fusion product 1) gene is an essential member of the ubiquitin family. Ubiquitin is a small protein with 76 amino acids and about 8.6 kDa. It is ubiquitous and highly conserved in eukaryotes. Ubiquitin can play a crucial role in tissue remodeling and development, gametogenesis and maturation, fertilization, and early pregnancy through the ubiquitin-proteasome pathway (UPP) [21]. Kobayashi's research on mouse embryos confirmed that *uba52* regulates ribosomal protein complexes and simultaneously provides *rpl40* and ubiquitin to ribosomes. *Uba52*-deficient mice die during embryogenesis, indicating that *uba52* can maintain embryos' developmental function [22]. Mao et al. found that the *uba52* gene is essential for early embryogenesis in pigs [23].

By comparing the transcriptome and bioinformatics analyses of G_O and H_O, we predict that the ribosome signaling pathway may be closely related to snail reproduction. In addition, we determined that *rpl23a* and *uba52* genes play an essential role in snail reproduction. Of course, the specific mechanisms and functions of these pathways and genes need to be verified through many biological experiments to provide solid evidence for understanding the reproductive mechanism of Pomacea canaliculata.

Data Availability

The data of this study are available from the corresponding author.

Conflicts of Interest

The authors declare no conflicts of interest.

Acknowledgments

References

[1] D. L. Strayer, "Alien species in fresh waters: ecological effects, interactions with other stressors, and prospects for the future," *Freshwater Biology*, vol. 55, pp. 152–174, 2010.

[2] G. M. Luque, C. Bellard, C. Bertelsmeier et al., "The 100th of the world's worst invasive alien species," *Biological Invasions*, vol. 16, no. 5, pp. 981–985, 2013.

[3] D. P. Sarikaya, S. H. Church, L. P. Lagomarsino et al., "Reproductive capacity evolves in response to ecology through common changes in cell number in Hawaiian Drosophila," *Current Biology*, vol. 29, no. 11, pp. 1877–1884, 2019.

[4] C. H. Kyle, A. L. Plantz, T. Shelton, and R. L. Burks, "Count your eggs before they invade: identifying and quantifying egg clutches of two invasive apple snail species (Pomacea)," *PloS One*, vol. 8, no. 10, article e77736, 2013.

[5] L. Jun, H. Yue-jin, T. Ji-cai et al., "Characteristics of Pomacea canaliculata reproduction under natural conditions," *Chinese Journal of Applied Ecology*, vol. 23, no. 2, pp. 559–565, 2012.

[6] N. E. Tamburi and P. R. Martín, "Effects of food availability on reproductive output, offspring quality and reproductive efficiency in the apple snail Pomacea canaliculata," *Biological Invasions*, vol. 13, no. 10, pp. 2351–2360, 2011.

[7] N. E. Tamburi and P. R. Martín, "Reaction norms of size and age at maturity of Pomacea canaliculata (Gastropoda: Ampullariidae) under a gradient of food deprivation," *Journal of Molluscan Studies*, vol. 75, no. 1, pp. 19–26, 2009.

[8] T. Nurhayati, T. Hidayat, and M. A. Ameliawati, "Profile of macro-micro mineral and carotenoids in Pomacea canaliculata," *Current Research in Nutrition and Food Science*, vol. 7, no. 1, pp. 287–294, 2019.

[9] T. Yang, Z. Wu, and Z. Lun, "The apple snail Pomacea canaliculata, a novel vector of the rat lungworm, Angiostrongylus cantonensis: its introduction, spread, and control in China," *Hawai'i Journal of Medicine & Public Health*, vol. 72, Supplement 2, pp. 23–25, 2013.

[10] M. E. Seuffert and P. R. Martín, "Thermal limits for the establishment and growth of populations of the invasive apple snail Pomacea canaliculata," *Biological Invasions*, vol. 19, no. 4, pp. 1169–1180, 2017.

[11] M. E. Seuffert, L. Saveanu, and P. R. Martín, "Threshold Temperatures and degree-day estimates for embryonic development of the invasive apple snail Pomacea canaliculata (Caenogastropoda: Ampullariidae)," *Malacologia*, vol. 55, no. 2, pp. 209–217, 2012.

[12] B. Thaewnon-ngiw, S. Klinbunga, K. Phanwichien, N. Sangduen, N. Lauhachinda, and P. Menasveta, "Genetic diversity of introduced (Pomacea canaliculata) and native (PILA) apple snails in Thailand revealed by randomly amplified polymorphic DNA (RAPD) analysis," *ASEAN Journal on Science & Technology for Development*, vol. 20, pp. 289–306, 2017.

[13] M. P. Cadierno, M. S. Dreon, and H. Heras, "Validation by qPCR of reference genes for reproductive studies in the invasive apple snail Pomacea canaliculata," *Malacologia*, vol. 62, no. 1, pp. 163–170, 2018.

[14] A. Ben-Shem, N. Garreau de Loubresse, S. Melnikov, L. Jenner, G. Yusupova, and M. Yusupov, "The structure of the eukaryotic ribosome at 3.0 A resolution," *Science*, vol. 334, no. 6062, pp. 1524–1529, 2011.

[15] H. Khatter, A. G. Myasnikov, S. K. Natchiar, and B. P. Klaholz, "Structure of the human 80S ribosome," *Nature*, vol. 520, no. 7549, pp. 640–645, 2015.

[16] H. Khatter, A. G. Myasnikov, L. Mastio et al., "Purification, characterization and crystallization of the human 80S ribosome," *Nucleic Acids Research*, vol. 42, no. 6, pp. 49-50, 2014.

[17] K. K. Steffen, V. L. MacKay, E. O. Kerr et al., "Yeast life span extension by depletion of 60s ribosomal subunits is mediated by Gcn4," *Cell*, vol. 133, no. 2, pp. 292–302, 2008.

[18] S. Klinge, F. Voigts-Hoffmann, M. Leibundgut, S. Arpagaus, and N. Ban, "Crystal structure of the eukaryotic 60S ribosomal

subunit in complex with initiation factor 6," *Science*, vol. 334, no. 6058, pp. 941–948, 2011.

[19] E. Provost, C. A. Weier, and S. D. Leach, "Multiple ribosomal proteins are expressed at high levels in developing zebrafish endoderm and are required for normal exocrine pancreas development," *Zebrafish*, vol. 10, no. 2, pp. 161–169, 2013.

[20] P. Hu, X. He, C. Zhu, W. Guan, and Y. Ma, "Cloning and characterization of a ribosomal protein L23a gene from Small Tail Han sheep by screening of a cDNA expression library," *Meta Gene*, vol. 2, pp. 479–488, 2014.

[21] L. H. Dong, M. L. Ran, Z. Li, F. Z. Peng, and B. Chen, "The role of ubiquitin-proteasome pathway in spermatogenesis," *Hereditas*, vol. 38, no. 9, pp. 791–800, 2016.

[22] M. Kobayashi, S. Oshima, C. Maeyashiki et al., "The ubiquitin hybrid gene UBA52 regulates ubiquitination of ribosome and sustains embryonic development," *Scientific Reports*, vol. 6, no. 1, article 36780, 2016.

[23] J. Mao, C. O'Gorman, M. Sutovsky, M. Zigo, K. D. Wells, and P. Sutovsky, "Ubiquitin A-52 residue ribosomal protein fusion product 1 (Uba52) is essential for preimplantation embryo development," *Biology Open*, vol. 7, no. 10, pp. 1–10, 2018.

Research Article

The Association between *Helicobacter pylori* Seropositivity and Bone Mineral Density in Adults

Jinke Huang ⬤,[1] Zhihong Liu ⬤,[2] Jinxin Ma ⬤,[2] Jiali Liu ⬤,[1] Mi Lv ⬤,[1] Fengyun Wang ⬤,[1] and Xudong Tang ⬤[3]

[1]*Department of Gastroenterology, Xiyuan Hospital, China Academy of Chinese Medical Sciences, Beijing, China*
[2]*Department of Gastroenterology, Peking University Traditional Chinese Medicine Clinical Medical School (Xiyuan), Beijing, China*
[3]*China Academy of Chinese Medical Sciences, Beijing, China*

Correspondence should be addressed to Fengyun Wang; wfy811@163.com and Xudong Tang; txdly@sina.com

Objectives. Current evidence on the associations between *Helicobacter pylori* (*H. pylori*) infection and bone mineral density (BMD) is conflicting. Therefore, a nationally representative sample of adults was analyzed to investigate the associations of *H. pylori* seropositivity and BMD in this study. *Methods*. A retrospective cross-sectional study was conducted with 2555 subjects aged 40-85 years in the US National Health and Nutrition Examination Survey (NHANES) 1999–2001. Multivariable logistic regression models were performed to evaluate the associations between *H. pylori* seropositivity and BMD. Subgroup analyses stratified by sex, age, race, and body mass index (BMI) were performed. *Results*. No association was found between *H. pylori* seropositivity and BMD ($\beta = 0.006$, 95% CI: -0.003 to 0.015, $P = 0.177$). In the subgroup analyses stratified by age, a positive association was observed between the *H. pylori* seropositivity and total BMD among subjects aged 40-55 years ($\beta = 0.018$, 95% CI: 0.004 to 0.033, $P = 0.012$); in the subgroup analyses stratified by sex, a positive association was observed between the *H. pylori* seropositive and total BMD in male ($\beta = 0.019$, 95% CI: 0.007 to 0.032, $P = 0.003$); in the subgroup analyses stratified by age and sex, the total BMD was higher in men aged 40-55 years with *H. pylori* seropositive than those with *H. pylori* seronegative ($\beta = 0.034$, 95% CI: 0.013 to 0.056, $P = 0.002$). *Conclusions*. In conclusion, no association between *H. pylori* seropositive and total BMD was demonstrated among most middle-aged and elderly adults. *H. pylori* infection may not be one key factor in the loss of BMD.

1. Introduction

Helicobacter pylori (*H. pylori*) is the most common chronic bacterial colonizing the human stomach. *H. pylori* infection is prevalent [1], with a prevalence of approximately 35.6% in the United States [2]. *H. pylori* infection has been well known to be associated with a variety of gastric diseases, including chronic gastritis, peptic ulcers, gastric cancer, and mucosa-associated lymphoid tissue lymphoma [3]. Furthermore, several extra gastric disorders have also been proven to be associated with *H. pylori* infection, such as metabolic, neurological, and cardiovascular diseases [4].

Osteoporosis is a silent health problem characterized by deterioration of bone structure due to low bone mineral density (BMD) and disruption of bone homeostasis [5]. As one of the most common metabolic bone diseases worldwide, osteoporosis mostly affects middle-aged and elderly populations [6]. Patients with osteoporosis are susceptible to bone fragility and osteoporotic fractures, and the occurrence of these fractures affects morbidity, mortality, and quality of life, making osteoporosis a growing health and health-economic problem worldwide [7, 8]. Therefore, understanding the risk factors is essential for the prevention, early diagnosis, and management of osteoporosis.

It is reported that *H. pylori* infection can induce inflammatory and immune reactions in individuals, which may modulate bone turnover [9]. However, evidence for the association between *H. pylori* infection and BMD is limited and controversial [10, 11]. Therefore, to investigate the association between *H. pylori* seropositivity and BMD, a
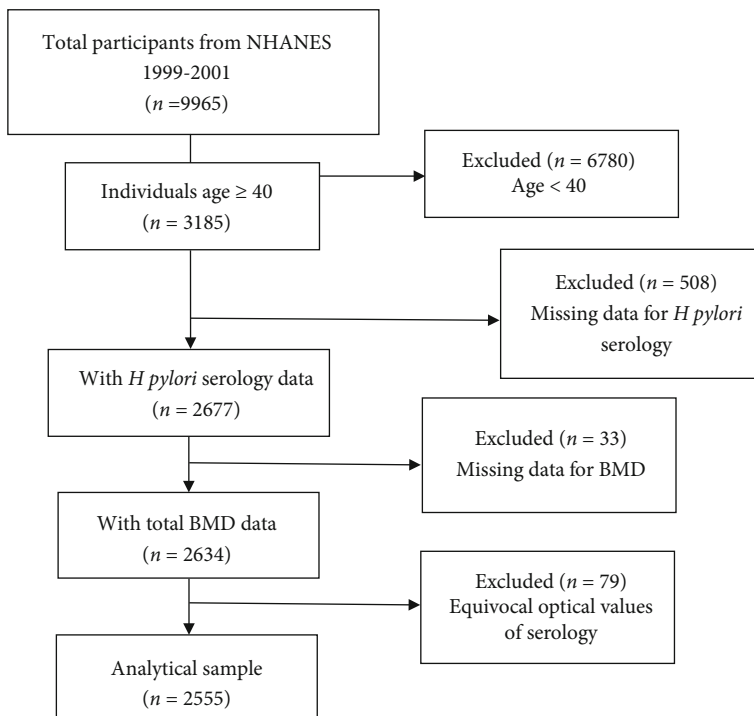
FIGURE 1: The sample selection flow chart.

population-based sample from the National Health and Nutrition Examination Survey (NHANES) was analyzed in this study.

2. Materials and Methods

2.1. Study Population. The NHANES is a representative survey of the national population of US, providing multitudinous information about the nutrition and health of the general US population using a complex, multistage, and probability sampling design [12]. Data for this study was obtained from the 1999–2001 continuous cycle of the US NHANES dataset. The number of subjects in this cycle was 9965. After excluding subjects without information on laboratory and demographic variables, 2555 subjects were finally included for analyses. The sample selection flow chart is presented in Figure 1.

2.2. Variables. In this study, the dependent variable was *H. pylori* seropositivity, and the targeted independent variable was total BMD. *H. pylori* seropositivity was measured by the Wampole Laboratories *H. pylori* IgG Enzyme-Linked Immunosorbent Assays (ELISA). For each specimen, immune status ratio values of >1.1 and <0.9 were considered as seropositive and seronegative, respectively, whereas 0.9– 1.1 were an equivocal value [13]. Subjects with equivocal values were excluded to prevent misleading statistical outcomes in this study. The measurements of total BMD were determined by DEXA scans. For covariates, sex, race, educational level, physical activity, body mass index (BMI), smoking behavior, and other disease status were used as categorical variables; age, poverty to income ratio, days drink

in year, serum uric acid, total calcium, blood urea nitrogen, serum creatinine, total cholesterol, bone alkaline phosphatase, and dietary calcium intake were used as continuous variables. More detailed information on *H. pylori* seropositivity, total BMD, and the covariates is publicly available at http://www.cdc.gov/nchs/nhanes/.

2.3. Statistical Analysis. The design of complex sampling strategies and appropriate weight were incorporated in all analyses. Weighted multivariate linear regression models were performed to evaluate the associations between *H. pylori* seropositivity and total BMD. The other variables were considered potential effect modifiers. For continuous variables, the weighted linear regression model was used to calculate the differences among different groups. For categorical variables, the weighted chi-square test was used. All analyses were conducted in R (http://www.R-project.org, The R Foundation) and EmpowerStats software (http://www. http://empowwerstats.com/, X&Y Solutions, Inc., Boston, MA).

3. Results

3.1. Characteristics of Included Subjects. A total of 2555 subjects were included in final analyses, of which 1263 (49.43%) subjects were *H. pylori* seronegative and 1292 (50.57%) subjects were *H. pylori* seropositive. In these two groups, race, educational level, income poverty ratio, physical activity, days drink in year, smoking behavior, diabetes status, serum creatinine, bone alkaline phosphatase, dietary calcium intake, and total BMD were significantly different ($P < 0.05$). More details are presented in Table 1.

TABLE 1: Weighted characteristics of included subjects.

	H. pylori seronegative (n = 1263)	H. pylori seropositive (n = 1292)	P value
Age (years)	60.493 ± 13.239	61.158 ± 12.959	0.200
Sex (%)			0.433
Male	48.219	49.768	
Female	51.781	50.232	
Race (%)			<0.001
Non-Hispanic white	67.379	27.941	
Non-Hispanic black	12.747	22.755	
Mexican American	14.727	38.854	
Other races	5.146	10.449	
Educational level (%)			<0.001
Less than high school	26.920	59.211	
High school	25.178	17.492	
College graduate or above	47.902	23.297	
Ratio of family income to poverty	6.821 ± 2.856	5.794 ± 2.568	<0.001
Body mass index (100%)			0.398
Undernutrition	2.142	1.208	
Normal	30.038	29.890	
Overweight	35.224	35.551	
Obese	32.596	33.351	
Smoking behavior (%)			0.044
None	48.614	47.988	
Past	35.154	32.198	
Current	16.231	19.814	
Days drink in year	96.090 ± 97.198	79.335 ± 78.680	<0.001
Physical activity (MET-based rank) (100%)			<0.001
0	24.149	38.313	
1	32.225	30.186	
2	16.706	11.842	
3	26.920	19.659	
Any hypertension (%)			0.197
None	57.641	55.108	
Yes	42.359	44.892	
Any diabetes (%)			<0.001
None	86.936	81.115	
Yes	13.064	18.885	
Any coronary artery disease (%)			0.774
None	94.458	94.195	
Yes	5.542	5.805	
Serum uric acid (mg/dL)	5.408 ± 1.558	5.462 ± 1.637	0.389
Total calcium (mg/dL)	9.349 ± 0.898	5.462 ± 1.637	0.255
Blood urea nitrogen (mg/dL)	15.777 ± 6.508	15.630 ± 6.294	0.563
Serum creatinine (μmol/L)	1.419 ± 0.470	1.454 ± 0.515	0.070
Total cholesterol (mg/dL)	203.684 ± 42.647	204.084 ± 43.037	0.813
Bone alkaline phosphatase (mg/dL)	362.894 ± 85.213	372.056 ± 83.924	0.006
Dietary calcium intake (mg)	795.699 ± 493.174	671.269 ± 505.352	<0.001
Total bone mineral density (g/cm^2)	1.088 ± 0.130	1.074 ± 0.129	0.007

Mean ± SD for continuous variables: P value was calculated by a weighted linear regression model. % for categorical variables: P value was calculated by a weighted chi-square test.

Table 2: Association of *H. pylori* seropositive and total bone mineral density.

Effect modifier	Model I (β, 95% CI, P)	Model II (β, 95% CI, P)	Model III (β, 95% CI, P)
Total	-0.015 (-0.025, -0.006) 0.001	-0.002 (-0.011, 0.007) 0.665	0.006 (-0.003, 0.015) 0.177
Age groups			
40-55 years ($n = 977$)	-0.001 (-0.016, 0.013) 0.850	0.004 (-0.011, 0.019) 0.590	0.018 (0.004, 0.033) 0.012
~70 years ($n = 921$)	-0.019 (-0.035, -0.003) 0.0188	-0.014 (-0.029, 0.001) 0.064	-0.010 (-0.025, 0.004) 0.169
~85 years ($n = 657$)	0.007 (-0.012, 0.026) 0.487	0.008 (-0.008, 0.023) 0.329	0.009 (-0.007, 0.024) 0.257
Sex			
Male ($n = 1252$)	0.002 (-0.011, 0.015) 0.746	0.013 (-0.000, 0.026) 0.056	0.019 (0.007, 0.032) 0.003
Female ($n = 1303$)	-0.031 (-0.044, -0.018) <0.001	-0.014 (-0.025, -0.002) 0.023	-0.002 (-0.014, 0.009) 0.730
Race			
Non-Hispanic White ($n = 1212$)	-0.023 (-0.039, -0.007) 0.004	-0.003 (-0.016, 0.010) 0.655	0.008 (-0.005, 0.021) 0.237
Non-Hispanic Black ($n = 455$)	-0.019 (-0.043, 0.006) 0.131	-0.018 (-0.039, 0.003) 0.100	-0.013 (-0.035, 0.008) 0.230
Mexican American ($n = 688$)	0.006 (-0.013, 0.025) 0.514	-0.004 (-0.020, 0.013) 0.672	0.003 (-0.014, 0.020) 0.703
Other races ($n = 200$)	0.018 (-0.013, 0.049) 0.256	0.024 (-0.004, 0.051) 0.089	0.015 (-0.010, 0.041) 0.244
BMI categories			
Undernutrition ($n = 36$)	-0.081 (-0.199, 0.037) 0.188	0.020 (-0.093, 0.134) 0.728	-0.000 (-0.282, 0.281) 0.997
Normal ($n = 695$)	-0.015 (-0.034, 0.004) 0.131	0.001 (-0.017, 0.018) 0.951	0.017 (-0.001, 0.035) 0.064
Overweight ($n = 953$)	-0.010 (-0.026, 0.006) 0.234	0.005 (-0.009, 0.019) 0.515	0.007 (-0.007, 0.022) 0.304
Obese ($n = 871$)	-0.023 (-0.039, -0.007) 0.0056	-0.008 (-0.022, 0.006) 0.270	-0.003 (-0.017, 0.011) 0.668

Model I: no covariates were adjusted; model II: age, sex, and race were adjusted; model III: age, sex, race, educational level, body mass index, ratio of family income to poverty, physical activity, smoking behavior, hypertension status, diabetes status, coronary artery disease status, serum uric acid, total calcium, blood urea nitrogen, serum creatinine, total cholesterol, bone alkaline phosphatase, and dietary calcium intake were adjusted.

3.2. Association between *H. pylori* Seropositivity and Total BMD

3.2.1. Multiple Regression Model. Three weighted univariate and multivariate linear regression models were constructed: model I, unadjusted; model II, age, sex, and race that were adjusted; and model III, covariates presented in Table 1 that were adjusted. In the unadjusted model, a negative association was found between *H. pylori* seropositivity and total BMD ($\beta = -0.015$, 95% CI: -0.025 to -0.006, $P = 0.001$). However, after variable adjustments, the association between *H. pylori* seropositivity and total BMD was not significant in model II and model III. Details are presented in Table 2.

3.2.2. Subgroup Analyses. In the subgroup analyses stratified by age, a positive association was observed between the *H. pylori* seropositivity and total BMD among subjects aged 40-55 years ($\beta = 0.018$, 95% CI: 0.004 to 0.033, $P = 0.012$); however, the total BMD was not related to *H. pylori* seropositivity in other groups. In the subgroup analyses stratified by sex, a positive association was observed between the *H. pylori* seropositive and total BMD in male ($\beta = 0.019$, 95% CI: 0.007 to 0.032, $P = 0.003$); however, the total BMD was not related to *H. pylori* seropositivity in female. In the subgroup analyses stratified by race and BMI categories, no association was found between *H. pylori* seropositivity and total BMD. Details are presented in Table 2.

In the subgroup analysis by age and sex, a positive association was observed between the *H. pylori* seropositivity and total BMD in male aged 40–55 years ($\beta = 0.034$, 95%

CI: 0.013 to 0.056, $P = 0.002$); however, no association was found between *H. pylori* seropositivity and total BMD in female aged 40–55 years. Moreover, in the groups of age over 55 years, no association was found between *H. pylori* seropositivity and total BMD neither male nor female. Details are presented in Table 3.

4. Discussion

The purpose of this study was to explore the associations between *H. pylori* seropositivity and total BMD using the data from NHANES. In summary, no association was found between *H. pylori* seropositivity and total BMD among most middle-aged and elderly adults. However, in the subgroup analyses stratified by age, a positive association was observed between the *H. pylori* seropositivity and total BMD among subjects aged 40-55 years; in the subgroup analyses stratified by sex, a positive association was observed between the *H. pylori* seropositive and total BMD in male; in the subgroup analyses stratified by age and sex, the total BMD was higher in men aged 40-55 years with *H. pylori* seropositive than those with *H. pylori* seronegative.

Osteoporosis, as one of the metabolic bone diseases, is characterized by constant loss of BMD. It is important to understand the risk factors for BMD loss, which can help in the prevention, early diagnosis, and management of osteoporosis. *H. pylori* has been coevolved with humans over 50,000 years. Infection with *H. pylori* is a common risk factor for susceptibility to metabolic diseases; however, the association between *H. pylori* infection and BMD is limited

TABLE 3: Total bone mineral density stratified by race and age.

Helicobacter pylori infection	Total bone mineral density (g/cm^2) (β, 95% CI, P)		
	40-55 years	56~70 years	71~85 years
Male	0.034 (0.013, 0.056) 0.002	-0.001 (-0.022, 0.020) 0.907	0.010 (-0.014, 0.015) 0.907
Female	0.005 (-0.014, 0.023) 0.616	-0.011 (-0.031, 0.009) 0.285	0.008 (-0.014, 0.029) 0.485

Adjusted for age, sex, race, educational level, body mass index, ratio of family income to poverty, physical activity, smoking behavior, hypertension status, diabetes status, coronary artery disease status, serum uric acid, total calcium, blood urea nitrogen, serum creatinine, total cholesterol, bone alkaline phosphatase, and dietary calcium intake.

and controversial. In most studies [14–21], no association between *H. pylori* infection and BMD or osteoporosis was observed, which is consistent with our observation. Recently, a meta-analysis including 1321 adults without other causes of osteoporosis or pathological bone disease at baseline showed that *H. pylori* infection was not associated with osteoporosis (OR = 1.49, 95% CI: 0.88 to 2.55) [11]. However, another pooled study [10] including 9655 subjects came to the opposite conclusion that *H. pylori* infection was associated with increased odds of osteoporosis (OR = 1.39, 95% CI: 1.13 to 1.71). Notably, as acknowledged by the authors, the reference value of the results needs to be further validated due to the heterogeneity of the included studies. Thus, heterogeneity between these studies, including differences in the study design, study simple, and the controlled confounding variables, may explain the controversial findings. In this study, a nationally representative sample of US was used, so the findings are highly relevant to the whole population. Additionally, we further performed subgroup analyses for more appropriate representation of the dataset as recommended by the STROBE statement [22], and a special group was found; that is, a positive association was found between *H. pylori* seropositive and total BMD in male aged 40–55 years. As recently reported, sex and age are also predictors of *H. pylori* infection and BMD [9]. Furthermore, an interesting finding was reported; that is, 63.6% studies conducted in Eastern countries have observed an association between *H. pylori* infection and BMD status, whereas only 22.2% studies conducted in Western countries have observed such association [9]. The difference in the prevalence of *H. pylori* infection (about 30% in developed countries and up to 80% in developing countries) seems to contribute to the understanding of these findings [20].

The mechanism by which *H. pylori* infection increases the risk of osteoporosis and fracture remains to be elucidated in detail. Based on the evidence available to date, several potential mechanisms may underlie the association between *H. pylori* infection and osteoporosis. First, proinflammatory cytokines can act on mesenchymal stem cells and osteoclast precursors to enhance osteoclast-mediated bone resorption [23]. It was reported that high levels of circulating inflammatory markers were associated with increased bone loss or increased fracture risk [24, 25]. Therefore, it is likely that *H. pylori* increases the risk of osteoporosis by promoting an inflammatory response to produce proosteoclastogenic cytokines such as TNFα, IL-1, IL-6, and IL-8 [23]. Second, *H. pylori* infection was associated with reduced levels of estrogen, total estradiol, free estradiol, and bioavailable estradiol in both genders [26]. It was found that decreased estrogen production was associated with a sustained increase in the spontaneous secretion of osteoclastogenic cytokines by T cells, mononuclear cells, and bone marrow stromal cells, leading to net bone loss with increased bone resorption and decreased bone formation [27]. Third, chronic H. pylori infection may be associated with gastric mucosal atrophy. Atrophy of the gastric mucosa can inhibit acid secretion and thus affect calcium absorption and consequently adversely affect bone mass [15]. However, a recent cross-sectional study of 268 healthy men showed that decreased bone mineral density was not associated with *H. pylori*-associated estradiol levels or gastric mucosal atrophy [21]. Similarly, the chronic use of proton pump inhibitors for treatment for gastroduodenal mucosal injury may result in low levels of gastric acid, which is believed to impair calcium solubility and lead to malabsorption, thereby exacerbating bone mineral density loss secondary to hypocalcemic hyperparathyroidism, osteoclast activation, and bone resorption [28, 29]. Overall, the current available data are equivocal, and further mechanistic studies are still necessary.

To the best of our knowledge, this is the first study to explore the association between *H. pylori* seropositive and BMD using the data from NHANES. The NHANES features a rigorous sampling design from the national population of US, high-quality research measurement, detailed quality control procedures, and a more representative population. However, limitations must be acknowledged. First, all data in NHANES are cross-sectional; this study cannot draw the causal relationship between *H. pylori* seropositive and total BMD. Second, the bias caused by other potential confounding factors that did not be adjusted in this study is not excluded. Furthermore, this study did not include the inflammation status of the subjects, which can possibly explain the relationship between *H. Pylori* seropositive and bone health.

5. Conclusion

In conclusion, no association between *H. pylori* seropositive and total BMD was demonstrated in our study. *H. pylori* infection may not be one key factor in the loss of BMD.

Abbreviations

H. pylori: *Helicobacter pylori*
BMD: Bone mineral density

NHANES: National Health and Nutrition Examination Survey.

Data Availability

The datasets analyzed during the current study are available in the NHANES repository (https://wwwn.cdc.gov/nchs/nhanes/Default.aspx).

Disclosure

Jinke Huang and Zhihong Liu are the co-first authors.

Conflicts of Interest

The authors declare that there is no conflict of interest.

Authors' Contributions

Jinke Huang and Zhihong Liu initiated the study design. Jinke Huang drafted the manuscript. Zhihong Liu, Jinxin Ma, Jiali Liu, and Mi Lv helped with implementation of this work. Fengyun Wang and Xudong Tang contributed to the methodology, review, and editing of the manuscript. All authors read and approved the final manuscript.

Acknowledgments

References

[1] M. Zamani, F. Ebrahimtabar, V. Zamani et al., "Systematic review with meta-analysis: the worldwide prevalence of Helicobacter pylori infection," *Alimentary Pharmacology & Therapeutics.*, vol. 47, no. 7, pp. 868–876, 2018.

[2] C. Burucoa and A. Axon, "Epidemiology of Helicobacter pylori infection," *Helicobacter*, vol. 22, Supplement 1, pp. 1–5, 2017.

[3] J. C. Atherton, "The pathogenesis ofHelicobacter pylori-induced gastro-duodenal diseases," *Annual Review of Pathology*, vol. 1, no. 1, pp. 63–96, 2006.

[4] T. Wang, X. Li, Q. Zhang et al., "Relationship betweenHelicobacter pyloriinfection and osteoporosis: a systematic review and meta-analysis," *BMJ Open*, vol. 9, no. 6, article e027356, 2019.

[5] A. Klibanski, L. Adams-Campbell, and T. Bassford, "Osteoporosis prevention, diagnosis, and therapy," *Journal of the American Medical Association*, vol. 285, no. 6, pp. 785–795, 2001.

[6] O. Johnell and J. A. Kanis, "An estimate of the worldwide prevalence and disability associated with osteoporotic fractures," *Osteoporosis International*, vol. 17, no. 12, pp. 1726–1733, 2006.

[7] N. F. Ray, J. K. Chan, M. Thamer, and L. J. Melton, "Medical expenditures for the treatment of osteoporotic fractures in the United States in 1995: report from the National Osteoporosis Foundation," *Journal of Bone and Mineral Research*, vol. 12, no. 1, pp. 24–35, 1997.

[8] C. R. Lyles, A. L. Schafer, and H. K. Seligman, "Income, food insecurity, and osteoporosis among older adults in the 2007-2008 National Health and Nutrition Examination Survey (NHANES)," *Journal of Health Care for the Poor and Underserved*, vol. 25, no. 4, pp. 1530–1541, 2014.

[9] F. Leon, F. Alexander, and N. Smith Paul, "Helicobacter pylori related diseases and osteoporotic fractures (Narrative Review)," *Journal of Clinical Medicine*, vol. 9, no. 10, p. 3253, 2020.

[10] T. Wang, X. Li, Q. Zhang et al., "Helicobacter pylori Relationship between infection and osteoporosis: a systematic review and meta-analysis," *BMJ Open*, vol. 9, no. 6, article e027356, 2019.

[11] S. Upala, A. Sanguankeo, K. Wijarnpreecha, and V. Jaruvongvanich, "Association between Helicobacter pylori infection and osteoporosis: a systematic review and meta-analysis," *Journal of Bone and Mineral Metabolism*, vol. 34, no. 4, pp. 433–440, 2015.

[12] L. R. Curtin, L. K. Mohadjer, S. M. Dohrmann et al., "The national health and nutrition examination survey: sample design, 1999–2006," *Vital and Health Statistics*, vol. 2, pp. 1–39, 2012.

[13] Centers for Disease Control and Prevention, *Helicobacter pylori ELISA measurement in NHANES*, 2008.

[14] A. M. Kakehasi, C. M. Mendes, L. G. Coelho, L. P. Castro, and A. J. A. Barbosa, "The presence of Helicobacter pylori in post-menopausal women is not a factor to the decrease of bone mineral density," *Arquivos de Gastroenterologia*, vol. 44, no. 3, pp. 266–270, 2007.

[15] A. M. Kakehasi, C. B. Rodrigues, A. V. Carvalho, and A. J. A. Barbosa, "Chronic gastritis and bone mineral density in women," *Digestive Diseases and Sciences*, vol. 54, no. 4, pp. 819–824, 2009.

[16] M. Fotouk-Kiai, S. R. Hoseini, N. Meftah et al., "Relationship between helicobacter pylori infection (Hp) and bone mineral density (BMD) in elderly people," *Caspian Journal of Internal Medicine*, vol. 6, pp. 62–66, 2015.

[17] M. R. Kalantarhormozi, M. Assadi, K. Vahdat et al., "Chlamydia pneumoniae and helicobacter pylori IgG seropositivities are not predictors of osteoporosis-associated bone loss: a prospective cohort study," *Journal of Bone and Mineral Metabolism*, vol. 34, no. 4, pp. 422–428, 2016.

[18] D. Chinda, T. Shimoyama, C. Iino, M. Matsuzaka, S. Nakaji, and S. Fukuda, "Decrease of estradiol and several lifestyle factors, but not Helicobacter pylori infection, are significant risks for osteopenia in Japanese females," *Digestion*, vol. 96, no. 2, pp. 103–109, 2017.

[19] B. Heidari, A. Muhammadi, Y. Javadian, A. Bijani, R. Hoseini, and M. Babaei, "Associated factors of bone mineral density and osteoporosis in elderly males," *International Journal of Endocrinology and Metabolism*, vol. 15, no. 1, article e39662, 2016.

[20] L. J. Lu, N. B. Hao, J. J. Liu, X. Li, and R. L. Wang, "Correlation between Helicobacter pylori infection and metabolic abnormality in general population: a cross-sectional study," *Gastroenterology Research and Practice*, vol. 2018, Article ID 7410801, 6 pages, 2018.

[21] D. Chinda, T. Shimoyama, K. Sawada et al., "Lifestyle factors rather thanHelicobacter pyloriinfection or estradiol level are

associated with osteopenia in Japanese men," *American Journal of Men's Health*, vol. 13, no. 3, p. 155798883193948421, 2019.

[22] E. von Elm, D. G. Altman, M. Egger, S. J. Pocock, P. C. Gøtzsche, and J. P. Vandenbroucke, "The Strengthening the Reporting of Observational Studies in Epidemiology (STROBE) statement: guidelines for reporting observational studies," *Journal of Clinical Epidemiology*, vol. 61, no. 4, pp. 344–349, 2008.

[23] K. Papamichael, G. Papaioannou, M. A. Cheifetz, and A. S. Cheifetz, "Bone of contention: Helicobacter pylori and osteoporosis-is there an association?," *Digestive Diseases and Sciences*, vol. 64, no. 10, pp. 2736–2739, 2019.

[24] C. Ding, V. Parameswaran, R. Udayan, J. Burgess, and G. Jones, "Circulating levels of inflammatory markers predict change in bone mineral density and resorption in older adults: a longitudinal study," *The Journal of Clinical Endocrinology and Metabolism*, vol. 93, no. 5, pp. 1952–1958, 2008.

[25] B. Abrahamsen, V. Bonnevie-Nielsen, E. N. Ebbesen, J. Gram, and H. Beck-Nielsen, "Cytokines and bone loss in a 5-year longitudinal study-hormone replacement therapy suppresses serum soluble interleukin-6 receptor and increases interleukin-1-receptor antagonist: the Danish Osteoporosis Prevention Study," *Journal of Bone and Mineral Research*, vol. 15, no. 8, pp. 1545–1554, 2000.

[26] L. Gennari, D. Merlotti, N. Figura et al., "Infection by CagA-positive helicobacter pylori strains and bone fragility: a prospective cohort study," *Journal of Bone and Mineral Research*, vol. 36, no. 1, pp. 80–89, 2021.

[27] T. Ueyama, N. Shirasawa, M. Numazawa et al., "Gastric parietal cells: potent endocrine role in secreting estrogen as a possible regulator of gastro-hepatic axis," *Endocrinology*, vol. 143, no. 8, pp. 3162–3170, 2002.

[28] Y. Nassar and S. Richter, "Proton-pump inhibitor use and fracture risk: an updated systematic review and meta-analysis," *Journal of Bone Metabolism*, vol. 25, no. 3, 2018.

[29] Y. X. Yang, "Chronic proton pump inihibitor therapy and calcium metabolism," *Current Gastroenterology Reports*, vol. 14, no. 6, pp. 473–479, 2012.